Alexandre Rodrigues Coelho

Study of RNA-binding protein networks in colorectal cancer cells

Universidade do Algarve

Faculdade de Medicina e Ciências Biomédicas

2021

Alexandre Rodrigues Coelho

Study of RNA-binding protein networks in colorectal cancer cells

Mestrado em:

Oncobiologia – Mecanismos Moleculares do Cancro

Trabalho efetuado sob a orientação de:

Bruno Miguel Correia Pereira, PhD

Bibiana Isabel da Silva Ferreira, PhD

Raquel Maria da Silva Graça Almeida, PhD

Universidade do Algarve

Faculdade de Medicina e Ciências Biomédicas

2021

Study of RNA-binding protein networks in colorectal cancer cells

Declaração de autoria de trabalho

Declaro ser o autor deste trabalho, que é original e inédito. Autores e trabalhos consultados estão devidamente citados no texto e constam da listagem de referências incluída.

_____

Alexandre Rodrigues Coelho

If you want to build a ship, don't drum up the men to gather wood, divide the work, and give orders. Instead, teach them to yearn for the vast and endless sea.

- Antoine de Saint-Exupéry

Acknowledgments

Agradecimentos, por onde começar? Foi a ajuda de muitos que me permitiu estar aqui a escrever isto mesmo que não se tenham dado conta do seu contributo.

Começar, sem dúvida, pelo meu orientador, Bruno, que me acompanhou de perto nesta jornada de 1 ano nas diferentes etapas. Agradeço por me ter recebido e por toda a sua ajuda e conselhos que me permitiram executar este trabalho e a levá-lo na melhor direção. Pela enorme paciência para me explicar e ensinar, e sobretudo no início com as constantes perguntas, "Desculpe, onde é que está o…?". Agradeço por partilhar o seu olhar crítico que muito me ensinou e que tornou as coisas mais claras. São estas características que nos acompanham no nosso percurso. Obrigado.

Agradeço também à Drª Raquel por me ter acolhido e dado a oportunidade de desenvolver a minha dissertação no seu laboratório.

À Catarina não só pela preciosa ajuda na realização de algumas das experiências, mas também pelas conversas na sala de cultura e pela partilha de experiências.

Agradeço aos restantes elementos do grupo Differentiation & Cancer, à Patrícia, às Dianas, à Mariana e à Sara, por me fazerem sentir bem-vindo e ajudado no que precisei.

À Prof.ª Bibiana por ter aceite ser co-orientadora deste trabalho e pelo rigor e exigência que nos incutiu nas suas aulas.

A todos os incríveis docentes que possibilitaram aqui chegar.

Uma palavra de agradecimento também à Prof.ª Leonor Cancela por me ter ajudado a encontrar o laboratório.

À malta de OncoMeMoCa por todos os bons momentos do 1º ano, que infelizmente acabou por ser mais curto.

Aos meus amigos que mesmo longe senti-os perto.

Aos meus pais por tudo o que fizeram por mim e continuam a fazer. Agradeço todo o apoio e segurança que sempre me deram e as palavras de encorajamento. À minha irmã, aos meus avós e a todos os outros que sempre acreditaram em mim.

E por último à minha Daniela. Agradeço o teu constante apoio nas pequenas e grandes coisas. Tornaste tudo sem dúvida mais fácil ao longo deste ano e não sei como te agradecer pela tua cumplicidade, carinho e amizade.

Obrigado a todos.

Abstract

Colorectal cancer (CRC) is one of the leading cancer-related deaths in the world, causing the death of almost 1 million people every year, thus highlighting the need for better prognostic biomarkers and reliable therapeutic targets. It is increasingly evident that RBPs are major players in stem cell biology and carcinogenesis, namely in CRC, and have the potential to regulate several cancer-related phenotypes when dysregulates. Therefore, we aimed at identifying new RBPs with a functional impact in the context of CRC.

An *in silico* approach led us to three potential stemness-related RBPs: ASPM, TIMELESS and ZBTB16. The characterization of a cohort of human CRC cases showed that ASPM and ZBTB16 were preferentially overexpressed in tumoral tissue, whereas TIMELESS was expressed at low and high levels in the same proportion of cases. However, an association with a MSS status was found, indicating that TIMELESS might have a predictive prognostic value.

TIMELESS knockdown induced several functional changes in CRC cell lines, some in a cell line-specific manner. TIMELESS depletion led to a prominent reduction of cells in S phase and sensitized them for apoptosis or necrosis which was further amplified by the exposure to the chemotherapeutic agent 5-FU. Furthermore, we observed that TIMELESS expression was restricted to the crypt base in normal tissue and the expression of several known ISC markers was altered upon TIMELESS removal. The phenotypic alterations also occurred at the level of mRNA metabolism in SW480 cells through a reduction of P-body aggregates.

Our results show that TIMELESS might be implicated in key tumorigenic processes, such as promotion of cell proliferation and cell death avoidance. This work highlights the relevance of putative RBPs in CRC and the understanding of their functional impact opens an avenue for novel cancer therapies.

Keywords: Colorectal cancer; RNA-binding protein; Intestinal stem cells; TIMELESS; ASPM; ZBTB16.

Resumo

O epitélio intestinal é o tecido que mais rapidamente se regenera em mamíferos, sendo renovado a cada 3-5 dias. Esta incrível capacidade é assegura por células estaminais localizadas no fundo das criptas intestinais identificadas pela expressão de Lgr5, um gene alvo da via de sinalização Wnt. Porém, as células $Lgr5^{+}$ já foram identificadas como as células de origem do cancro colorectal (CCR), sendo fundamentais não só para o seu crescimento como também para a sua disseminação e resistência a quimioterapia.

O CCR é atualmente a segunda causa de morte por cancro em Portugal e no mundo, tendo causado cerca de 940.000 mortes em 2020. A sua incidência está principalmente associada a estilos de vida típicos de países desenvolvidos que compreendem 60% das mortes. A etiologia e os mecanismos moleculares responsáveis tanto pelo aparecimento como pela progressão da doença já foram extensamente estudados ao longo das últimas décadas. Contudo, maioria dos pacientes apresenta doença metastática, sobretudo no fígado, na altura do diagnóstico e a remoção cirúrgica do tumor continua a ser a melhor opção de tratamento, o que a que a sobrevida a 5 anos em pacientes em estadio avançado ronde os 10%. Isto demonstra a falta de melhores biomarcadores com valor prognóstico e do desenvolvimento de terapias mais eficazes.

Os mecanismos de regulação pós-transcricionais têm um papel fundamental na expressão génica, os quais são sobretudos mediados por proteínas de ligação ao ARN. Estas representam alvos terapeuticamente interessantes tendo em conta que são capazes de regular a expressão de múltiplas proteínas relevantes para o processo cancerígeno. A desregulação das proteínas de ligação ao ARN tem sido associados à biologia das células estaminais e à carcinogénese, nomeadamente no CCR. Desta forma, o nosso trabalho tem como objetivo a identificação de novas proteínas de ligação ao ARN relacionadas com o potencial estaminal e que desempenhem funções relevantes em células de CCR.

Partindo de uma abordagem bioinformática selecionámos três candidatos associados a estaminalidade e diferencialmente expressos em casos de CCR: ASPM, TIMELESS e ZBTB16. A caraterização de uma série de 192 casos de CCR revelou que ASPM e ZBTB16 estão preferencialmente sobreexpressos em tumores, enquanto que TIMELESS estava expresso em baixos e altos níveis na mesma proporção de casos. Além disso, procurámos ainda associar os dados de expressão com as características clinino-

patológicas dos pacientes que revelaram uma correlação estatisticamente significativa da elevada expressão de ASPM e TIMELESS com estabilidade de microssatélites tipicamente associada a um pior prognóstico.

De seguida, e tendo em conta as observações anteriores e a disponibilidade de ferramentas molecular, prosseguimos o estudo do papel de TIMELESS na biologia do CCR. Considerando o papel central da via de sinalização Wnt nas células estaminais e no desenvolvimento de CCR, começámos por tentar esclarecer se TIMELESS é regulado pela via Wnt em cultura de organóides intestinais de ratinho. De facto, a estimulação da via Wnt levou a um aumento na expressão de TIMELESS, embora não expressiva a nível de ARNm, sugerindo que TIMELESS poderá não ser um alvo da via Wnt mas sim estar associado à expansão da população de células $Lgr5^{+}$ induzida pela ativação da via.

A inibição de TIMELESS por siARN produziu várias alterações a nível funcional nas linhas celulares de CCR HCT116 e SW480. A depleção de TIMELESS afetou a progressão das células no ciclo celular, aumentando as células nas fases G1 e G2/M, e diminuindo a fase S. Além disso, a remoção de TIMELESS também afetou a morte celular embora de forma distinta nas duas linhas celular. Nas células HCT116, a inibição de TIMELESS induziu a morte por apoptose, mas a combinação com o agente quimioterapêutico 5-FU potenciou a necrose. Por outro lado, a ausência de TIMELESS nas células SW480 causou principalmente morte por necrose, enquanto a adição de 5-FU teve um efeito considerável no aumento de células em apoptose. Este efeito específico das linhas celulares dever-se-á provavelmente ao seu perfil mutacional, pois as células HCT116 não apresentam p53 defeituoso, sendo, por isso, mais capazes de desencadear a morte celular programada, ao contrário das células SW480 que são mutantes em p53. Coletivamente, estas observações sugerem que a expressão de TIMELESS promove a proliferação celular ao prevenir a paragem do ciclo celular e está envolvida na manutenção da viabilidade celular ao evitar mecanismos de morte celular incluindo na presença de stress genotóxico. No entanto, e contrariamente ao que já havia sido publicado, não conseguimos associar TIMELESS à capacidade migratória de células de CCR, possivelmente devido ao facto da transfeção transiente não produzir alterações significativas no fenótipo celular visíveis por 24h.

Além disso, a depleção de TIMELESS resultou ainda num aumento a expressão de alguns marcadores de células estaminais intestinais, contradizendo os resultados anteriores. Isto poderá indicar um possível mecanismo compensatório para as alterações

causadas pela depleção de TIMELESS. Alterações essas que se estendem ao metabolismo de ARNm, pelo menos nas células SW480, visto que a ausência de TIMELESS afetou a dinâmicas dos corpos P, isto é, agregados citoplasmáticos de ARNm cuja tradução foi reprimida. Apesar do número de agregados se manter constante na inibição de TIMELESS, verificámos uma diminuição na área destes agregados que se refletiu também numa menor intensidade de fluorescência.

Considerando os resultados obtidos, concluímos que TIMELESS está efetivamente implicado na biologia do CCR, estando envolvido tanto na proliferação como nos mecanismos de morte celular e estaminalidade. Trabalhos futuros serão necessários para determinar os mecanismos moleculares por detrás destes processos em CCR bem como esclarecer o seu papel na homeostasia do epitélio intestinal e mais concretamente nas células $Lgr5^{+}$. Além disso, também demonstrámos que ASPM e ZBTB16 estão preferencialmente sobreexpressos em tumores humanos. Desta forma, ao determinar o envolvimento destas três proteínas em mecanismos de regulação pós-transcricional, permitirá uma melhor compreensão e enquadramento dos mecanismos subjacentes ao desenvolvimento e progressão do CCR, que permanece uma das principais causas de mortes mundialmente.

Assim, o presente trabalho permitiu identificar três novas potenciais proteínas de ligação ao ARNm, tendo uma delas, TIMELESS, sido demonstrada a sua relevância a nível funcional, o que abre novas perspetivas para novos biomarcadores e potenciais terapias para o CCR.

Palavras-chave: Cancro colorectal; Proteína de ligação ao ARNm; Células estaminais intestinais; TIMELESS; ASPM; ZBTB16.

Table of contents

Figures index

Tables index

Abbreviations

A

ABCB1: ATP Binding Cassette Subfamily B Member 1

ALPI: Alkaline Phosphatase, Intestinal

AP-1: Activator *protein 1*

APC: Adenomatous polyposis coli

ASCL2: Achaete-scute complex homolog 2

ASPM: Abnormal spindle-like primary microcephaly associated

ATCC: *American Type Culture Collection* ATOH1: Protein atonal homolog 1

B

BCL9: B-cell lymphoma 9 *protein*

BMI1: Polycomb complex *protein* BMI-1

BMP: *Bone morphogenetic protein*

BRAF:

C

CAMKII: Ca2+/calmodulin-dependent protein kinase-II

CBC: Crypt base columnar

CBP: CREB-binding protein

CD: Cluster of differentiation

CDC42: Cell division control *protein* 42 homolog

CDK1: Cyclin Dependent Kinase 1

ChIP: Chromatin immunoprecipitation

CHK1: Checkpoint kinase 1

CIMP CpG island methylation phenotype

CK1: Casein kinase I

CRC: Colorectal cancer

CRY: Cryptochrome

CSC: Carcer stem cell

CTNNB1: Catenin Beta 1

D

DKK: Dickkopf-related *protein*

DLL: Delta Like Canonical Notch Ligand

DMSO: Dimethyl sulfoxide

DNA: Deoxyribonucleic acid

dsRBD: Double-stranded RNA-binding domain

DVL: Dishevelled

E

ECM: Extracellular matrix

EDC4: Enhancer of mRNA-decapping *protein* 4

EGF: Epidermal growth factor

eIF2: Eukaryotic translation initiation factor 2A

EMT: Epithelial-mesenchymal transition

EpCAM: Epithelial Cell Adhesion Molecule

F

FAP: Familial adenomatous polyposis coli

FBS: Fetal bovine serum

FOXL1: Forkhead box protein L1

FZD: Frizzled

G

GFP: Green fluorescent protein

GPCR: G protein-coupled receptors

GSK-3: Glycogen synthase kinase 3

H

HDAC: *Histone Deacetylase*

HDI: *Human Development Index*

Hh: Hedgehog

HIPK2: Homeodomain Interacting *Protein* Kinase 2

HNPCC: Hereditary Nonpolyposis Colorectal Cancer

hnRNPA1: Heterogeneous Nuclear Ribonucleoprotein A1

HOPX: Homeodomain-only *protein* homeobox

I

IDR: Intrinsically disordered region

IGFBP3: Insulin-like growth factor-binding *protein* 3

IMP: insulin-like growth factor mRNA-binding *protein*

IRES: Internal ribosome entry site

ISC: Intestinal stem cell

J

JNK: c-Jun N-terminal kinase

K

kDa: kilodalton

KH: K Homology domain

KRAS: Kirsten rat sarcoma virus

L

LARP: La-related *protein*

LDL: Low Density Lipoprotein

LEF: Lymphoid enhancer factor

LGR: Leucine-rich repeat-containing G-*protein* coupled receptor

LOH: Loss of heterozygosity

LRIG1: leucine rich repeats and immunoglobulin like domains 1

LRP: LDL receptor related protein

M

miRNA: micro-RNA

MMP: Matrix metalloproteinases

MMR: Mismatch repair

mRNA: Messenger RNA

MSH: MutS Homolog

MSI: Musashi

MSI: microsatellite instability

MSS: Microsatellite stable

mTERT: Mouse Telomerase Reverse Transcriptase

N

NFAT: Nuclear factor of activated T cells

O

OLFM4: Olfactomedin-4

P

PARP-1: Poly(ADP-ribose) polymerase 1

PAT1: *protein* interacting with APP tail-1

P-body: Processing *bodies*

PCP: Planar cell polarity protein

PER: Period

PKC: Protein kinase C

PLK1: Polo-like Kinase 1

PORCN: Porcupine protein

PPAR: Peroxisome proliferator-activated receptor

PTM: Post-translational modification

Q

QKI: Quaking homolog protein

R

RBD: RNA-binding domain

RBP: RNA-binding protein

RBPMS2: RNA-Binding *Protein* with Multiple Splicing-2

RNA: Ribonucleic acid

RNF43: Ring Finger Protein 43

RNP: Ribonucleoprotein

ROCK: Rho-associated *protein* kinase

RRM: RNA recognition motif

RYK: Receptor Like Tyrosine Kinase

S

SALL2: Sal-like protein 2

SAM68: Src associated in mitosis, of 68 kDa

sFRP: Secreted Frizzled-related *protein*

siRNA: Small interfering RNA

SLC12A2: Solute Carrier Family 12 Member 2

SOX: SRY-Box

SRSF: Serine/Arginine (SR)-rich splicing factor

SSA: sessile serrated adenoma

T

TA: Transit-amplifying

TCF: T cell *factor*

TGF-β: Transforming growth factor beta

TLE: Transducin-like enhancer

TP53: Tumour protein P53

U

UTR: Untranslated region

V

VEGF: *Vascular endothelial growth factor*

Z

ZBTB16: Zinc finger and BTB domain-Containing protein 16

ZNRF3: Zinc and Ring Finger 3 protein

Chapter 1 – Introduction

1.1. The adult intestinal epithelium

The intestinal tract is a tubular organ derived from the embryonic endoderm and it is anatomically divided into two segments in vertebrates: the small intestine and the large intestine (1). The small intestine starts after the pylorus and extends for 6 to 8 meters, being further divided into three proximal-distal portions: duodenum, jejunum, and ileum. The large intestine is about 1,5 meters, from the ileocecal valve to the anus and it includes the colon and the rectum. The colon is mainly responsible for the absorption of water and electrolytes, and for the formation of feces and its movement towards the rectum (1,2).

1.1.1. Tissue and cellular organization

The intestinal wall comprises four concentric tissue layers (fig. 1.1). The inner layer called mucosa is composed of a single-cell epithelium, the lamina propria, and the muscularis mucosa. The second layer, the submucosa, consists of connective tissue with blood and lymph vessels, nervous plexuses, and immune cells. The third layer is formed by two muscular sheets, the internal circular smooth muscle and the external longitudinal smooth muscle, together with nerve fibers from the enteric nervous system that orchestrate the contractions responsible for moving forward the intestinal content. Finally, the entire organ is covered by the fourth layer, the serosa (1).

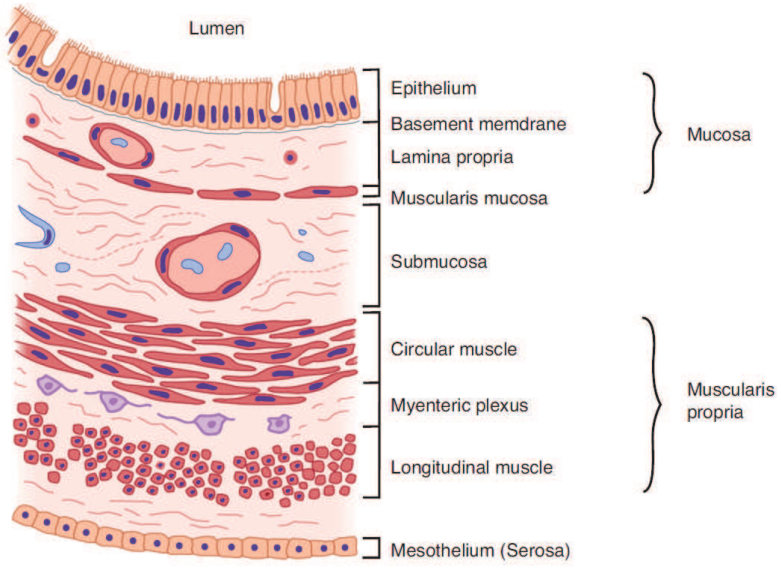

Figure 1.1. Organization of the intestinal wall into functional layers. From Barrett *et al.* (3).

The luminal epithelium is responsible for promoting the digestion and absorption of nutrients, and for the compaction of stool (2). For that, the small intestinal surface area is maximized through well-defined structures of luminal projections of the mucosa, called villi, and tubular-shaped invaginations, called crypts of Lieberkühn (fig. 1.2A) (4). Each intestinal villus consists of a simple columnar epithelium and is surrounded by at least six crypts, whereas the mucosa of the large intestine does not show villi and the crypts reach the submucosa (2). Four major types of differentiated cells can be found in these structures: enterocytes, enteroendocrine cells, goblet cells, and Paneth cells (1,2). Enterocytes or absorptive cells are the main constituents in the long villi that compose the duodenum and jejunum, but also in the colon (colonocytes). Enterocytes secrete hydrolytic enzymes, namely peptidases and enterokinases, to facilitate the digestion of food and exhibit microvilli into the lumen for the absorption of nutrients. Goblet cells are mainly located in the epithelium of short and flat villi in the ileum and in the colon, where they produce mucus as the stool becomes more compacted. Enteroendocrine cells represent less than 1% of the intestinal epithelium and can secrete various hormones, including serotonin, secretin, and peptide hormones such as cholecystokinin, which regulate the digestive functions of other intestinal cells. Paneth cells are phagocytic cells that secrete lysozymes and antimicrobial agents to protect the gut environment against microorganisms and toxins. Importantly, Paneth cells are found at the base of the crypts in the small intestine, cecum and very rarely in the distal colon in humans, and are completely absent in the mouse colon epithelium (1,2,5).

The constant maintenance of the intestinal epithelium is ensured by multipotent, self-renewing, and actively cycling crypt base columnar (CBC) intestinal stem cells (ISCs) capable of rapidly originating all the epithelial cell types of the small intestine and colon. CBC cells are located at the crypt base, and in the small intestine are intercalated by Paneth cells (2,4). From the crypts, these stem cells permanently generate highly proliferative transit-amplifying (TA) cells that migrate upwards while progressively differentiating into the secretory or absorptive cell lineages (fig. 1.2B). Once out of the crypts, they stop dividing and fully differentiate into the functional cell types mentioned above that form the villi and the upper half of the colon crypts. However, differentiated cells continue migrating upward until the tips of the villi where they undergo anoikis, detach, and are shed into the intestinal lumen. TA cells also migrate down towards the

base of the crypts to give rise to Paneth cells, which are phagocytized by neighbouring Paneth cells after dying (1,4).

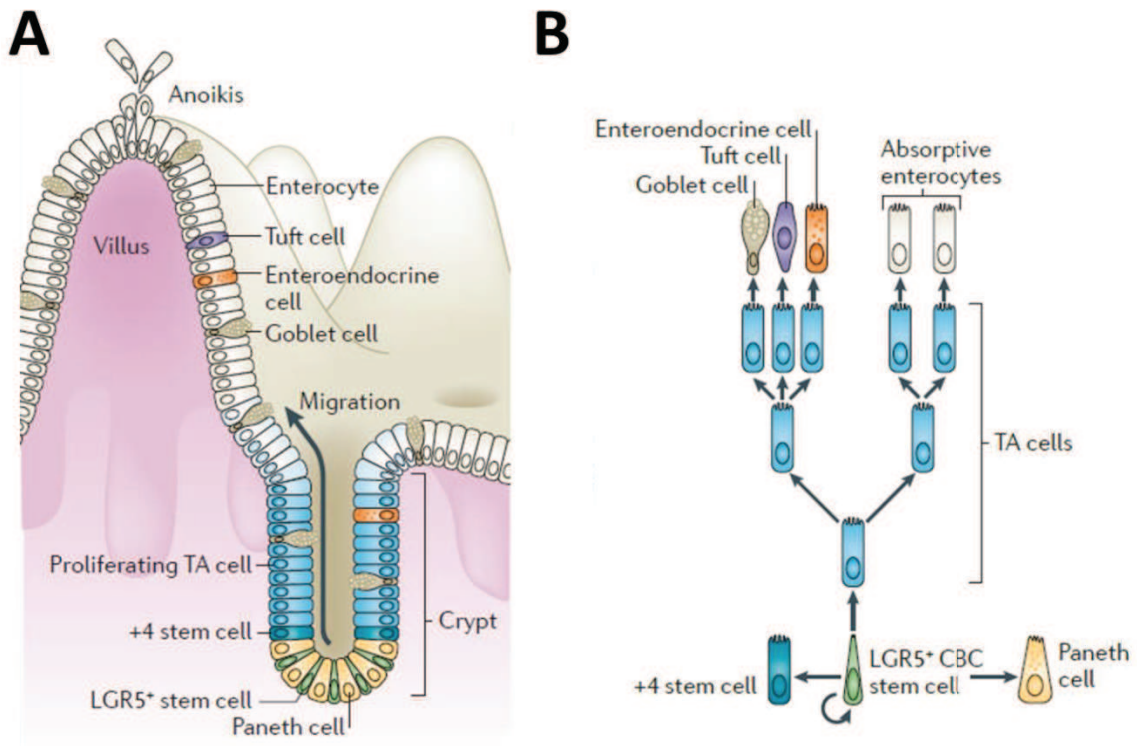

Figure 1.2. The intestinal epithelium architecture. (A) In the small intestine, the epithelium is organized in well-defined structures of villi and crypts. ISCs reside at the base of the crypts intercalated with Paneth cells and TA cells occupy the remainder of the crypt, whereas the differentiated cells are located in the villus. **(B)** LGR5^{+} stem cells produce rapidly proliferating TA cells that migrate upwards and differentiate into the absorptive or secretory lineage to originate the different cell types found in the villi. Paneth cells migrate downwards and remain at the crypt bottom. The +4 stem cell population acts as reserve stem cells. TA: transit-amplifying. Adapted from Barker N. *et al.* (2).

1.1.2. Intestinal stem cell identity

For a long time, linking putative stem cell populations to their progeny was a difficult task. The emergence of specific markers helped overcoming this issue. The Leucine rich repeat-containing G-protein coupled receptor 5 (LGR5) was the first marker identified to be restricted to the CBC cells within crypts (6). LGR5^{+} cells average cycling time is 24h, repopulating the entire small intestinal epithelium every 3-5 days in homeostatic conditions (6). Lineage tracing in mice by genetic labelling has shown that LGR5^{high} cells divide symmetrically around each crypt base, which leads to stem cells

being continuously lost and readily replaced by neighbouring stem cell clone expansion (7,8). Therefore, stem cell renewal occurs at the population level, where expanding clones randomly compete with each other towards monoclonality within each crypt in a mechanism known as neutral drift. A few months after the mouse in born, an entire intestinal crypt will be derived from the last surviving stem cell clone and hence its progeny will migrate upwards to occupy clonal villi. Thus, homeostatic tissue turnover is ensured by around 14 symmetrically proliferating CBC cells that compete for the niche microenvironment at the crypt base. Stem cells displaced from the niche lose stemness and commit to differentiation, resulting in the expansion of the remaining clones within the niche (7,8). $LGR5^+$ cells are a heterogeneous cell population with different self-renewal potentials according to their anatomical position within the crypt base compartment (9). $LGR5^+$ cells closer to the niche boundary tend to be displaced into the TA compartment and replaced. Whereas "functional" stem cells (5-7 per crypt) located at the bottom of the crypt are biased towards survival and thus more likely to colonize a crypt and to drive epithelial renewal (9,10).

In addition to $LGR5^+$ cells, it has been proposed the existence of another population of ISCs positioned at or near the +4 position (counting from the bottom of the crypt) forming a ring above the crypt base. These cells are defined as quiescent or slow-cycling cells that do not contribute to the homeostatic tissue turnover but are capable of giving rise to all intestinal epithelial lineages, including $LGR5^+$ ISCs following acute damage. The $LGR5^+$ population is radiation sensitive and responsive to Wnt pathway modulation (see below) with its gene expression signature spanning many Wnt target genes, for example, *Ascl2*, *Sox9*, *Ephb-3* and *Axin2*. On the other hand, the +4 cell pool is described as radiation resistant and refractory to Wnt signal modulation. Interestingly, many of the proposed +4 cell markers, such as *Bmi1*, *mTert*, *Hopx*, *Lrig1*, and *Dll1*, have broad expression patterns within the crypt and therefore are also highly expressed in $LGR5^+$ cells and in committed progenitor cells, raising doubts about the existence of a second independent ISC population (11,12). Several studies have now proposed that the two populations of ISCs coexist in the crypts in a non-hardwired system, as already observed in other tissues (13).

The intestinal epithelium is endowed with great plasticity resulting from the localized microenvironment that provides the necessary signals to convert non-stem cell epithelial cells into functional ISCs. This allows the rapid restoration of crypt homeostasis

in response to tissue damage and consequent loss of the resident stem cell population (4). During injury-induced regeneration, many cell types have the potential to restore the stem cell compartment, which enables the dedifferentiation of both progenitor and differentiated cells. The regenerative capacity of progenitor cells after irradiation is mediated by the expression of high levels of the transcription factor ASCL2, a Wnt target restricted to $LGR5^+$ cells and involved in the maintenance of stem cells in the adult intestinal epithelium. *Ascl2* activation in the crypt middle region following ISC ablation in the mouse is required for absorptive and secretory precursors to dedifferentiate and drive $LGR5^+$ ISC repopulation (14,15). Upon active ISC ablation, $DLL1^+$ secretory progenitors have the ability to originate $LGR5^+$ cells and to be mobilized into the crypt base. Similarly, $ALPI^+$ enterocyte precursors dedifferentiate and revert to $LGR5^+$ cells following damage to the stem cell pool (16). Likewise, radiation-induced depletion of $LGR5^+$ ISCs activates Notch signalling in a small subset of mature Paneth cells that regain proliferation capacity and stem cell features in order to repair the epithelium (17).

1.1.3. The intestinal niche signalling pathways

ISCs reside in a specialized niche that strictly modulates their self-renewal, proliferation and differentiation, and is thus crucial to maintain ISC homeostasis. The ISC niche encompasses elements of the extracellular matrix, adjacent epithelial cells and mesenchymal cells that supply ISCs with extrinsic signalling molecules, which are summarized in fig. 1.5. Several signalling pathways ensure intestinal epithelial homeostasis, strictly regulating ISCs fate.

1.1.3.1. Wnt signalling

Wnt signalling plays a key role in multiple developmental processes as well as in adult stem cells. The Wnt family comprises at least 19 members which are cysteine-rich glycoproteins that act as paracrine factors on neighbouring cells (18). WNT proteins consist of a single-chain polypeptide synthesized in the endoplasmic reticulum, and a hydrophobic palmitate group is then covalently attached near the N-terminus by the enzyme Porcupine (PORCN), a critical modification for transporting it to the cell

membrane and enable receptor binding. Wnt proteins are then secreted by multiple mechanisms, either by free diffusion, exosomes, or within lipoprotein assemblies (19).

The receptors that recognize WNT ligands belong to the Frizzled (FZD) family, seven-pass transmembrane α helices proteins that are included in the G-protein coupled receptor (GPCR) superfamily, with 10 members in humans and mice (18). In the absence of WNT ligands, the Wnt transcriptional co-activator β-catenin is sequestrated by a multimeric protein aggregate known as the destruction complex composed by the scaffolding protein AXIN, the tumour suppressor adenomatous polyposis coli (APC), the glycogen synthase kinase 3 (GSK-3) and the casein kinase 1 (CK1) (20,21). Phosphorylation of the N-terminal portion of β-catenin by CK1 and GSK3 primes β-catenin for ubiquitination and subsequent proteasomal degradation, preventing its nuclear translocation. In this scenario, a repressive complex containing DNA-bound T cell factor/lymphoid enhancer factor (TCF/LEF) and transducing-like enhancer protein (TLE/Groucho) recruits histone deacetylases (HDACs) to repress transcription of Wnt responsive genes (fig. 1.3) (20). On the contrary, the selective binding of different WNT members to their specific FZD receptors triggers distinct intracellular signalling pathways. For example, WNT1, WNT3A, WNT7B and WNT8 association with the respective FZD receptors activates the canonical β-catenin-dependent pathway (18). In the canonical Wnt pathway, when WNT ligands interact with FZD and the low-density lipoprotein receptor related protein (LRP)5 and 6 co-receptors at the cellular membrane, Dishevelled (DVL) is recruited. DVL induces LRPs phosphorylation, which promotes AXIN recruitment and β-catenin stabilization. Once stabilized, β-catenin translocates to the nucleus where it serves as a co-activator of TCF, leading to the transcription of Wnt responsive genes (21).

Once WNT proteins reach a target cell, a series of negative feedback mechanisms control Wnt signalling overactivation (22). These mechanisms include the blockage of receptors by the secreted inhibitor Dickkopf-1 (DKK1), the cleavage of WNT proteins acyl group by the hydrolase NOTUM at the responding cell, or the sequestration of secreted WNT proteins in the ECM by secreted Frizzled-related proteins (sFRPs) (22).

Other WNT proteins, such as WNT4, WNT5A and WNT11, bind to different FZD family members and the co-receptors ROR1, ROR2 and RYK that preferentially trigger the non-canonical Wnt pathways: the planar cell polarity (PCP) and the Ca^{2+}-dependent pathway (23,24). In the PCP pathway, activated DVL associates with the small GTPases

RAC1 and RHO inducing ROCK- and JNK-mediated actin cytoskeleton rearrangement important for cell polarity and cell migration. The Ca^{2+}-dependent pathway provokes phospholipase C-induced intracellular calcium fluxes, stimulating calcium-dependent kinases such as PKC, CAMKII, and calcineurin. These kinases trigger cytoskeletal reorganization namely through CDC42, and activate NFAT-mediated gene transcription, thus promoting cell motility and invasion (23,24).

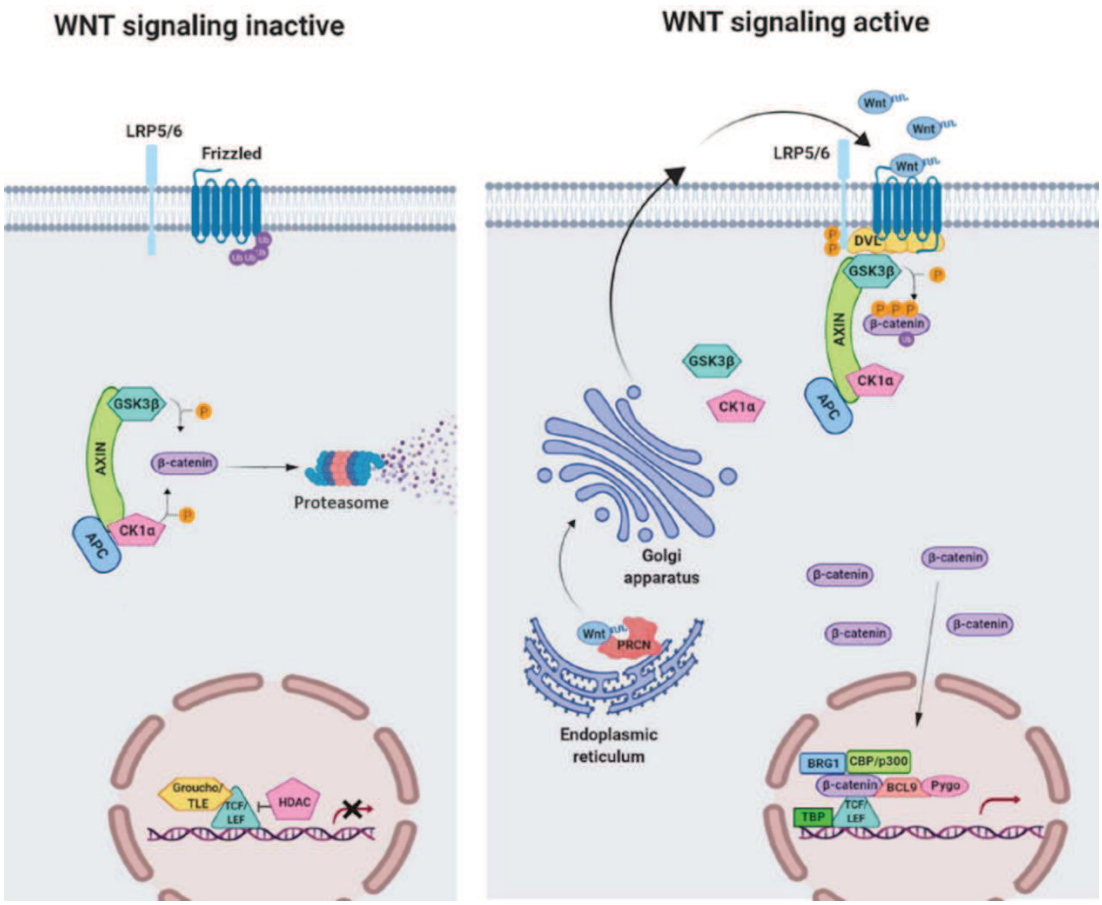

Figure 1.3. The canonical Wnt signalling pathway. In the absence of Wnt (left panel), β-catenin is sequestrated by the destruction complex which promotes its phosphorylation and subsequent ubiquitination. This turns β-catenin recognizable for proteasome-mediated degradation, thereby repressing gene transcription. In the presence of Wnt ligands (right panel), the interaction between FZD receptors and LRP5/6 co-receptors triggers the phosphorylation of DVL and the recruitment of the destruction complex. The disassembly of the destruction complex prevents β-catenin from being degraded allowing its translocation to the nucleus, where it promotes gene transcription with several other co-activators. Adapted from Martin-Orozco E. *et al.* (23).

In the intestine, WNT ligands are secreted by different populations of pericryptal stromal cells and by epithelial cells, namely Paneth cells. Paneth cell depletion alone does not impact intestinal homeostasis, which suggests a redundant role of WNT ligands from the stromal microenvironment (25–27). For instance, $FOXL1^+$ mesenchymal fibroblasts represent a major source of WNT ligands and its ablation suppresses ISC proliferation and disrupts the intestinal villus-crypt architecture (28). Wnt signalling is highly active at the bottom of crypts where cycling cells are located, and gradually loses its strength as cells move upwards to the differentiated villus (29). Wnt signalling disruption affects crypt cell proliferation leading to a loss of ISCs, whereas its aberrant activation potentiates rapid cell proliferation within the crypt eventually originating hyperplasia (30,31). Wnt signalling also imposes a gradient of EphB-Ephrin B that regulates the compartmentalization of intestinal epithelial cells. Wnt signals promote the expression of the membrane receptors EphB2 and EphB3 and thus cells exiting the crypt environment gradually lose receptor expression and start exhibiting Ephrin B ligand expression. EphB-Ephrin B complexes induce alterations in cell adhesion capacity and cell-ECM attachment, ultimately causing the migration of Ephrin B-expressing cells towards the villi, whereas EphB-expressing cells remain in the crypt (32). Another consequence of Wnt signalling is the expression of LGR4/5/6 in ISCs.

1.1.3.2. The LGR family

The LGR family belongs to the rhodopsin superfamily of GPCRs and is formed by 8 seven-pass transmembrane receptors. LGR 4-6 constitute a subgroup within the LGR family, which contains a large extracellular domain with 17 leucine-rich repeats, and are Wnt target genes that encode receptors for R-spondins, a family of cysteine-rich glycoproteins with two Furin domains (33,34). This family is present in all vertebrates and is formed by four secreted proteins in humans, R-spondin 1-4, all of them able to bind LGR 4-6 (35).

LGR5 allows ISCs to recognize R-spondin agonists and cancel out a mechanism of negative feedback mediated by two highly homologous membrane E3 ubiquitin-protein ligases ZNRF3 and RNF43 (fig. 1.4). These two ubiquitin ligases are also Wnt target genes and are specific to $LGR5^+$ intestinal crypt cells (33). In the absence of R-spondin, these ligases promote poly-ubiquitination of lysines in the cytoplasmic loops of

FZD in a DVL-dependent manner. Upon WNT binding the entire complex together with the Wnt ligand and the bound destruction complex suffers endocytosis and is degraded in lysosomes, therefore removing receptors from the cell surface and allowing β-catenin to be active only for a short period of time (33). On the contrary, upon R-spondin binding, LGR5 becomes linked to RNF43/ZNRF3 by the Furin domains of R-spondin, removing the ligases from the membrane through clathrin-mediated endocytosis. This enables the accumulation of FZD-LRP complexes on the cell surface and thus positively regulates the Wnt signalling and extends its duration (33).

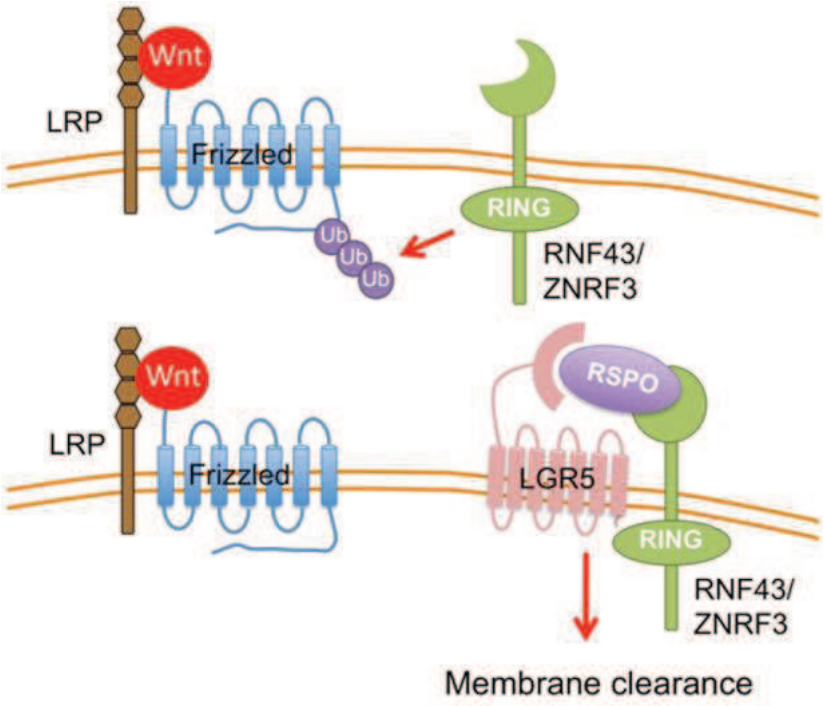

Figure 1.4. Regulation of FZD receptor availability at the cell surface by R-spondin. In the absence of R-spondin (top panel), the E3 ligases RNF43 and ZNRF3 ubiquitinate FZD inducing its internalization and degradation, limiting Wnt signalling. In the presence of R-spondin (bottom panel), the ligases form a complex with LGR receptors and are removed from the membrane, therefore amplifying Wnt signalling. From Yu J. *et al.* (21).

1.1.3.3. Notch and BMPs

Notch signalling is also important for ISC homeostasis and fate determination. Paneth cells express the membrane ligands DLL1 and DLL4 which further support the self-renewal ability and maintenance of the stem cell population that expresses the Notch receptor (36). Notch signalling plays a significant role in stem cell fate decision by specifying the differentiation of progenitor cells towards the secretory or the absorptive lineage (37). High levels of Notch drive absorptive lineage differentiation by promoting HES1 expression which silences ATOH1, the transcriptional factor that triggers secretory lineage specification (37).

The Wnt and Notch signalling are balanced by Bone Morphogenetic Protein (BMP) signals that negatively regulate the self-renewal and proliferation capacity of ISCs (38). BMPs belong to the TGF-β superfamily of ligands which stimulate the phosphorylation of cytoplasmatic R-SMADs for signal transduction. BMP ligands are expressed by intravillus and pericryptal mesenchymal cells, hence BMP signalling is primarily active in the villus compartment (31). The BMP signalling is involved in the terminal differentiation of intestinal lineages in the villi. Deletion of the BMP receptor in the mouse intestine impairs cell maturation and induces the uncontrolled expansion of the stem cell compartment, showing that BMP signals are critical to restrain Wnt signalling activity to crypts and preventing intestinal hyperplasia (31,39). Moreover, intestinal subepithelial myofibroblasts and smooth muscle cells in the submucosal crypt region express BMP antagonists, such as Noggin, Gremlin1/2 and Chordin-1, which repress BMP signalling at the crypt bottom (40).

The comprehension of these major signalling pathways mediating stem cell maintenance and fate determination in the intestinal epithelial allowed the establishment of *in vitro* three-dimensional structures from a single $LGR5^+$ cell. Intestinal organoids maintenance in culture is achieved with a mix of growth factors, such as Noggin, R-spondin 1, and EGF, which recapitulate the intestinal epithelium architecture and cellular composition without a mesenchymal niche (41).

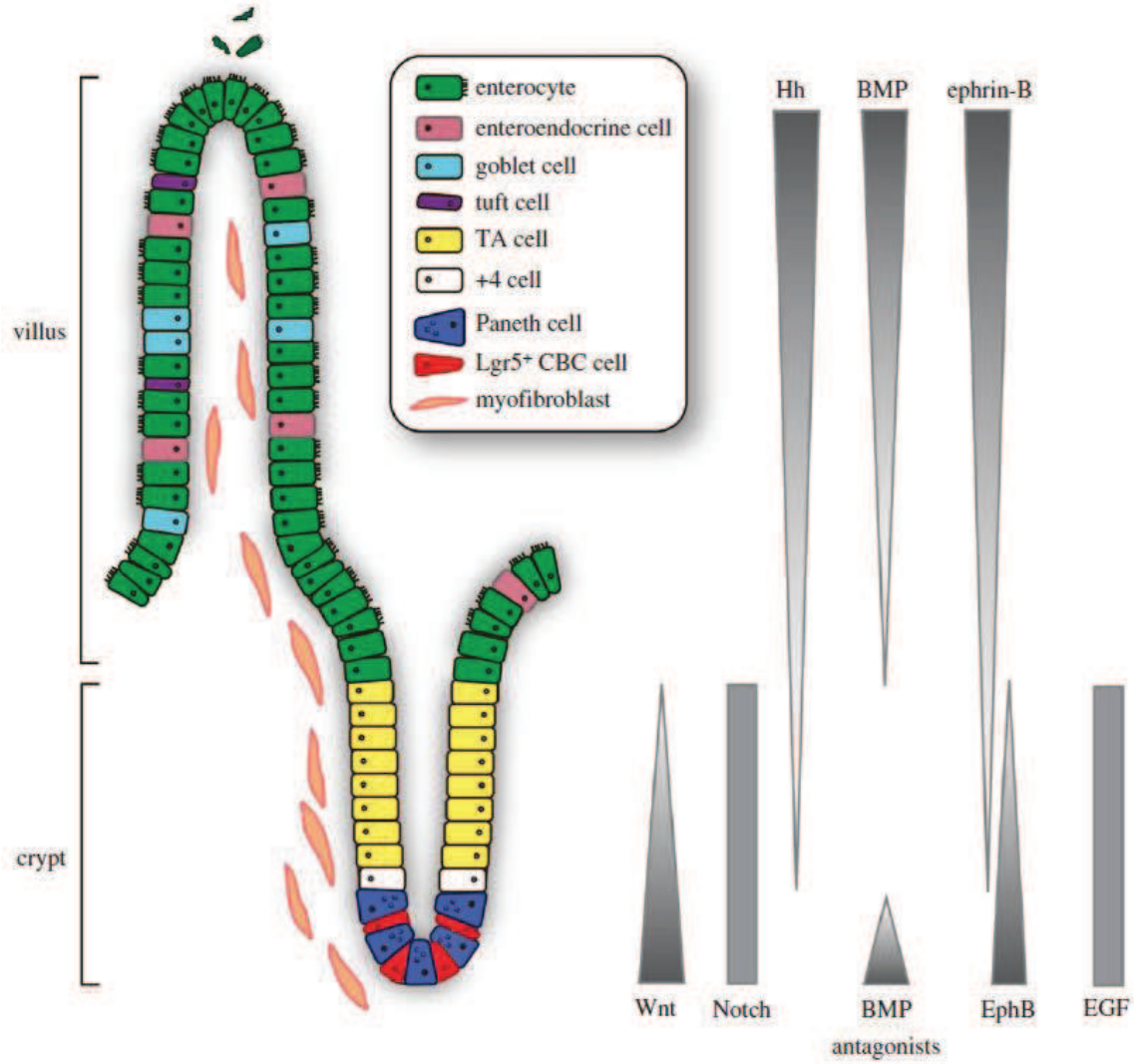

Figure 1.5. Signalling pathways controlling cell fate and intestinal epithelium homeostasis. TA: transit-amplifying. From Spit M. *et al.* (40).

1.2. Colorectal cancer

Colorectal cancer (CRC) is the third most common cancer and the second leading cause of cancer-related deaths in Portugal and worldwide, being responsible for around 940.000 deaths in 2020 (GLOBOCAN 2020, https://gco.iarc.fr/). Its incidence is higher in males and strongly correlated with age, dramatically increasing after 50 years, being the median age at diagnosis about 70 years. Most cases of CRC are sporadic and its risk factors are largely associated with the western lifestyle, being Europe, North America, Australia, and New Zealand the regions with higher incidence rates (fig. 1.6) (42). Countries with a very high human development index (HDI) account for over two-thirds of all CRC cases and had incidence rates (>40 per 100 000) six times greater than countries with a low HDI in 2012. On the contrary, comparisons of incidence-to-mortality showed higher case fatalities in countries with lower HDI, although almost 60% of all deaths occurred among countries with a high or very high HDI (43). The existence of previous colonic polyps, and environmental factors, such as a sedentary lifestyle with no exercise, obesity, high alcohol consumption, tobacco smoking, high consumption of red and processed meats, and a high-fat/low-fiber diet, have been established as contributing factors to CRC onset in several epidemiological studies (42,44). Other factors with increased risk for CRC might include inflammatory bowel disease (ulcerative colitis and Crohn's disease), diabetes mellitus, and infectious agents, such as *Fusobacterium spp* (42).

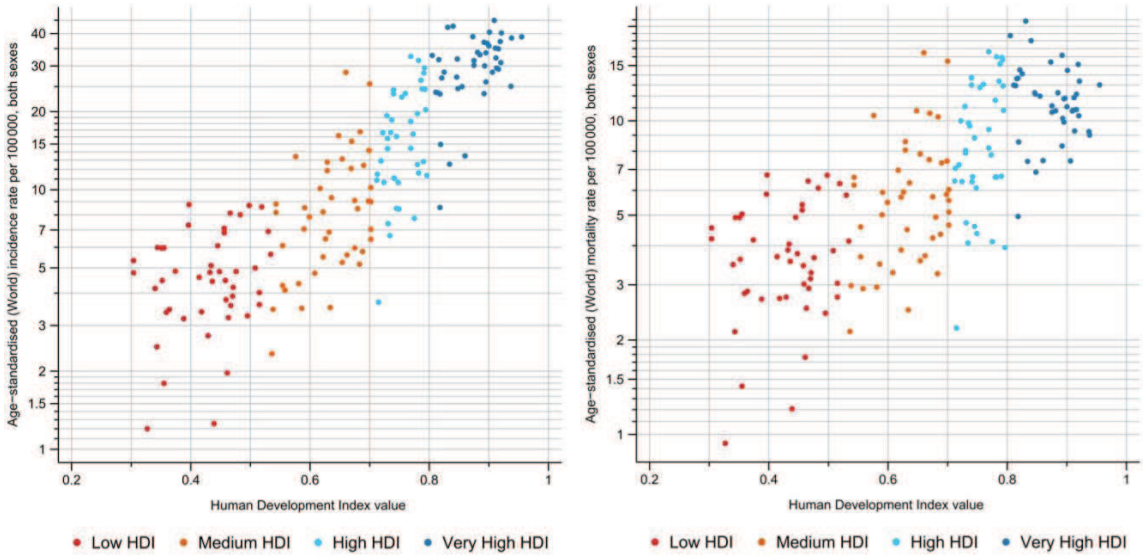

Figure 1.6. Relationship between age-standardised CRC incidence (left panel) and mortality (right panel) rates and HDI in both sexes combined. From GLOBOCAN 2012, Arnold M. *et al.* (43).

CRC patients can present a range of gastrointestinal symptoms, which may include blood in stool, alterations in bowel habits, and abdominal pain, in addition to others more broad, such as fatigue, anaemia, and weight loss (45). However, the disease is usually asymptomatic until it reaches an advanced stage. Hence, about 20% of CRC patients already present distant metastasis at the time of diagnosis, mainly in the liver (46). The gold standard for CRC diagnosis is rectosigmoidoscopy or total colonoscopy. This method, although invasive, is necessary to assess tumour location and allows biopsy sampling for histological characterization and molecular profiling (45). According to their histological staging and assessment of lymphatic, perineural and venous invasion, CRCs are classified through the local invasion depth (T stage), lymph node involvement (N stage), and presence of distant metastases (M stage) staging system (table 1.1) which dictates subsequent therapeutic management (46). The prognosis for CRC patients is largely determined by the stage at diagnosis, and the 5-year survival rate has been slowly improving during the last decade due to the successful implementation of screening programmes for early detection, especially in high-income countries (42,46). 5-year survival rate is 70-90% for stages I and II, 50-70% for stage III, and 10-14% for stage IV. The best treatment option remains surgical resection of the affected intestinal segment and surrounding lymph nodes for CRC confined to the intestinal wall, whereas adjuvant chemotherapy is recommended for more advanced stages (42).

Table 1.1. Classification of CRC according to the TNM staging system. Adapted from Brenner H. *et al.* (42).

Stage	Characteristics
Local invasion depth (T stage)	
Tx	No information about local tumour infiltration available
T0	No evidence of primary tumour
Tis	Carcinoma *in situ* : Tumour restricted to mucosa, no infiltration of lamina muscularis mucosae
T1	Infiltration through lamina muscularis mucosae into submucosa, no infiltration of lamina muscularis propria
T2	Infiltration into, but not beyond, lamina muscularis propria
T3	Infiltration into subserosa or non-peritonealised pericolic or perirectal tissue, or both
T4a	Infiltration of the serosa
T4b	Infiltration of neighbouring tissues or organs
Lymph node involvement (N stage)	
Nx	No information about lymph node involvement available
N0	No lymph node involvement
N1a	Cancer cells detectable in 1 regional lymph node
N1b	Cancer cells detectable in 2-3 regional lymph nodes
N1c	Tumour satellites in subserosa or pericolicor perirectal fat tissue, regional lymph nodes not involved
N2a	Cancer cells detectable in 4-6 regional lymph nodes
N2b	Cancer cells detectable in 7 or greater regional lymph nodes
Distant metastases (M stage)	
Mx	No information about distant metastases available
M0	No distant metastases detectable
M1a	Metastasis to 1 distant organ or distant lymph nodes
M1b	Metastasis to more than 1 distant organ or set of distant lymph nodes or peritoneal metastasis

1.2.1 The genetics of colorectal cancer

As most cancers, CRC evolves through a multistep process that can take up to 30 years until it becomes invasive and metastatic (46). In the case of CRC, it starts by localized lesions, termed polyps, that rise above the surrounding mucosa starting from an aberrant crypt. Polyps can be pathologically classified as nonneoplastic hamartoma, hyperplastic mucosal proliferation, or adenomatous (44). The vast majority of CRCs is originated from adenomatous polyps through the adenoma-carcinoma sequence model and can be grouped into molecular subtypes based on their genomic profile (47) (fig. 1.7).

Most sporadic cases (about 84%) present chromosomal instability (CIN) and are aneuploid as a result of chromosomal amplifications and translocation, and loss of heterozygosity (LOH) in several loci, including 5q, 8p, 17p, and 18p (44). These tumours are predominantly well differentiated, rarely mucinous and exhibit low peritumoral lymphocytic infiltration. Inactivating mutations on the tumour suppressor gene *APC* are often the initial event in CRC tumorigenesis and a common feature of 70-80% of colorectal adenomas leading to increased Wnt signalling (42). Further growth is promoted by activating mutations in the *KRAS* oncogene and inactivation of *TP53* (48). A small fraction of tumours presenting CIN (<1%) occur in the form of familial adenomatous polyposis coli (FAP), a hereditary cancer syndrome with an estimated allele frequency of 1:10000 and characterized by germinal mutations in the *APC* gene (42).

However, approximately 12% of sporadic CRC cases follow a distinct molecular pathway. These tumours arise from sessile premalignant lesions in the proximal colon called serrated precursor lesions, and exhibit high-frequency microsatellite instability (MSI) as opposed to CIN-containing tumours, although some overlap is possible depending on the genes dysregulated (44). Microsatellites are short tandemly repeated nucleotide sequences (1 to 4 nucleotides) throughout the genome. Epigenetic gene silencing or inactivating mutations in mismatch repair (MMR) genes, such as *MLH1*, *MSH2*, *MSH6*, and *PMS2*, compromise the ability of detecting and correcting errors during DNA replication, which leads to insertions and deletions in microsatellites altering their length (49). Moreover, MMR gene deficiency contributes for hypermutated genomes through missense and frameshift mutations, namely in apoptotic genes and growth factors (49). These tumours are often characterized by poor differentiation, mucinous histology and increased peritumoral lymphocytic infiltration (44). In MSI-high

sporadic cases, the MMR silencing is accomplished by hypermethylation of CpG islands (CIMP) in the promoter region of *MLH1*, and additional activating mutations in *KRAS* and *BRAF* are also common (46). The remaining 3% of CRC cases are caused by hereditary non-polyposis colon cancer (HNPCC) or Lynch syndrome, which is characterized by germline mutations in MMR genes that give an 80% risk of developing CRC before the age of 50. Lynch syndrome is an autosomal dominant disorder with an estimated allele frequency of 1:1700 to 1:350 and leads to tumours with elevated levels of MSI (42).

The progressive accumulation of genetic mutations and epigenetic alterations accentuates the loss of tumour suppressor genes and activation of oncogene, and thus greatly contributes to malignant transformation of cancer cells (45,48). Somatic mutations that confer a selective advantage over the remaining cells are termed driver mutations and are responsible for triggering tumour initiation and progression (48). Noteworthy, each driver mutation is associated to the progression of tumour to specific steps of the tumorigenic model and cancer cell clone harbouring this mutation is then selected by clonal expansion. For example, *APC* mutations are typically implicated in tumour initiation, whereas *KRAS* mutations contribute to adenoma development but are not required for its initiation (48). Other genetic defects, such as loss of *TGFβIIR* or *TP53*, are important do drive the transition of adenomas to carcinomas and possibly the acquisition of invasive properties. P53 is a transcriptional factor essential for cellular response upon DNA damage by promoting the expression of cell cycle inhibitors and proapoptotic proteins, hence stimulating G1/S- or G2/M checkpoint-mediated cell cycle arrest and programmed cell death (or apoptosis) (50). For metastatic disease development, a larger cellular reprogramming must happen to change their phenotype from epithelial-like to mesenchymal-like features (EMT). This grants cells with invasion capacity enabling cancer cell dissemination through blood vessels and the colonization of other organs (51).

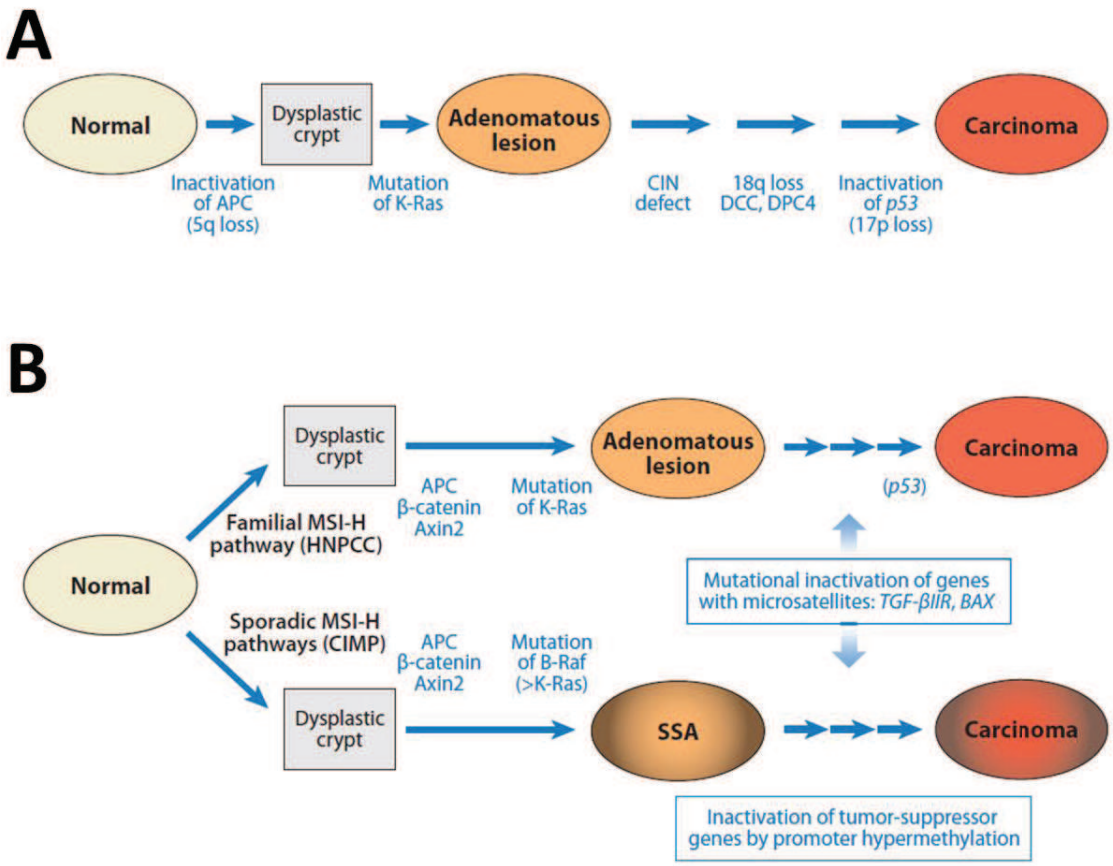

Figure 1.7. Genetic model of CRC. (A) Most sporadic CRC cases arise from adenomatous polyps that accumulate genetic mutations that activate oncogenes and inactivate tumour suppressor genes through a multistep process that takes years or decades to form a carcinoma and became invasive. **(B)** Tumours carrying defects in MMR genes present MSI. In the HNPCC syndrome, there is a genetic predisposing for CRC from germline mutations in MMR genes, while in sporadic cases the *MLH1* promoter region is commonly hypermethylate the and originates serrated adenomas. In both MSI-high tumours, inactivation of TGFβIIR and BAX, whose coding sequences contain microsatellites, contribute for further tumour progression. From Fearon E. *et al.* (48).

1.2.2. Stem cells in colorectal cancer

The intestinal epithelium is the fastest self-renewing tissue in mammals as a result of the high rate of cell death, with around 10^{11} epithelial cells being lost every day in humans (2). The constant replacement of cells is ensured by the small population of $LGR5^{+}$ cells at the base of the crypts. It is not surprising that this remarkable ability, together with the exposure to the harsh luminal environment, turns ISCs quite susceptible to accumulate mutations and originate cancers (2). In fact, the lifetime risk of developing cancer in a given tissue has been directly correlated to the total number of stem cell divisions in that tissue during the average lifetime of a human (52). The cancer stem cell

(CSC) theory emerged as a comprehensive explanation to cancer clonal expansion and progression based on the endogenous stem cell-driven tissue homeostasis. CSCs are defined as a small population of cancer cells with stem-like properties, such as self-renewing capacity, alongside with abnormal characteristics, such as uncontrolled proliferation, which are responsible for generating more cancer cells and thus tumour heterogeneity (53). Therefore, CSCs fuel tumour growth and maintenance, but they are slow-cycling when compared to other cancer cell populations, which render them resistant to most of the common therapeutic drugs, hence leading to tumour recurrence (54,55).

The first evidence that CRC contained CSCs came from the isolation of a putative population of tumorigenic and undifferentiated cells with a surface marker profile, including expression of CD133, CD44, EpCAM and CD116, which are broadly expressed and not specific to the CSC population (56–58). Xenotransplantation and lineage tracing experiments in mouse tumour models showed that the adenomatous clonogenic core could be traced back to a cell population marked by LGR5 expression, with a similar gene signature to the normal $LGR5^+$ cells. The clonogenic capacity of these cells is essential to sustain the growth of intestinal adenomas by generating not only additional $LGR5^+$ cells but also all the other differentiated cells in the tumour (59,60). Furthermore, Wnt signalling activation through *APC* loss, an early event in most CRCs, is extremely efficient in inducing neoplasia formation from stem cells but not TA cells, reinforcing the notion that crypt $LGR5^+$ cells are the cell-of-origin of CRCs (61). Likewise, in humans, the analysis of the expression patterns of 19 ISC markers in colorectal adenocarcinomas revealed that 74-85% of CRC cases might arise from $LGR5^+/ASCL2^+$ crypt stem cells (62).

Importantly, $LGR5^+$ cells carrying oncogenic mutations crucial for cancer development, such as in *KRAS*, have an increased cell division rate that enables them to outcompete other nonmutant $LGR5^+$ cells and colonize the crypts. This potentiates the clonal expansion of these mutant crypts via crypt fission predisposing the tissue for further mutations and tumour growth (63). Furthermore, a LGR5+ cell-specific gene signature has been proved to correlate with tumour-initiating capacity as well as long-term self-renewal potential having predictive value for disease relapse (64).

The epigenetic down-regulation of regulators of the Wnt signalling negative feedback loop have been showed to potentiate early CRC development or its progression

to advance stages of tumorigenesis through further activation of the Wnt signalling. Interestingly, chromosome translocations involving the R-spondin 2 and 3 generate higher levels of functional proteins and were found in a subset of colon tumours that express the receptors LGR (65). Furthermore, R-spondin fusions-containing tumours did not carried *APC* and *CTNNB1* mutations, but had mutations in the RAS pathway, suggesting that R-spondin gene fusions induce the Wnt signalling and may promote colon tumorigenesis similarly to *APC* mutations, reinforcing the importance of this pathway for CRC development (65).

Recent studies support a more dynamic model in which all tumour cells can originate CSCs under the right microenvironment-derived signals. Wnt signalling activity appears to play a major role in the reprogramming of differentiated cells, being directly associated to the tumorigenic potential of colon CSCs (66). As mentioned above, intestinal epithelial cells are endowed with plasticity that enables their dedifferentiation to regain stem-like features, and such plasticity is also capable of giving rise to tumour-initiating cells in CRCs (67,68). It has been demonstrated that the depletion of $LGR5^+$ cells impairs primary tumour growth and cell dissemination in the mouse, which is then followed by $LGR5^+$ CSC pool restoration at the expense of differentiated $LGR5^-$ cancer cells (69,70). Remarkably, human tumour xenografts revealed that $LGR5^-$ cells are the main constituent of circulating CRC cells and are capable of establishing distant metastasis in which $LGR5^+$ cells re-emerged to sustain long-term metastasis growth (71). Furthermore, higher levels of LGR5 expression were associated with a poor clinical outcome in CRC patients and its expression correlated with chemoresistance to 5-Fluoracil and oxaliplatin treatments due to overexpression of the extrusion pump ABCB1 (72). The plasticity capacity of cancer cells is an additional pitfall for anti-cancer therapies, suggesting that future therapeutics should not only target CSCs and/or the microenvironmental niche but also the mechanisms underlying endogenous cellular plasticity (71).

1.3. Post-transcriptional regulation: RNA-binding proteins

It is now evident that post-transcriptional control plays a key role in gene expression regulation and cell plasticity. The large majority of eukaryotic mRNAs are subject to multiple regulatory processes during their life-span (73). Essentially every step of mRNA metabolism, from stability and location to translation and degradation, is regulated by functional units termed ribonucleoprotein complexes (RNP) formed by the mRNA, small non-coding RNAs, such as miRNAs, and RNA-binding proteins (RBPs) (73).

RBPs strictly support mRNAs throughout their life cycle, starting from transcription where they are essential for splicing and polyadenylation. After nuclear exportation, RBPs determinate the subcellular location by coupling them with cytoskeleton-associated motor proteins, which dictate the fate of cytoplasmatic mRNAs (74). mRNAs can either be translated through the translation initiation complex, or repressed by the assembly of translation repression factors (fig 1.8) (75). In the latter, mRNAs are then aggregated and stored in larger subcellular compartments of untranslated mRNAs called Processing Bodies or P-bodies, formed by decapping enzymes, exonucleases, translation repressors, RNA helicases, and miRNAs. mRNAs complexed at P-bodies can either be degraded or re-enter translation, for example through the formation of stress granules (75,76). Stress granules are cytoplasmatic RNP granules for mRNAs stalled in translation initiation complexed with translation initiation factors and 40S ribosomal subunits. mRNA aggregation into stress granules occurs in response to different stress stimuli through the phosphorylation of eIF2. This induces the local concentration of the translation machinery to overcome limiting conditions for translation initiation (76). The mRNA translational status is the result of the constant competition between the assembly of the translation or the repression/decay machinery, in which RBPs associated to a mRNA can play a determinant role by interacting with these complexes (75).

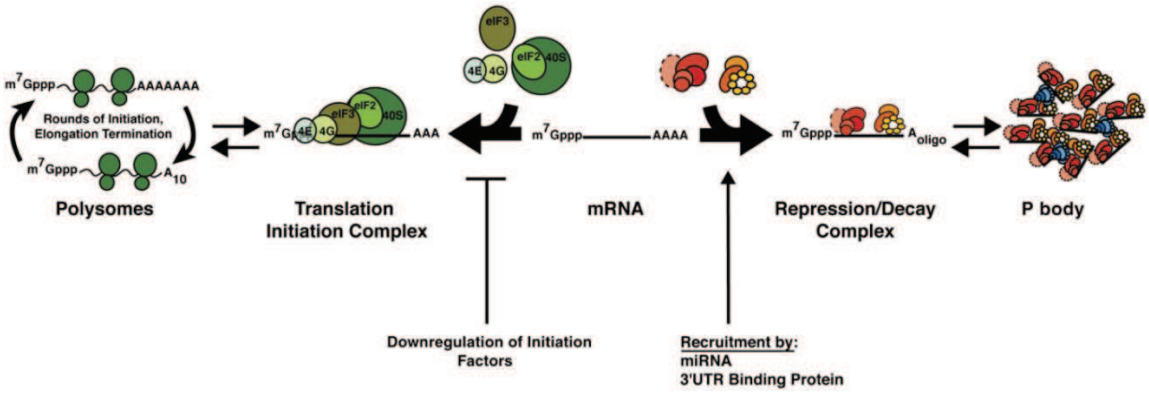

Figure 1.8. Fate of cytoplasmatic mRNAs. mRNA translational status is regulated by the assembly of the translation initiation complex and the translation repressor complex, in which RBPs play a major role. Adapted from Parker R. *et al.* (75).

Recently, a large-scale study analysed computational and experimental proteomic data and identified a total of 2961 human RBPs representing around 14,4% of all protein-coding genes in humans, many of them evolutionary conserved across eukaryotic species (77,78). This highlights the importance of RBPs role in the expression of many other proteins and their potential impact on diseases when dysregulated. It has been suggested that protein abundance is predominantly controlled at the translational level by post-transcriptional mechanisms, for instance through mRNA stability and half-life (79,80). Moreover, RBPs are dynamic and subjected to many levels of regulation themselves, including genomic alterations, transcriptional and post-transcriptional control, and post-translational modifications (PTMs) (81).

RBPs act in a RNA-specific manner by binding to secondary structures, such as IRES, and/or sequence-specific motifs through well-defined recognition modules called RNA-binding domains (RBDs). RBPs may contain a wide variety of RBDs, each one with different specificities and affinities, which allows them to interact with a large array of target mRNAs, mostly, but not exclusively, in the 3'- UTR so that the translation machinery is not disturbed. Some RBPs are highly specific and only regulate a restricted number of target RNAs, while others have a broader number of targets binding to over a thousand RNAs, probably coordinating the expression of mRNAs encoding proteins with related cellular functions (82). The most common RBDs include the RRM and dsRBD domains, which recognize single-stranded and double-stranded RNAs, respectively, and the KH domain, which binds to specific nucleotide sequences. However, almost 40% of the human RBPs identified are non-canonical, meaning that they do not contain any

known RBD for their RNA-interacting ability. This is mainly accomplished through structures termed intrinsically disordered regions (IDRs) that exhibit elevated conformational flexibility enabling their adaptation to the binding partners (81).

1.3.1. RNA-binding proteins dysregulation in cancer

The RNP granules are increasingly associated with cancer initiation and progression by modulating cellular responses to stresses from the tumour microenvironment (83). External stresses, such as hypoxia, inflammation, nutrient starvation, oxidative stress, and often chemotherapeutics, enhance P-body and stress granules formation to regulate a rapid cellular adaptation. This response is largely orchestrated by RBPs with signalling properties that transduce the incoming stress into a functional response (83).

It is thus becoming clear that cancer cells are able to exploit the RBPs machinery to their advantage to selectively regulate mRNA translation, enabling them to adapt to stress and support malignant transformation. The number of RBPs implicated in carcinogenesis is continuously growing and its dysregulation associated to numerous cancer types. RBP disruption can lead to a large-scale rewiring of downstream networks and facilitate tumour-specific reprogramming of gene expression (84,85). Altered expression or aberrant activity of a single RBP might impact multiple targets, including oncoproteins and tumour-suppressor proteins (81). In CRC, post-transcriptional alterations and RBPs dysfunction have major repercussions in cancer cell function playing a key role in every hallmark of cancer, as shown in table 1.2. Furthermore, it has been reported that RBPs are involved in intestinal epithelium homeostasis and the establishment and maintenance, or the differentiation of stem cells in response to several stimuli (86,87).

However, the underlying mechanisms and the functionally relevant oncogenic targets are yet to be established. The identification of functionally relevant RBPs in CRC could pave the path for new prognostic biomarkers and cancer therapies considering their influence in the regulation of multiple genes related to many cancer features (81). Indeed, new therapies targeted to RBPs, for instance HuR, hnRNPA1, IGFBP3 and SAM68, are starting to emerge and under evaluation (88,89).

Table 1.2. Summary of CRC-related RBPs. Adapted from Pereira B. *et al.* (81).

RBP	Molecular mechanism	Cellular phenotype	Carcinogenic potential	Refs.
ESRP1/2	Alternative splicing; mRNA translation	EMT, migration, invasion and metastasis; sustaining proliferation	Proto-oncogenic	(90–92)
	Alternative splicing	EMT, migration, invasion and metastasis; sustaining proliferation	Tumour-suppressing	
	mRNA translation	Sustaining proliferation	Tumour-suppressing	
hnRNPD (AUF1)	mRNA stability; mRNA translation	EMT, migration, and invasion; evading apoptosis; replicative immortality; sustaining proliferation;	Proto-oncogenic	(93)
HuR	mRNA stability; mRNA translation	Angiogenesis; avoiding immune surveillance; evading apoptosis; invasion and metastasis; sustaining proliferation	Proto-oncogenic	(94)
IMP1	mRNA localization; mRNA stability; mRNA translation	EMT, migration, invasion and metastasis; sustaining proliferation	Proto-oncogenic	(95)
IMP3	mRNA stability; mRNA translation	Evading apoptosis, migration; sustaining proliferation	Proto-oncogenic	(96)
LARP1	mRNA stability, mRNA translation	Evading apoptosis; Migration and invasion; sustaining proliferation	Proto-oncogenic	(97)
LIN28A/B	miRNA processing	EMT, invasion, migration and metastasis; sustained proliferation;	Proto-oncogenic	(98,99)
MSI1/2	mRNA translation	Evading apoptosis; EMT; sustained proliferation	Proto-oncogenic	(100)
QKI	Alternative splicing	Sustained proliferation	Tumour-suppressing	(101)
SRSF1	Alternative splicing	EMT and migration; evading apoptosis; sustaining proliferation	Proto-oncogenic	(102)

An example of an RBP with a putative relevant role in CRC is MEX3A. MEX3A is the vertebrate orthologue of the nematode *Caenorhabditis elegans* MEX-3 protein, a translational regulator involved in germline totipotency (103). In mice, *Mex3a* mRNA was found to belong to the $LGR5^+$ stem cell gene signature and its expression labels a subpopulation of $LGR5^+$ cells around the crypt +3/+4 cell position. These cells are slow-cycling and resistant to chemotherapy- and irradiation-induced damage (104). Importantly, it was observed that *Mex3a* deletion impairs epithelial turnover through a dramatic decrease in the LGR5+ ISC pool (105). Furthermore, MEX3A overexpression in human CRC cell lines potentiates cell proliferation, impacts their metabolism, and impairs intestinal differentiation, while correlated to increased expression of ISC markers (106).

Chapter 2 - Objectives

CRC remains one of the leading causes of cancer-related deaths despite the extensively characterization of the driver mutations and molecular mechanisms underlying its development and progression. This is mainly due to the lack of predictive biomarkers in early disease and effective therapeutic agents. RBPs have been implicated in many carcinogenic processes and represent potentially interesting targets to accomplish a broader effect in fundamental cancer players. Taking this into account, the main objective of this work is to identify new potential stemness-related RBPs and further evaluate if they have functionally-relevant role in CRC cell lines. We also aimed to assess their expression profile and a putative association with clinicopathological features in human CRC cases.

Chapter 3 – Materials and Methods

3.1. Bioinformatic analysis

The selection of potential RBPs was achieved through the RNA-sequencing data of CRC patients from TCGA database (https://portal.gdc.cancer.gov) and the known RBPs deposited in the EuRBPDB database (http://eurbpdb.syshospital.org). The GEPIA web server was used to compare the mRNA expression profile of each individual candidate in cohorts of colon and rectal cancer cases to the expression level in normal tissue counterparts available from the TCGA and GTEx databases (https://gtexportal.org/home/).

3.2. Cell culture and treatments

The human colorectal carcinoma cell lines Caco-2, DLD-1, HCT116, Ls174T and SW480 (ATCC, American Type Culture Collection) (table 3.1) were cultured under standard conditions in Dulbecco's Modified Eagle's Medium supplemented with 10% (v/v) fetal bovine serum (FBS) and maintained at 37ºC and 5% CO_2. The culture medium was renewed every 2 or 3 days and cells were subcultured before reaching confluency. To determine cell concentration, cells were mixed with Trypan Blue and counted under a Neubauer chamber. For the characterization of RBPs expression in cell lines, $2x10^5$ cells were seeded per well in 6-well plates for DLD-1, HCT116 and SW480; $5x10^5$ for Ls174T; and $1x10^5$ and $7{,}5x10^5$ for Caco-2 (pre and post-confluence conditions, respectively). Cells were maintained in culture for 72h and then collected. For CHIR99021 and IWP-2 treatments, $2x10^5$ DLD-1, HCT116 and SW480 cells were seeded on 6-well plates. At 24h, they were treated with 3µM CHIR99021, 2µM IWP-2 or vehicle-treated with DMSO, and were harvested 48h after the treatment. All collected cells were washed twice with filtered PBS.

Table 3.1. CRC cell lines and their characteristics. Dukes classification: Dukes' type A- limited to muscularis propria; Dukes' type B- extending beyond muscularis propria; Dukes' type C- nodes involvement; Dukes' type D- distant metastasis. Adapted from ATCC.

		Caco-2	DLD-1	HCT116	Ls174T	SW480
Organism		*Homo sapiens*	*Homo sapiens*	*Homo sapiens*	*Homo sapiens*	*Homo sapiens*
Tissue		Colon	Colon	Colon	Colon	Colon
Cell type		Epithelial cells	Epithelial cells	Epithelial cells	Epithelial cells	Epithelial cells
Morphology		Epithelial-like	Epithelial	Epithelial	Epithelial	Epithelial
Culture properties		Adhrent	Adhrent	Adhrent	Adhrent	Adhrent
Disease		Colorectal adenocarcinoma	Dukes' type C Colorectal adenocarcinoma	Colorectal adenocarcinoma	Dukes' type B Colorectal adenocarcinoma	Dukes' type B Colorectal adenocarcinoma
Mutational profile	Mutations		RAS P53	RAS		RAS P53
	Upregulated		MYC MYB RAS FOS SIS P53		C-MYC N-MYC MYB H-RAS N-RAS FOS P53	C-MYC MYB K-RAS H-RAS N-RAS FOS SIS P53
	Downregulated		ABL ROS SRC		SIS ABL ROS SRC	ABL ROS SRC

3.3. siRNA transfection

For the TIMELESS knockdown experiments, HCT116 and SW480 cells were plated on 6-well plates and allowed to grow for 24h, after which they were washed with PBS and transiently transfected with an esiRNAs (pmol) (EHU053831, Merck) to Lipofectamine 2000 reagent (µL) ratio of 20:1 in Opti-MEM medium. At 24h, the culture medium was changed for regular medium and, in the case of apoptosis analysis, exposed to 5-FU or DMSO, and cells were harvested after 24h.

3.4. Protein extraction and quantification

Cells were lysed for 30min on ice with a RIPA lysis buffer (20mM Tris-HCl pH 7,5; 150mM NaCl; 2mM EDTA pH 7,5; 1% (v/v) SDS; and 0,1% (v/v) sodium deoxycholate) supplemented with 1x Complete protease inhibitor cocktail (Roche Applied Science), 1mM PMSF, 20mM NaF and 1mM Na_3VO_4 (all three Sigma-Aldrich). Lysates were centrifuged at 17000xg for 15min at 4ºC and the supernatant recovered. Protein concentration was calculated using the BCA Portein Assay Reagent (Thermo Fisher Scientific). Briefly, 5µL of each protein extract was diluted 10x and placed on 96-well plates in duplicates along with BSA standard solutions. Reagent B was diluted 1:50 in Reagent A and 195µL of this solution was added to each well. The plate was incubated at 37ºC for 30min, after which the absorbance at 560nm was readily measured on SynergyMX Multimode Microplate Reader (BioTek). Protein concentration was determined using the standard curve method.

3.5. SDS-PAGE and western blotting analysis

Samples for SDS-PAGE were prepared by mixing 20-50µg of protein extract with 1:4 of a loading buffer containing 4x Laemmli buffer (250 mM Tris-HCl pH 6,8; 8% SDS; 40% glycerol), 5% (v/v) 2-mercaptoethanol and 5% (v/v) bromophenol blue. Samples were denaturated at 95ºC for 5min and were run on 1mm 8% SDS-PAGE with a molecular marker (Precision Plus Protein Dual Color Standards, Bio-Rad) in Tris-Glycine-SDS running buffer (Bio-Rad) at 130V. For gradient gels, NuPAGE 3-8% Tris-Acetate gradient gels were purchased at Thermo Fisher Scientific and samples run was

performed in NuPAGE Tris-Acetate SDS running buffer (Thermo Fisher Scientific). Proteins were transferred to a nitrocellulose membrane (GE Healthcare Life Sciences) in Tris-Glycine transfer buffer (Bio-Rad) with 20% (v/v) methanol for 2h at 60V on ice and with a magnetic stirring bar.

After visual confirmation of successful transfer with Ponceau S solution (Sigma-Aldrich), membranes were blocked for unspecific antibody binding with 5% (w/v) BSA in 0,1% TBS-T [1x TBS with 0,1% (v/v) Tween-20 (Sigma-Aldrich)) for 30min with agitation. Membranes were then incubated with appropriate primary antibody (table 3.2) diluted in blocking solution or 5% (w/v) milk (Molico) in 0,1% TBS-T according to the manufacturer at 4ºC with agitation overnight. Afterwards, membranes were washed three times in 0,1% TBS-T for 10min each, incubated with the secondary antibody (table 3.3) diluted in 5% (w/v) milk in 0,1% TBS-T for 1h at RT with agitation, and washed three times in 0,1% TBS-T for 10min each. Protein signals were revealed using ECL Western Blotting Detection Reagents (GE Healthcare Life Sciences) for 5min at RT. β-actin or GAPDH levels were used to normalize protein expression, and quantification was performed using the Fiji 1.46n version software (https://imagej.net/software/fiji/).

Table 3.2. List of primary antibodies used.

Antigen	Description	Manufacturer	Commercial reference	Dilution		
				WB	IHC	IF
ASPM	Rabbit polyclonal	Invitrogen	PA5-99790	1:1000	1:200	1:100
TIMELESS	Rabbit monoclonal (JE51-39)	Invitrogen	MA5-34880		1:50	1:50
TIMELESS	Mouse monoclonal	Santa Cruz Biotechnology	sc-393122	1:500		
ZBTB16	Rabbit polyclonal	Invitrogen	PA5-81949		1:200	1:50
ZBTB16	Mouse monoclonal	Santa Cruz Biotechnology	sc-28319	1:500		
EDC4	Rabbit polyclonal	Cell Signalling Technology	2548		1:400	
MEX3A	Rabbit polyclonal	Sigma-Aldrich	PRS4869	1:2000		
β-actin	Mouse monoclonal	Santa Cruz Biotechnology	sc-47778	1:3000		
GAPDH	Mouse monoclonal	Santa Cruz Biotechnology	sc-47724	1:6000		

Table 3.3. List of secondary antibodies used.

Secondary	Description	Manufacturer	Commercial reference	Application	Dilution
Goat anti-mouse IgG	HRP-conjugated	Santa Cruz Biotechnology	sc-2005	WB	1:3000
Goat anti-rabbit IgG	HRP-conjugated	Cell Signalling Technology	7074	WB	1:10000
Goat anti-rabbit IgG	AlexaFluor 488 conjugated	Invitrogen	A-11032	IF	1:100

3.6. Immunohistochemistry staining

Tissue samples from 192 patients treated at the Centro Hospitalar Universitário de São João were processed at the Histology and Electron Microscopy service at i3S. Formalin-fixed paraffin embedded (FFPE) tissue sections in the form of tissue microarrays (TMA) were deparaffinized in two xylene solutions for 10min each and rehydrated in a sequence of 100% ethanol, 100% ethanol, 70% ethanol and in continuous renovation of tap water for 5min each. For heat-induced epitope retrieval, slides were placed in 10mM citrate buffer (pH=6) in a steamer set for 40min followed by 20min at RT. Slides were washed three times in 0,05% TBS-T [1x TBS with 0,05% (v/v) Tween-20] for 2min each and inhibition of endogenous peroxidase activity was achieved with 3% hydrogen peroxidase in an aqueous solution for 10min followed by three washes in 0,05% TBS-T for 2min each. Unspecific antibody binding was blocked with a solution of 1:5 normal goat serum in an antibody diluent solution (Thermo Fisher Scientific) for 30min at RT in a humidified chamber and slides were incubated with the appropriate primary antibody (table 3.2) diluted in antibody diluent solution overnight at 4ºC in a humidified chamber. Afterwards, slides were washed twice in 0,05% TBS-T for 5min each, incubated with an amplifying polymer HRP-conjugated system (REAL EnVision, Dako) for 30min in a humidified chamber, and washed twice in 0,05% TBS-T for 5min each. For signal detection 3-3'-diaminobenzidine (DAB) chromogen (Dako) was prepared according to the manufacturer and applied for 1min, after which slides were rinsed with distilled water and washed in continuous renovation of tap water for 5min. Counterstaining was achieved with haematoxylin for 45s and then slides were washed in continuous renovation of tap water for 5min. Slides were dehydrated in a sequence of 70% ethanol, 100% ethanol, 100% ethanol and diaphanization was performed in two xylene solutions for 10min each. Bio MountHM (Bio-Optica) mounting medium was used to mount slides.

All the tissues were evaluated in a semi-quantitative fashion according to their signal intensity and the percentage of positive cells, and classified as negative, weak, intermediate and strong. The expression level of each protein was categorized as low or high: negative and weak cases were considered low-expressing CRC cases, whereas intermediate and strong cases were considered high-expressing CRC cases.

3.7. Immunofluorescence

For immunofluorescence cell staining, 22mm autoclaved coverslips were placed at cell plating. Coverslips were washed twice in PBS and fixation/permeabilization was performed with -20ºC methanol on ice for 10min. Cells were rehydrated by three steps with PBS for 5min each, and then blocked with a solution of 1:5 normal goat serum in antibody diluent solution for 30min. Incubation with appropriate primary antibody (table 3.2) diluted in antibody diluent solution was performed overnight at 4ºC in a humidified chamber. Afterwards, coverslips were washed three times in PBS for 5min each, incubated with appropriate AlexaFluor-conjugated secondary antibody (table 3.3) diluted in antibody diluent solution for 45min at RT, and washed three times in PBS for 5min each. Nuclear counterstaininh was achieved with 10µg/µL 4'-6'-Diamidino-2-Phenylindole (DAPI) diluted 1:100 in PBS for 5min and then coverslips were washed three times in PBS for 5min each. Coverslips were mounted with VECTASHIELD® Mounting Medium for Fluorescence with DAPI (Vector Laboratories).

For fluorescence analysis, coverslips were visualized in a Zeiss Axio Imager Z1 microscope and images were acquired with a 40x objective. In case of EDC4 immunostaining, a Z stack was acquired and the images aligned into one 2D image. Approximately 100 cells per coverslip were analysed for fluorescence intensity, number of puncta per cell and puncta area with the Fiji software.

3.8. IC50 determination

For determination of the half maximal inhibitory concentration (IC50) at 24h, 15000 HCT116 and SW480 cells were seeded in 96-well plates and allowed to grow for 48h, after which they were treated with the following concentrations of 5-FU diluted in the culture medium: vehicle-treated with DMSO; 1; 2,5; 5; 10; 25; 50; 100; and 250µM. Cells were exposed for each concentration in triplicates. After 24h, cells were incubated with 10% (v/v) PrestoBlue Cell Viability Reagent (Invitrogen) in DMEM supplemented with 5% (v/v) FBS at 37ºC for 45min. Then, the absorbance at 570nm and 600nm was read and the percentage of viable cells calculated to determine the IC50.

3.9. *In vitro* wound healing assay

Sterile 2-well silicone insert with a defined cell-free gap (ibidi) were used for migration capacity assessment. 15000 HCT116 and SW480 cells were seeded in each well and allowed to grow in standard culture medium for 24h, after which they were transfected with si*TIMELESS* or si*GFP*. After 24h, the culture medium was changed for regular medium. The inserts were removed and non-adherent cells were carefully washed with PBS. DMEM supplemented with 5% (v/v) FBS was added to the adherent cells to minimize cell proliferation interference and cell migration was assessed with a Leica DMI6000 FFW microscope during 24h at 37ºC and 5% CO_2, after which cells were tripsinized for molecular analysis confirmation.

For the HCT116 cell line, phase contrast was used and the settings were 15ms of light exposure and a pixel intensity of 20. For the SW480 cell line, brightfield was used and the setting were 2ms of light exposure and a pixel intensity of 9. Image acquisition occurred every 30min with a 10x objective. Cell migration potential was defined as the percentage of wound area covered and determined with the Fiji software.

3.10. Flow cytometry analysis

The HCT116 and SW480 cell lines were assayed for the percentage of cells in each cycle phase after siRNA transfection. Cells were fixed with 70% (v/v) ethanol at -20ºC added dropwise during vortex to avoid the formation of cell aggregates and cells were incubated on ice for 30min with agitation. The ethanol was carefully discarded and cells washed twice with PBS. Cells were then resuspended in Cell Staining Buffer (BioLegend) and incubated, in the dark, with 5µL of 1mg/mL RNase A (Blirt) and 25µL of 0,5mg/mL propidium iodide (PI) solution (BioLegend) to a final volume of 500µL for at least 15min at RT. Unstained cells were used to define positive cell staining. PI is intercalated between the DNA base pairs and therefore enables to distinguish the cell cycle phase according to the PI staining intensity of each cell. The DNA content was measured with an Accuri C6 (Becton Dickinson) flow cytometer and the Watson model was applied to determine the cell cycle phases.

For apoptosis evaluation, the Pacific Blue Annexin V Apoptosis Detection Kit with 7-AAD (BioLegend) was used. The culture medium was also collected to save cells

in suspension. Harvested cells were washed twice with ice-cold Cell Staining Buffer and then Annexin V Binding Buffer (BioLegend) was added. Samples were incubated, in the dark, with 50µg/mL Pacific Blue Annexin V and 50µg/mL 7-aminoactinomycin D (7-AAD) for at least 15min at RT. Unstained and mono-labelled controls were also performed to define positive cell staining. The FACS Canto II (Becton Dickinson) flow cytometer was used to analyse cell staining with proper machine settings. Annexin V is an intracellular protein that bind to phosphatidylserine (PS) in a calcium-dependent manner. In early apoptotic cells, the integrity of the cell membrane is compromised and thus PS is translocated to the outer layer, allowing their identification based on Annexin V staining. On the other hand, 7-AAD is also a DNA intercalator and is only incorporated in latter stages of apoptosis and by necrotic cells, but not cells in early apoptosis. All the analysis were performed with the FlowJo 7.6 version software (https://www.flowjo.com/).

3.11. RNA extraction and quantification

For total RNA extraction, cells were lysed using the TRI reagent (Sigma-Aldrich) according to the manufacturer's guidelines for RNA isolation. Briefly, cells were vigorously resuspended in 500µL of the TRI reagent and left at RT for 5min, after which 100µL of chloroform (Sigma-Aldrich) was added. Lysates were vigorously mixed for 15s and incubated for 15min at RT. For separation of the organic and aqueous phases, samples were centrifuged at 17000xg for 15min at 4ºC and the aqueous phase containing the RNA was carefully recovered. RNA precipitation was achieved by mixing 250µL of isopropanol at RT and a centrifugation at 17000xg for 10min at 4ºC. The supernatant was discarded and the pellet washed twice with 70% ethanol at -20ºC. The pellets were dried at RT and then eluted in distilled water. The NanoDrop 1000 spectrophotometer (Thermo Fisher Scientific) was used to determine the total RNA concentration in each sample. The ratio of absorbance at 260nm and 280nm was used to assess the RNA purity, and the ratio of absorbance at 260nm and 230nm to inspect for potential contaminations with organic and aromatic compounds or chaotropic salts.

3.12. Reverse transcription and quantitative real-time PCR

The Superscript IV Reverse Transcription Kit (Life Technologies) was used to reverse transcribe the total RNA. 2-4µg of total RNA extracts was mixed with 1mM dNTPs and 0,01µg/µL of random hexamers. RNA secondary structures were denaturated at 65ºC for 5min in a thermal cycler (MyCycler, Bio-Rad) and samples were then incubated on ice for at least 2min. 1x SSIV buffer, 5mM DTT, 0,4U/µL RNAseOUT™ RNase Inhibitor and 5U/µL Superscript® IV Reverse Transcriptase were added to each sample to a final volume of 20µL. The reverse transcription reaction proceeded as follows: 23ºC for 10min; 52ºC for 10min; and 80ºC for 10min.

For mRNA expression analysis, the *Power* SYBR® Green PCR Master Mix (Applied Biosystems) and sequence specific primers spanning exon-exon junctions (table 3.4) were used. Each sample was amplified in technical triplicates in an ABI Prism 7500 system (Applied Biosystems). The reaction proceeded as follows: 95ºC for 2min; 95ºC for 10min; and 40 cycles of 95ºC for 15s and 60ºC for 1min. Primer specificity was assessed by melting curves: 95ºC for 15s; 60ºC for 1min; 95ºC for 30s; and 60ºC for 15s. mRNA expression was calculated through the relative standard curve method or the $2^{-\Delta\Delta Ct}$ method. *18S* rRNA expression levels were used to normalize target gene expression.

Table 3.4. List of primers used.

Target gene	Primer sequence (5' -> 3')
Human *ASPM*	F: TCTCAAACGCCATCAGGAGAG
	R: TGAATGACGAGTGCTGCATTAAC
Human *TIMELESS*	F: GGTACAGATGGGACTGGCTG
	R: ATGACCCAGGACATCATCTGAG
Mouse *Timeless*	F: TTCCGGGACTCTGATGATGTTC
	R: TTGTATAGCTGCCTCCGCTC
Human *LGR5*	F: CAGCGTCTTCACCTCCTACCTA
	R: CCTTGGGAATGTATGTCAGAGC
Mouse *Lgr5*	F: AGCGTCTTCACCTCCTACCTG
	R: CTTGGGAATGTGTGTCAAAGC
Human *OLFM4*	F: TTGGAATTCACAGCTCATGTTC
	R: GATGTCAATTCGGACAGTTAGG
Human *BMI1*	F: GTCTACATTCCTTCTGTAAAACG
	R: CTTGGAGAGTTTTATCTGACC
18S	F: CGCCGCTAGAGGTGAAATTC
	R: CATTCTTGGCAAATGCTTTCG

3.13. Statistical analyses

All the results are presented either as mean ± standard deviation (SD) or mean ± standard deviation of the mean (SEM), such as specified in each experiment. Each experiment was executed at least three times unless otherwise stated. Statistical analysis was achieved through the IBM SPSS Statistics 25 version software (https://www.ibm.com/analytics/spss-statistics-software). To examine the relationship between the biomarkers and the clinicopathological features of the patients, we used the student's *t*-test to compare with age, the Fisher's exact test (2-sided) to compare gender, BRAF status and histograde, and the Pearson chi-square for the remaining parameters. The effect size, expressed as Phi (ϕ), was also considered to quantify the differences between two groups when the *P* value was statistically significant. The associations were weak when ϕ is around 0,1, moderate ϕ is around 0,3, and strong when ϕ is around 0,5 or greater. Results were considered as significantly different at a *P* value < 0,05.

Chapter 4 - Results

4.1. Bioinformatic identification of RBP candidates and prioritization

To identify potential RBPs whose expression levels are altered in CRC and are stemness-related, RNA-sequencing data from the TCGA database concerning colon cancer had been previously crossed with the RBPs deposited in the EuRBPDB database. This approach revealed 692 RBPs differentially expressed in colon cancer when compared to normal tissue (fig. 4.1A), most of them being upregulated in tumours as observed by GSEA analysis (Fig. 4.1B). This list included housekeeping factors, such as ribosomal proteins or the core spliceosome machinery that are essential for normal cell function. Therefore, they were excluded. The list was further curated based on a literature query with the term "stem cell" in any biological context. Thus, a stemness-related subset of 130 putative CRC-specific RBPs was defined, most of them with yet unknown functions in CRC. A shortlist of stemness-related RBPs upregulated and downregulated in CRC cases was selected and are shown in table 4.1. Among the upregulated RBPs, three belonged to the *Lgr5*$^{+}$ cell transcriptional signature (11), like MEX3A: ASPM, SLC12A2 and TIMELESS. On the other hand, the most significantly downregulated RBPs in CRC were ZBTB16, RBPMS2 and SALL2, although they do not belong to the *Lgr5*$^{+}$ cell transcriptional signature.

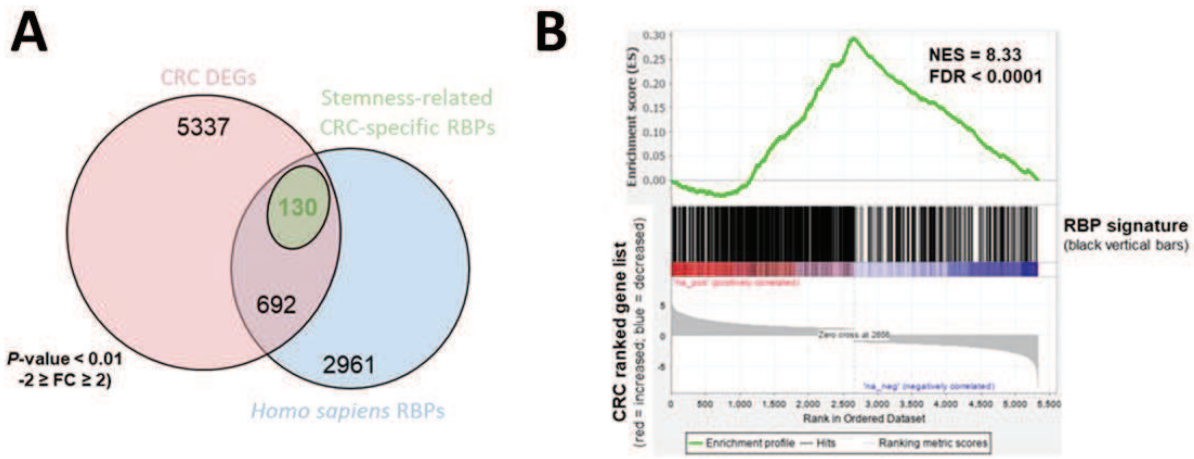

Figure 4.1. Bioinformatic analysis of CRC-altered RBPs. (A) Venn diagram representation of differentially expressed genes (DEGs) in CRC, the known human RBPs and stemness-related RBPs. **(B)** GSEA analysis showing the RBP signature for the 692 differentially expressed RBPs in CRC. Most of these RBPs are upregulated in CRC cases.

Table 4.1. Top hits of stemness-related RBPs upregulated and downregulated in CRC cases.

Gene	Fold-change	Log_2 fold-change	*P* value
ASPM	4,817	2,268	7.82E-124
SLC12A2	6,521	2,705	9.50E-121
TIMELESS	3,057	1,612	6.78E-101
ZBTB16	0,088	-3,51	1.93E-102
RBPMS2	0,021	-5,55	1.11E-89
SALL2	0,199	-2,326	5.72E-69

To focus our approach even more, a bibliographical search on PubMed was pursued to assess in which biological processes the candidate RBPs are involved, the functional consequences upon cell reprograming, their role in stemness regulation, and carcinogenesis, particularly in the context of colorectal cancer. For this literature survey, the following set of keywords was used: RNA-binding; stemness; stem cell; intestinal stem cell; self-renewal; differentiation; cancer; colorectal cancer; pluripotency; and Wnt signalling. Among the 6 candidates, ASPM, SLC12A2, and ZBTB16 showed to fulfil the largest number of criteria. However, SLC12A2 is a known ion cotransporter located at the plasma membrane, a function not easily reconciled with a role as a RBP. Hence, we focused on TIMELESS together with the other two.

ASPM is a microtubule-associated protein that also plays a role in the preservation of the proliferative and self-renewal capacities of progenitor cells by regulating the orientation of the mitotic spindle, cell cycle entrance, and activating Wnt signalling (107–109). The *TIMELESS* gene is the mammalian homologue of the *Drosophila melanogaster tim* gene, an evolutionary-conserved circadian clock gene (110). In humans, TIMELESS has been implicated in several cellular functions, including DNA replication as a critical component of the replication fork (111), DNA damage sensing and repair, S and G2/M checkpoints activation (112–114), sister chromatid cohesion (115,116), and telomere length maintenance (117). ZBTB16 is a transcriptional repressor and has a central role in myeloid lineage differentiation and maintenance of stem cells associated in developmental processes, namely in germline cells (118).

4.2. Candidate RBPs expression and its relationship with clinicopathological features in a cohort of human CRC cases

Through the GEPIA web server (http://gepia2.cancer-pku.cn/#index), it was possible to obtain the mRNA expression profile of each individual candidate in cohorts of colon and rectal cancer cases and compare it to the expression level in normal tissue counterparts available from the TCGA and GTEx databases. Indeed, *ASPM* and *TIMELESS* showed increased transcriptional levels both in colon and rectal cancer cases when compared to normal tissues (fig. 4.2A and B). On the contrary, ZBTB16 showed clearly downregulated expression levels in tumours when compared to normal tissue samples (fig. 4.2C).

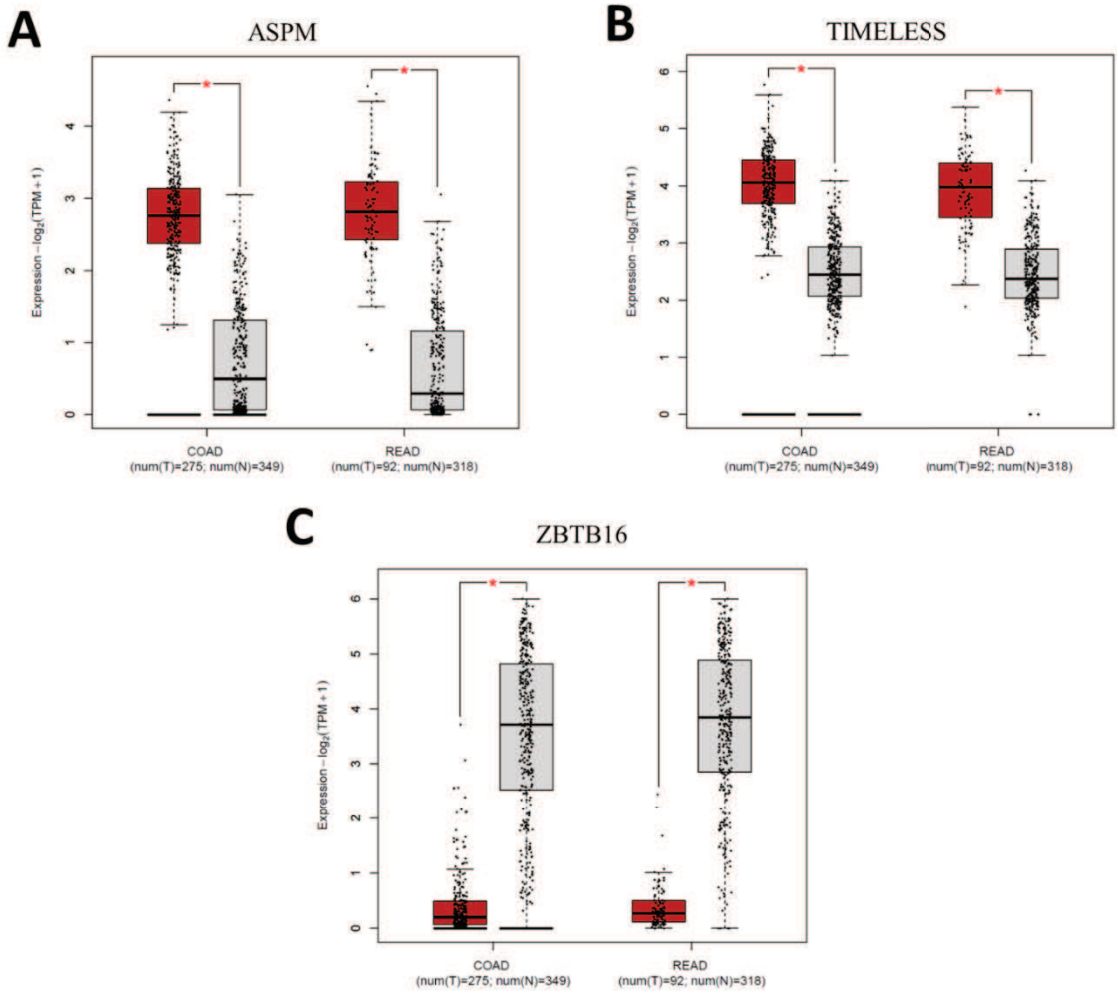

Figure 4.2. Transcriptional profile of the candidate RBPs. mRNA expression profile in cohorts of colon and rectal cancer cases compared to normal tissue counterparts available at the TCGA and GTEx databases for (A) ASPM (B) TIMELESS, and (C) ZBTB16. COAD: colon adenocarcinoma. READ: rectum adenocarcinoma (**P*<0,01).

To validate the expression profile of the chosen candidate RBPs in CRC, a cohort of stage II human CRC cases (n=192) in the form of tissue microarrays was evaluated by immunohistochemistry (fig. 4.3). A possible association between expression data and different clinicopathological features was then assessed (table 4.2).

Concerning ASPM expression, we observed that 36,4% (n=51) of the tumours analysed were either negative or had a weak staining pattern compared to 63,6% (n=89) of cases that exhibited moderate to high levels of ASPM in at least 60% of the cancer cells present, reinforcing the notion that ASPM expression is preferentially elevated in the context of CRC. In all positive cases, however, the staining was exclusively cytoplasmatic. On the contrary, in normal colonic tissue, we observed nuclear staining in the epithelial cells and also in the majority of the stromal compartment, indicating that ASPM expression is not restricted to epithelial cells. We found a significant association between ASPM expression levels and the microsatellite status (P=0,008; ϕ=-0,223), with higher ASPM-expressing tumours being mostly MSS when compared to low ASPM-expressing tumours. Tumours expressing higher levels of ASPM were also more frequently positive for the expression of the transcription factor SOX9 (P=0,027; ϕ=0,178).

The expression pattern of the TIMELESS protein was highly heterogeneous, with 49.3% (n=71) of tumours with low or absent expression and the remaining 50,7% (n=73) of cases having elevated expression levels, and so not a clear overexpression in tumour tissue as it was observed in the transcriptional data. TIMELESS localization was limited to the nucleus and it had a very characteristic staining pattern across the moderate- and high-expressing tumours, where only a subset of nearby cells (between 30% to 60%) were positive or either the whole tumour was strongly stained. Expression was not observed in the adjacent stroma in any of the cases. Remarkably, in the normal colonic tissue, TIMELESS expression was only detected in discrete cells at base of the crypts and less frequently in the upper crypt regions, being again absent from stromal cells. These observations suggest that TIMELESS expression might be restricted to the stem cell compartment of normal intestinal crypts. In line with this type of association, a weak correlation was observed between TIMELESS and MEX3A expression profiles (P=0,017; ϕ=0,199). Despite the very limited number of cases positive for the pluripotency transcription factor SOX2 included in this cohort, there was also a weak correlation detected between TIMELESS and SOX2 expression levels (P=0,009;

ϕ=0,220). High TIMELESS-expressing tumours also showed a slight correlation with the MSS status as opposed to the MSI status (*P*=0,022; ϕ=-0,199).

Regarding the ZBTB16 expression profile, we observed that ZBTB16 was expressed at low levels in 42,8% (n=59) of cases and at high levels in 57,2% (n=79) of cases. ZBTB16 staining was mainly cytoplasmatic and distinctively perinuclear in strongly positive cells. In low-expressing tumour cases, ZBTB16 expression became noticeable in stromal cells as opposed to tumours expressing more ZBTB16 in which the stromal cells lost its expression. Likewise, in the normal mucosa, ZBTB16 was almost exclusively detected in stromal cells, with very few positive epithelial cells

Curiously, the expression profiles of the three candidate RBPs showed some correlation between them. Tumours with increased levels of ASPM also presented higher levels of TIMELESS (*P*=0,016; ϕ=0,204) and ZBTB16 (*P*=0,017; ϕ=0,198) as well, being this the only statistically significant association found for ZBTB16. None of the putative RBPs expression profiles showed a significant correlation with any of the other clinicopathological variables evaluated, namely age at diagnosis, gender, site of tumour, histological grade, and BRAF mutational status. Furthermore, no significant differences were found between the three RBPs expression profiles and disease-free survival or overall survival when survival curves were plotted according to the Kaplan-Meier method and compared through the log-rank test (data not shown). Taken together, the selected RBPs demonstrated distinct expression patterns in the series of human CRC cases characterized. ASPM and ZBTB16 were preferentially overexpressed in tumour tissues, whereas TIMELESS was expressed at low and high levels in the same proportion of stage II CRC cases.

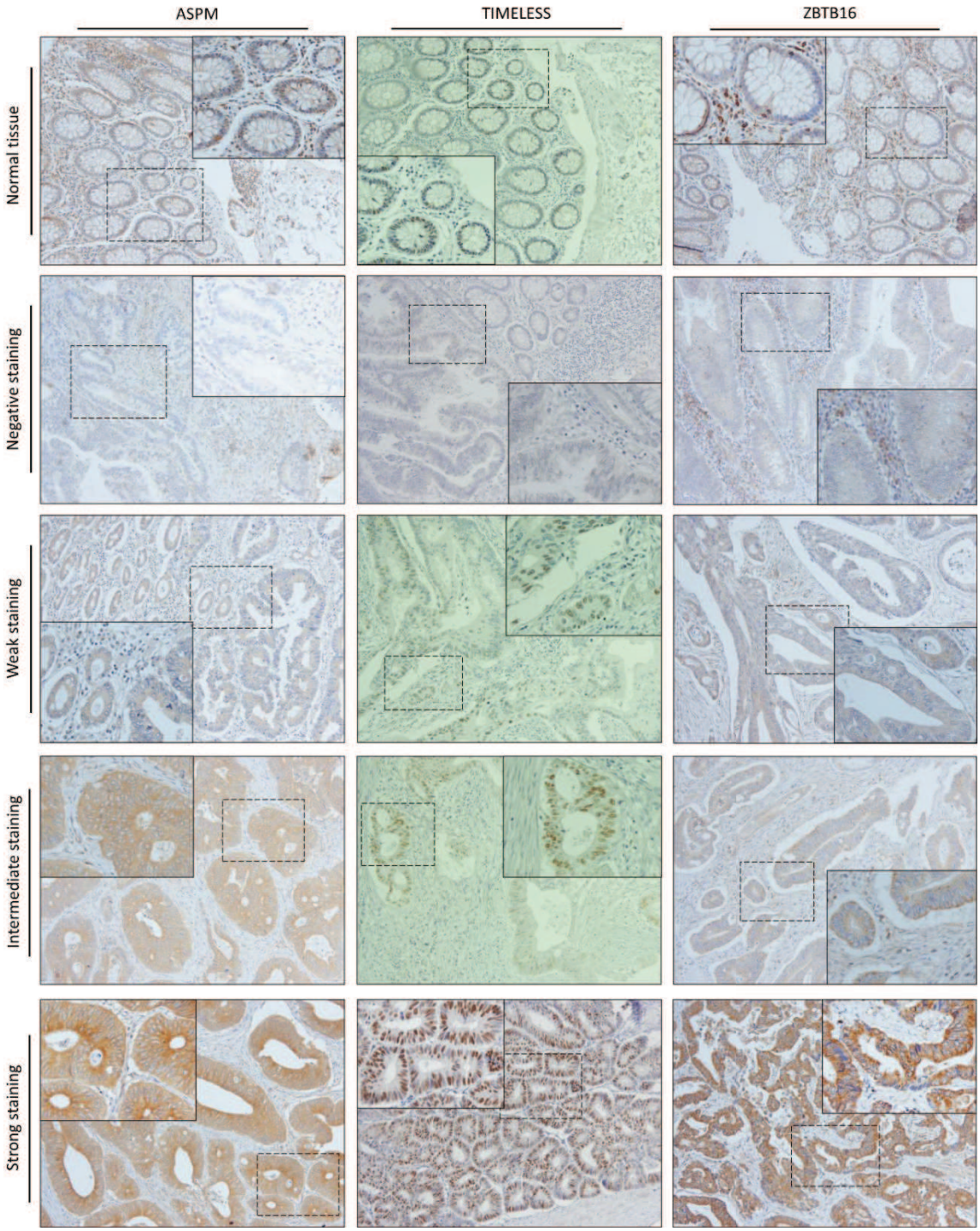

Figure 4.3. RBPs expression profiles in a series of 192 human CRC cases. Representative immunostaining images for ASPM, TIMELESS and ZBTB16. The RBPs expression pattern in normal colon tissue and representative cases for negative, weak, intermediate and strong cases are shown. Amplification of the original images is 100x and 200x for the amplified regions in the boxed areas.

Table 4.2. Association of clinicopathological features with ASPM, TIMELESS and ZBTB16 expression profiles in patients with CRC.

	ASPM			TIMELESS			ZBTB16		
Characteristic	Low	High	*P* value	Low	High	*P* value	Low	High	*P* value
Age (years)									
Mean ± SD	67,07 ± 11	70,31 ± 10,3	0,063	69,2 ± 10,2	69,9 ± 10,8	0,716	70,93 ± 10,1	68,49 ± 10,3	0,151
Range	35 - 92	44 - 91		45 - 91	35 - 92		48 - 92	35 - 86	
Gender									
Female	28 (17,7%)	40 (25,3%)	0,41	31 (21,5%)	29 (20,1%)	0,736	23 (15,2%)	41 (27,2%)	0,402
Male	31 (19,6%)	59 (37,3%)		40 (27,7%)	44 (30,6%)		38 (25,2%)	49 (32,5%)	
Site of tumor									
Proximal (including transverse)	26 (16,8%)	39 (25,2%)	0,573	26 (18,3%)	32 (22,5%)	0,376	30 (20,3%)	30 (20,3%)	0,053
Distal	32 (20,6%)	58 (37,4%)		44 (31%)	40 (28,2%)		30 (20,3%)	58 (39,2%)	
Histological grade									
G1	1 (0,6%)	2 (1,3%)		2 (1,4%)	1 (0,7%)		1 (0,7%)	2 (1,3%)	
G2	55 (34,8%)	90 (57%)	0,887	67 (46,5%)	65 (45,1%)	0,246	55 (36,4%)	84 (55,6%)	0,777
G3	3 (1,9%)	7 (4,4%)		2 (1,4%)	7 (4,9%)		5 (3,3%)	4 (2,6%)	
BRAF status									
WT	48 (31,2%)	78 (50,6%)	0,667	56 (39,4%)	58 (40,8%)	1	47 (32%)	73 (49,7%)	0,396
V600E	9 (5,8%)	19 (12,3%)		14 (9,9%)	14 (9,9%)		13 (8,8)	14 (9,5%)	
Microsatellite status									
MSS	24 (16,7%)	59 (41%)	**0,008**	31 (23,5%)	44 (33,3%)	**0,022**	30 (21,9%)	52 (38%)	0,212
MSI	31 (21,5%)	30 (20,8%)		35 (26,5%)	22 (16,7%)		26 (19%)	29 (21,2%)	
SOX9									
Negative	10 (6,5%)	6 (3,9%)	**0,027**	7 (5%)	6 (4,3%)	0,75	8 (5,5%)	6 (4,1%)	0,144
Positive	47 (30,7%)	90 (58,8%)		62 (44,6%)	64 (46%)		49 (33,6%)	83 (56,8%)	
SOX2									
Negative	52 (34%)	82 (53,6%)	0,292	67 (48,2%)	59 (42,4%)	**0,009**	52 (35,6%)	77 (52,7%)	0,387
Positive	5 (3,3%)	14 (9,2%)		2 (1,4%)	11 (7,9%)		5 (3,4%)	12 (8,2%)	
MEX3A									
Low	10 (6,3%)	14 (8,9%)	0,634	16 (11,1%)	6 (4,2%)	**0,017**	13 (8,6%)	10 (6,6%)	0,087
High	49 (31%)	85 (53,8%)		55 (38,2%)	67 (46,5%)		48 (31,8%)	80 (53%)	
ZBTB16									
Low	27 (18,5%)	31 (21,2%)	**0,017**	33 (23,9%)	26 (18,8%)	0,228			
High	24 (16,4%)	64 (43,8%)		36 (26,1%)	43 (31,2%)				
TIMELESS									
Low	32 (26,7)	17 (14,2%)	**0,016**						
High	19 (15,8%)	52 (53,3%)							

4.3. Candidate RBPs expression profile in CRC cell lines

To investigate the function of the selected RBPs in CRC cells, we began to characterize their expression levels in a panel of five CRC cells lines at the RNA and/or protein levels. The Caco-2 cell line was analysed before reaching confluency (Caco-2 Pre-confluency) and at confluency (Caco-2 Post-confluency), as a result of its ability to spontaneously differentiate after reaching confluency and acquire morphological and functional properties characteristic of enterocytes found in the small intestine, which turn them into an attractive *in vitro* model to study intestinal epithelial maturation and absorption (119).

We were unable to measure ASPM expression at the protein level due to what appeared to be a lack of antibody specificity (fig. 4.4A). The predicted protein size was 250kDa but the most intense detected band had a molecular weight of only 30kDa. Consequently, only the transcriptional analysis provided insight on its expression profile. *ASPM* mRNA was expressed at higher levels in the SW480 cell line, while the Caco-2 Pre-confluence, DLD-1, and HCT116 cells revealed the lowest expression levels.

TIMELESS protein expression was more elevated in the SW480 cell line and, surprisingly, in the Caco-2 Post-confluence followed by the HCT116 cell line (fig. 4.4B and C). Interestingly, *TIMELESS* mRNA was more expressed in the SW480 and Ls174T cell lines (fig. 4.4D).

For ZBTB16, the highest protein expression levels were detected in the SW480 and HCT116 cell lines (fig. 4.4B and C). The Caco-2 and DLD-1 showed to be cell lines that expressed less ZBTB16. Interestingly, ZBTB16 protein signal was only migrating at approximately 60kDa in the CRC cell lines rather than the expected 75kDa observed in the HEK293T cell line (data not shown). We were unable to assess *ZBTB16* mRNA expression due to lack of success in attaining good quality primer pairs to achieve specific amplification.

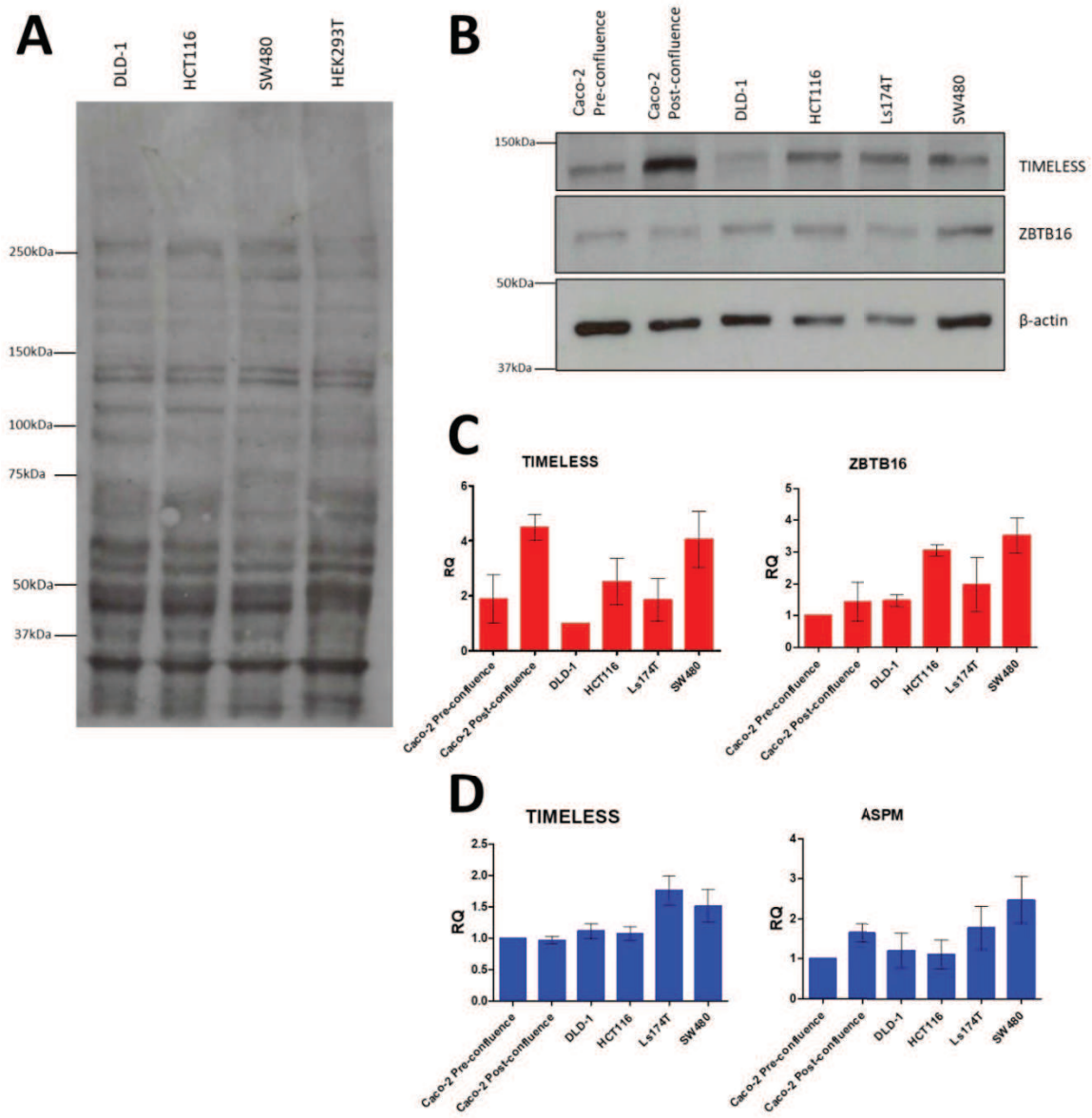

Figure 4.4. Candidate RBPs expression profile in a panel of CRC cell lines. (A) Western blot analysis of ASPM. **(B)** Western blot analysis of TIMELESS and ZBTB16. **(C)** Relative quantification of TIMELESS and ZBTB16 protein expression. **(D)** Relative quantification of *TIMELESS* and *APSM* mRNA expression. Values are expressed as mean ± SD (C, n=2 independent experiments; D, n=3 independent experiments).

To confirm these observations, we also performed immunofluorescence in some of the CRC cell lines (fig. 4.5). Indeed, ASPM was detected at higher levels in the SW480 cell line and in a positive control cell line, HEK293T, and at lower levels in the DLD-1 and HCT116 cell lines, which matched the data collected from the RNA expression. Moreover, ASPM was found mainly in the cytoplasm, as previously observed in positive CRC cases. TIMELESS and ZBTB16 expression levels were higher in the SW480 cell line, closely followed by the HCT116 cell line in both cases. TIMELESS was located exclusively in the cell nucleus, while ZBTB16 was detected in the nucleus and cytoplasm with a perinuclear staining pattern, reminiscent of the one observed in CRC tissues. These results show that the SW480 cell line was the CRC cell line that expressed higher levels of the selected RBPs according to our characterization at the transcriptional and protein levels.

At this point, based on the expression profile observed in our panel of CRC cell lines, and on the quality of the molecular tools available, we decided to further study TIMELESS functional role in CRC cell biology.

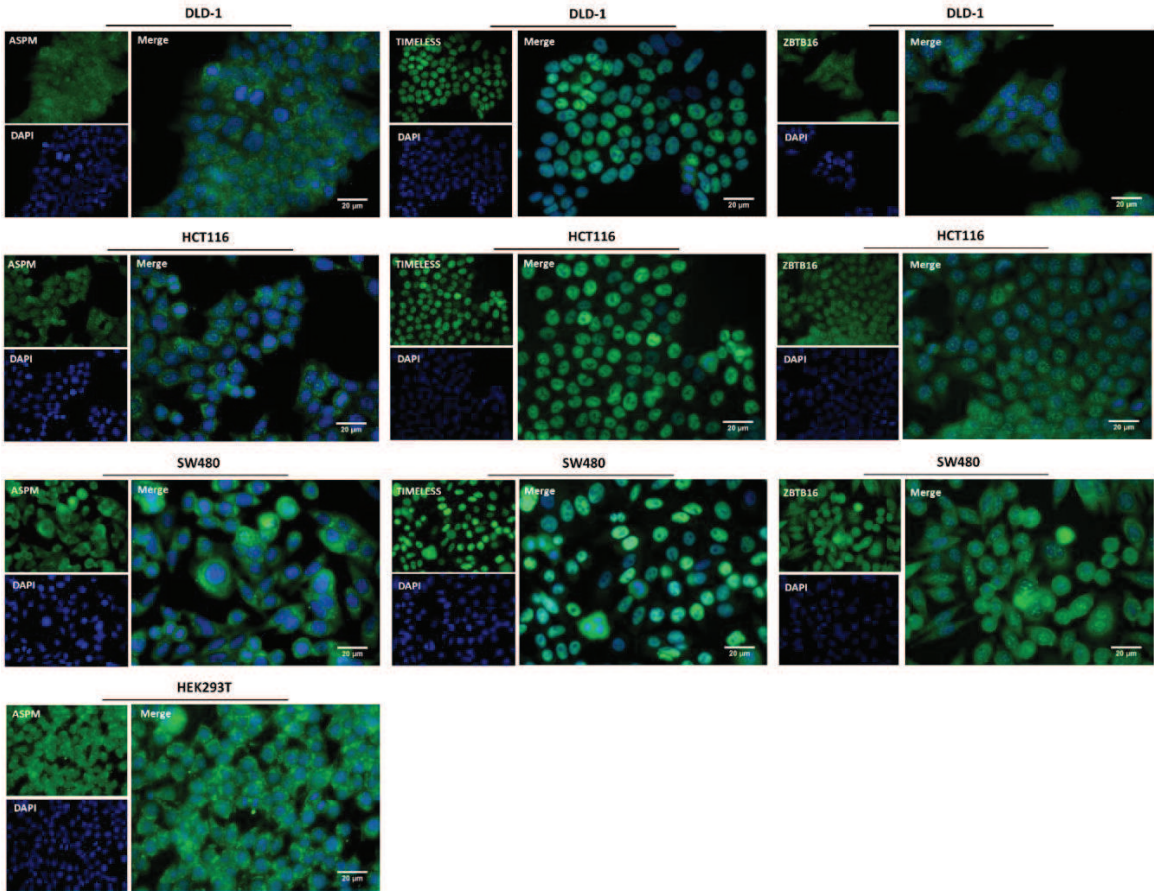

Figure 4.5. Immunofluorescence of the candidate RBPs in some CRC cell lines. Amplification of the original images is 400x.

4.4. TIMELESS expression is associated with the intestinal stem cell phenotype

Given the TIMELESS expression profile previously observed in tissues and cell lines, we started by addressing if TIMELESS is regulated by the Wnt signalling, considering the central role of this pathway in intestinal stem cell biology. The DLD-1, HCT116 and SW480 cell lines were treated with CHIR99021 (henceforward named CHIR) and IWP-2 to modulate Wnt signalling and then TIMELESS expression levels were measured. CHIR is a potent inhibitor of GSK3β and thus blocks β-catenin degradation, enhancing Wnt signalling. On the other hand, IWP-2 impedes Wnt proteins from being palmitoylated and secreted by inhibiting the O-acyltransferase PORCN, which results in the suppression of Wnt signalling. To verify if the treatments had the desired effects on the cell lines, we started by measuring the transcriptional levels of *LGR5*, a Wnt target gene. As showed in fig. 4.6A, the HCT116 cell line was the only one that presented the expected response in terms of *LGR5* expression levels according to each treatment: an increased expression in the presence of CHIR, and a clearly decreased expression in the presence of IWP-2. However, TIMELESS levels did not exhibit significant alterations in expression in any of the cell lines upon Wnt signalling modulation (fig. 4.6B). It is possible that the mutational background of each cell line prevents treatment-induced alterations, particularly because most CRC cell lines show abnormal Wnt signalling due to mutations in key elements of the pathway, noticeably APC and β-catenin.

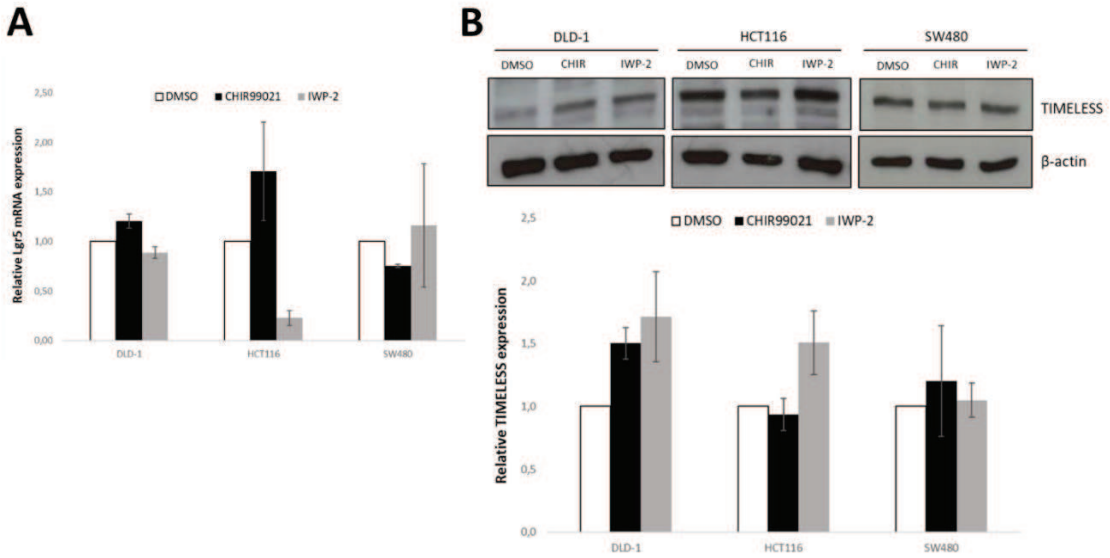

Figure 4.6. TIMELESS expression upon Wnt signalling modulation in DLD-1, HCT116 and SW480 cells. (A) qPCR analysis of *LGR5* mRNA expression levels on treatment with CHIR or IWP-2. **(B)** Western blot analysis and relative quantification of TIMELESS protein expression showing no significant alterations in expression. Values are expressed as mean ± SEM (A,B, n=2 independent experiments).

To overcome the limitation of CRC cell lines in addressing modulation by endogenous Wnt signalling, we assessed its influence in TIMELESS expression using intestinal organoids as a model with no genetic abnormalities, similar to the physiological conditions. For that, mouse small intestine was dissected and intestinal organoids established from isolated crypts. Conditioned medium with WNT3A was used together with CHIR to stimulate Wnt signalling, and IWP-2 for Wnt signalling downregulation. IWP-2-treated organoids were not able to grow due to the block on post-translational palmitoylation of endogenous WNT ligands (provided by Paneth cells in the organoids), which precluded further analysis (fig. 4.7A). However, intestinal organoids responded as expected when treated with WNT3A+CHIR (WENR medium). WENR organoids adopted a cyst-like structure rather than the stereotypical mini-guts with protrusions corresponding to crypt domains observed in control organoids (ENR medium). The former structures are expectedly composed of stem cells and Paneth cells, and as such showed higher levels of *Lgr5* expression (fig. 4.7B). We also detected a 3,73-fold increase in TIMELESS protein expression upon Wnt stimulation compared to the control organoids (fig. 4.7C), indicating that TIMELESS is associated with Wnt signalling. This was accompanied by a similar trend in *Timeless* mRNA levels, with a 2,42-fold increase in expression upon Wnt stimulation, although with a higher level of variability (fig. 4.7D), suggesting that TIMELESS might not be a direct transcriptional target of the Wnt signalling pathway. Moreover, TIMELESS appeared to be expressed at lower levels in mouse colon-derived organoids compared to the small intestinal ones (0,55-fold reduction).

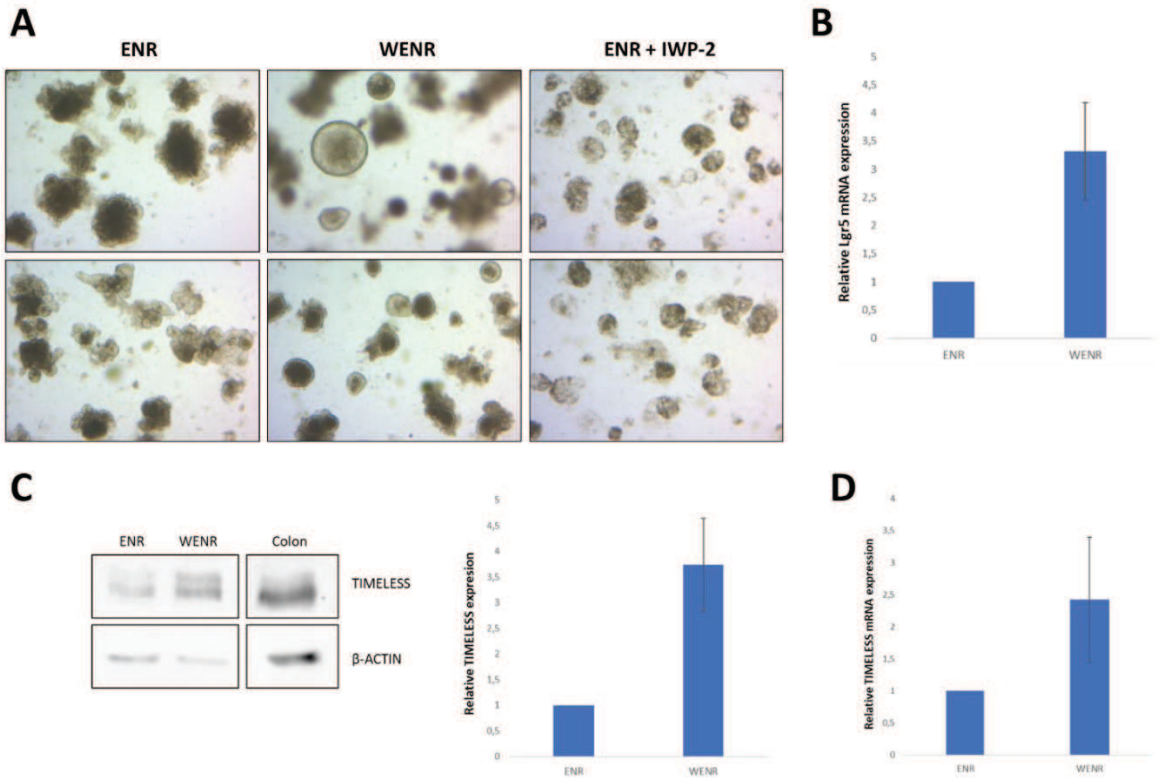

Figure 4.7. TIMELESS expression is increased upon Wnt activation in intestinal organoids. **(A)** Representative images of organoids in culture when treated with ENR medium, WENR medium or ENR+IWP-2 medium. **(B)** qPCR analysis of *LGR5* mRNA expression levels of organoids expanded in the different medium. **(C)** Western blot analysis and relative quantification of TIMELESS protein expression. (D) qPCR analysis of *TIMELESS* mRNA expression levels. Values are expressed as mean ± SEM (B-D, n=3 independent experiments).

4.5. TIMELESS depletion alters the cell cycle distribution of CRC cells

Our previous analysis of a panel of CRC cell lines showed that the SW480 cell line had consistently elevated expression of TIMELESS both at the RNA and protein levels. The Caco-2 (Post-confluence) and Ls174T cell lines also displayed high expression levels. However, these form 3D dome-like structures in culture and to avoid technically challenging transfections they were not selected. Therefore, SW480 and HCT116 were chosen to transiently knockdown TIMELESS expression and functionally assess its influence in the proliferation of CRC cells. For that, we studied the cell cycle profile of cells transfected with siRNAs against *TIMELESS* (siTIMELESS) or *GFP* (siGFP) as a control through flow cytometry (fig. 4.8A-E). We observed that TIMELESS depletion induced a slight increase in the percentage of cells in G1 (41,2% vs 39,2% for HCT116; and 41,6% vs 36,3% for SW480) as well as in G2/M (15,7% vs 12,6% for HCT116; and 13,8% vs 12,5% for SW480). But the common and most significant difference in both cell lines was a significant decrease in the number of cells undergoing S phase (39,8% vs 45,3% for HCT116; and 41,3% vs 48,1% for SW480). Together, these results show that TIMELESS ablation influences the cell cycle progression of CRC cells.

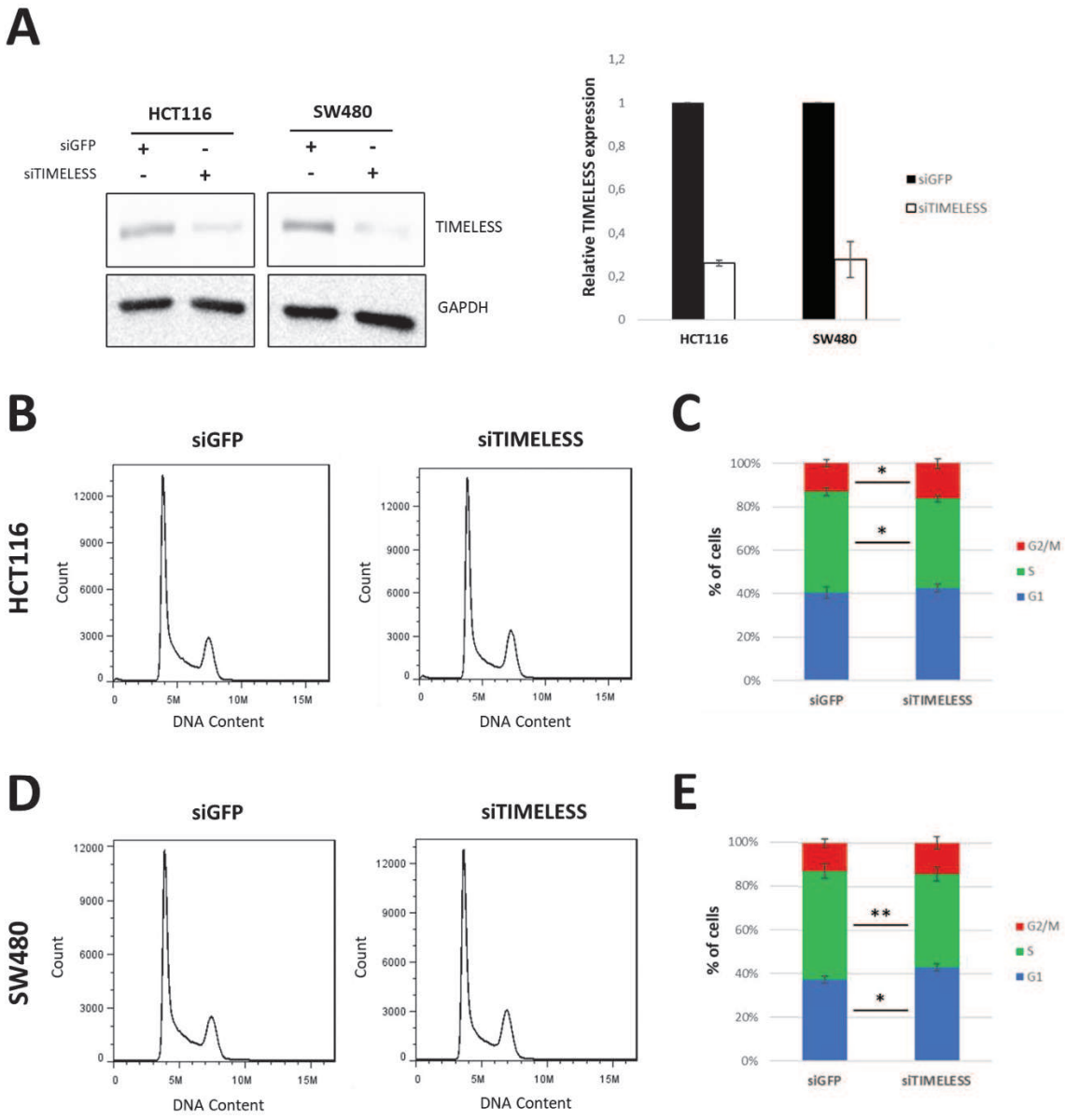

Figure 4.8. TIMELESS depletion influences the cell cycle progression of CRC cells. (A) Western blot analysis and relative quantification of TIMELESS expression in siTIMELESS- and siGFP control-transfected cells. **(B-C)** Quantification of the percentage of HCT116 cells in each phase of the cell cycle following PI staining. **(D-E)** Quantification of the percentage of SW480 cells in each phase of the cell cycle following PI staining. Values are expressed as mean ± SEM (A-E, n=3 independent experiments; Paired *t-test*, **P*<0,05; ***P*<0,01).

4.6. TIMELESS depletion sensitizes CRC cells to 5FU-induced cell death

We then proceeded to analyse TIMELESS involvement in mechanisms of cell death. For that, siRNA-transfected HCT116 and SW480 cells were subsequently treated with either 50μM of the chemotherapy drug 5-FU or vehicle-treated with DMSO at 24h, and cell death was studied by flow cytometry after proper staining. Knocking down TIMELESS (fig. 4.9A) expression caused an increase in the percentage of HCT116 cells undergoing both early and late apoptosis at the expense of a slight decrease in cell viability, compared to siGFP control-transfected cells (fig. 4.9B and C). 5-FU treatment caused mainly an increase in late apoptotic and necrotic cell populations, with the former induced to an extent similar to the one observed upon TIMELESS downregulation. Interestingly, 5-FU treatment induced a variable decrease in the expression levels of TIMELESS detected by immunoblotting. The combination of TIMELESS inhibition and 5-FU treatment resulted mainly in a higher portion of necrotic cells compared to the other conditions, accompanied by a reduction in the percentage of viable cells. The late apoptosis cell fraction was at similar levels compared to the individual experimental conditions.

Regarding the SW480 cell line, TIMELESS ablation only increased the population of necrotic cells (fig. 4.9D and E). On the other hand, 5-FU treatment caused an increase in late apoptotic and necrotic cell populations, an effect similar to the one observed in HCT116 treated cells. Likewise, diminished levels of TIMELESS were also detected in 5-FU-treated SW480 cells. The combination of TIMELESS inhibition and 5-FU treatment led to an increase in the percentage of cells in late stages of apoptosis specifically (2,3-fold increase), which was greater than the individual experimental conditions.

Taken together, these findings show that TIMELESS depletion impacts different cell death processes, apparently in a cell line-specific manner.

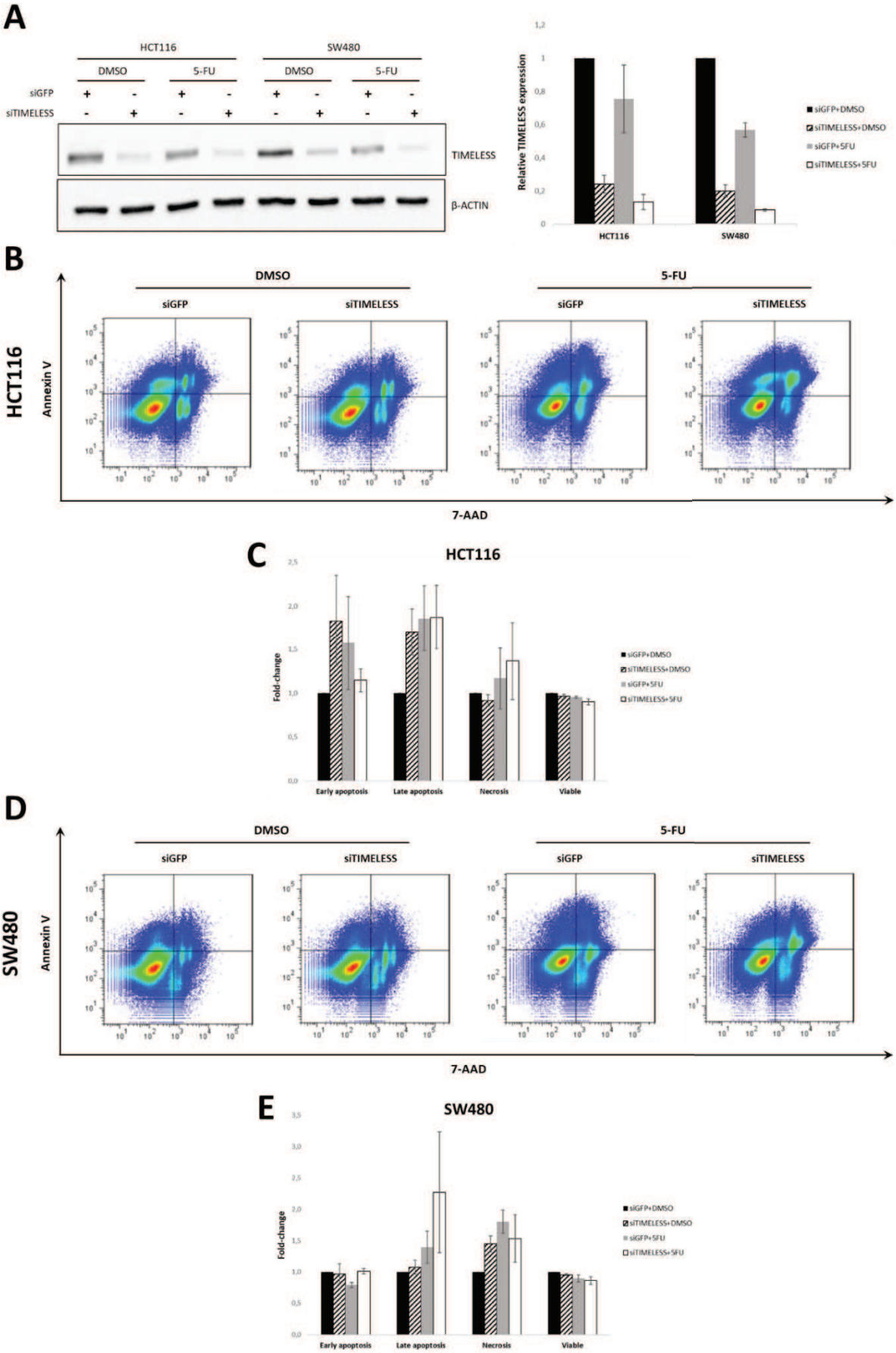
A
HCT116
SW480
DMSO
5-FU
DMSO
5-FU
siGFP
siTIMELESS
TIMELESS
β-ACTIN
Relative TIMELESS expression
HCT116
SW480
siGFP+DMSO
siTIMELESS+DMSO
siGFP+5FU
siTIMELESS+5FU
B
HCT116
DMSO
5-FU
siGFP
siTIMELESS
siGFP
siTIMELESS
Annexin V
7-AAD
C
HCT116
Fold-change
Early apoptosis
Late apoptosis
Necrosis
Viable
siGFP+DMSO
siTIMELESS+DMSO
siGFP+5FU
siTIMELESS+5FU
D
SW480
DMSO
5-FU
siGFP
siTIMELESS
siGFP
siTIMELESS
Annexin V
7-AAD
E
SW480
Fold-change
Early apoptosis
Late apoptosis
Necrosis
Viable
siGFP+DMSO
siTIMELESS+DMSO
siGFP+5FU
siTIMELESS+5FU

Figure 4.9. TIMELESS depletion renders cell more susceptible for cell death. (A) Western blot analysis and relative quantification of TIMELESS expression in siTIMELESS- and siGFP control-transfected cells on treatment with 5-FU or DMSO. **(B-C)** Quantification of the percentage of HCT116 cells stained with Annexin V and/or 7-AAD. **(D-E)** Quantification of the percentage of SW480 cells stained with Annexin V and/or 7-AAD. Values are expressed as mean ± SEM (A-E, n=3 independent experiments).

4.7. TIMELESS does not impact the migration phenotype of CRC cells

We also explored a role for TIMELESS concerning the migratory capacity of CRC cells as an additional functional assay in this context. For that, we followed siGFP- and siTIMELESS-transfected cells (fig. 4.10A) in a wound healing assay for approximately 24h and quantified the wound area closed throughout time. The HCT116 cell line showed greater motility and covered a larger area compared to the SW480 cell line after 24h (fig. 4.10B and C). Nevertheless, no differences in migratory potential were found in TIMELESS-depleted cells in both cell lines (fig. 4.10D and E), indicating that TIMELESS function is probably not related with the migration of CRC cells.

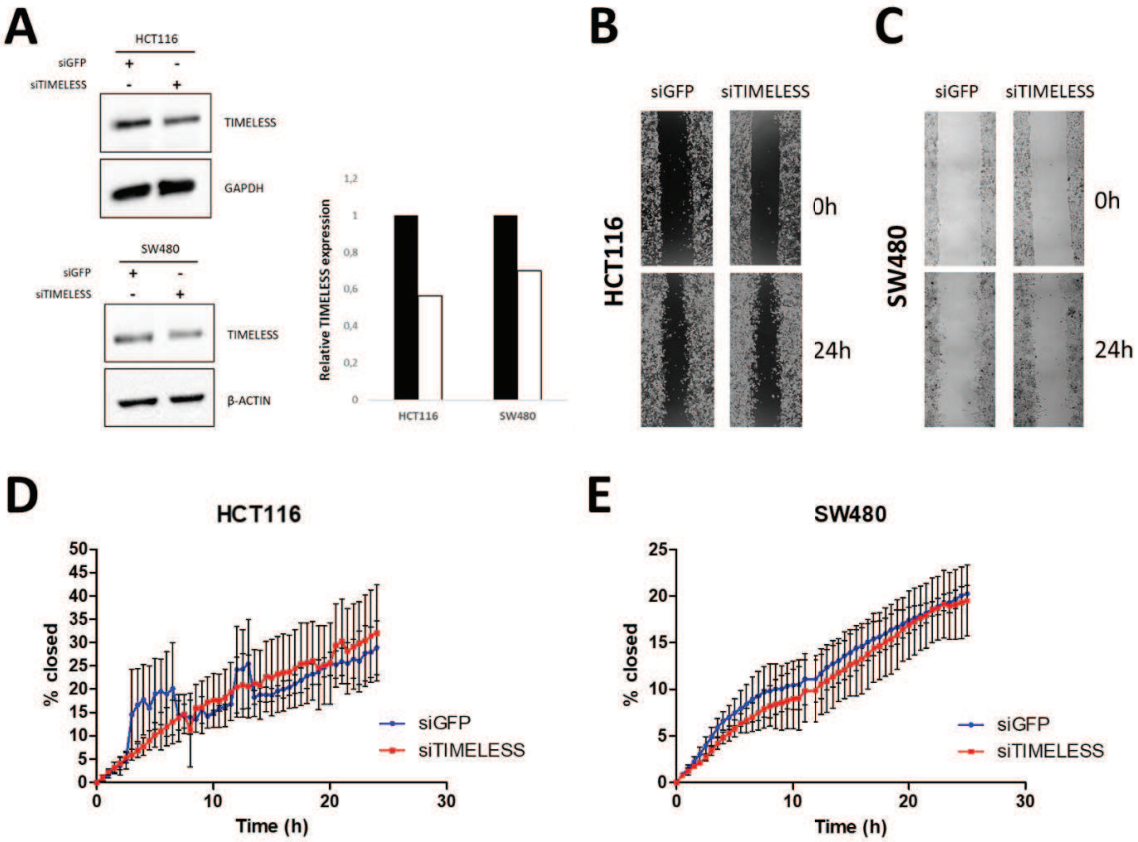

Figure 4.10. TIMELESS depletion does not affect the migration of CRC cells. (A) Western blot analysis and relative quantification of TIMELESS expression in siTIMELESS- and siGFP control-transfected cells. **(B)** Representative images the wound at 0h and 24h in HCT116 cells. **(C)** Representative images of the wound at 0h and 24h in SW480 cells. **(D)** Quantification of the percentage of wound area closed over 24h for HCT116 cells. **(E)** Quantification of the percentage of wound area closed over 24h for SW480 cells. Values are expressed as mean ± SD (n=1 experiment).

4.8. TIMELESS depletion influences the expression levels of ISC markers in CRC cells

To further investigate the relationship between TIMELESS expression and stemness potential, we measured the expression levels of several known ISC markers in siGFP- and siTIMELESS-transfected cells (fig. 4.11A and B). Upon TIMELESS-depletion in HCT116 cells, we found that the protein expression of MEX3A remained unchanged (fig. 4.11A and C), while *LGR5* (1,5-fold increase), *OLFM4* (1,3-fold increase) and *BMI1* (1,2-fold increase) mRNA levels were slightly elevated, although with a higher level of variability for *OLFM4* (fig. 4.11D).

On the contrary, in the SW480 cell line, TIMELESS abrogation led predominantly to increased expression of MEX3A protein (2,4-fold increase) and *OLFM4* mRNA (1,9-fold increase) compared to control siGFP-transfected cells (fig. 4.11C and E).

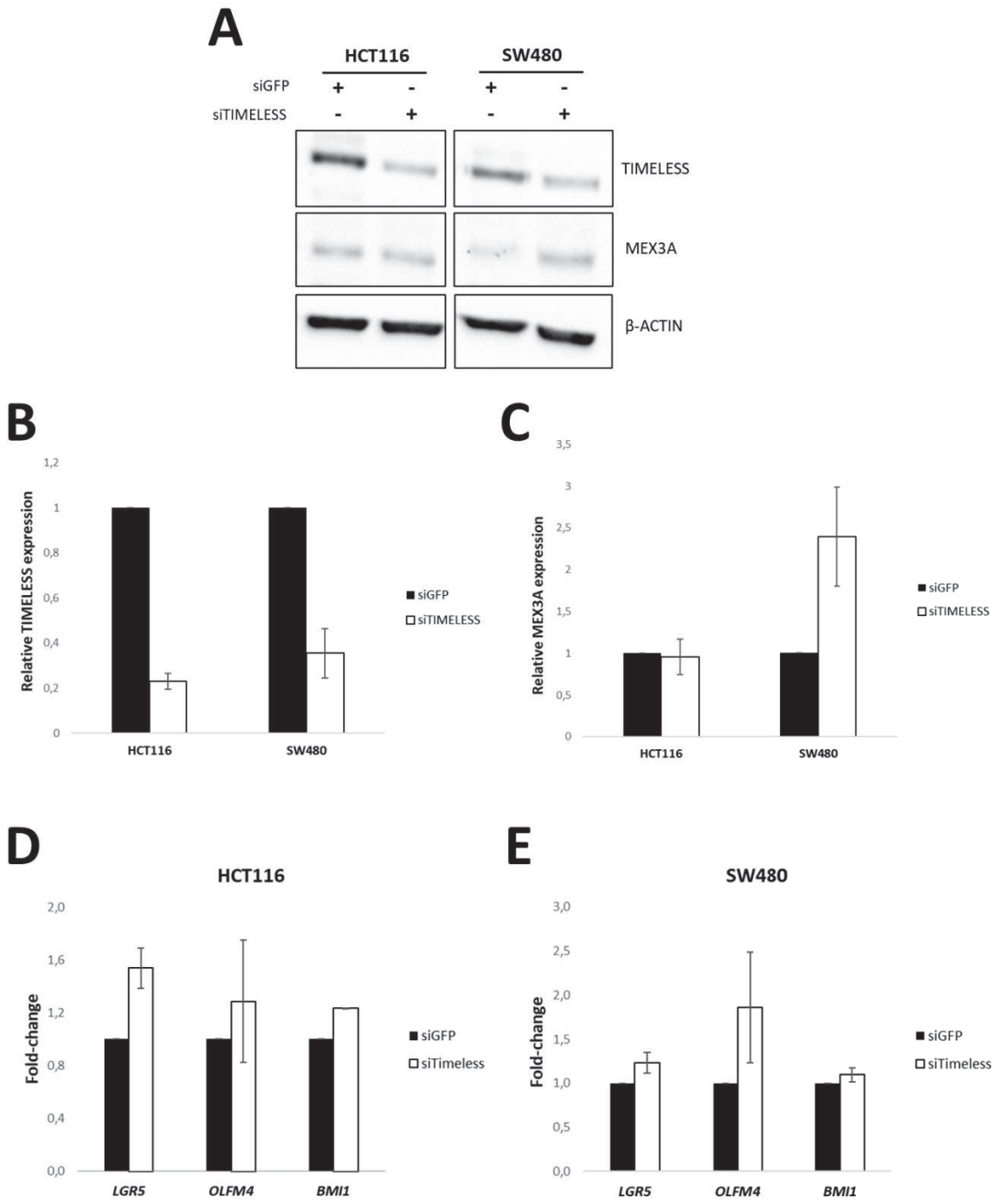

Figure 4.11. TIMELESS depletion alters the expression levels of ISC markers. (A) Western blot analysis of TIMELESS and MEX3A expression in siTIMELESS- and siGFP control-transfected cells. **(B)** Relative quantification of TIMELESS expression. **(C)** Relative quantification of MEX3A expression. **(D)** mRNA expression profiles of ISC markers in HCT116 cells. **(E)** mRNA expression profiles of ISC markers in SW480 cells. Values are expressed as mean ± SEM (C, n=6 independent experiment for HCT116 and n=5 independent experiments for SW480; D, n=2 independent experiments; E, n=3 independent experiments).

4.9. TIMELESS knockdown affects P-body dynamics in the SW480 cell line

To experimentally validate if TIMELESS does have a potential function as a RBP, we looked for alterations on P-body dynamics by performing immunostaining for EDC4, a mRNA decapping protein critical for P-body assembly, upon TIMELESS knockdown. As previously observed by western blot, the siRNA transfection significantly abrogated TIMELESS expression in both cell lines, with only a few cells retaining expression (fig. 4.12A).

In the HCT116 cell line, no significant differences were observed upon TIMELESS depletion compared to siGFP-transfected cells (fig. 4.12B), in terms of fluorescence intensity (fig. 4.12C), number of puncta per cell (fig. 4.12D) and puncta area (fig. 4.12E). On the other hand, TIMELESS depletion in the SW480 cell line led to a significant reduction of the fluorescence intensity (fig. 4.12C) and average size of EDC4 puncta (fig. 4.12E), but not in the average number of aggregates per cell (fig. 4.12D).

These findings demonstrate that TIMELESS expression directly or indirectly impacts P-bodies dynamics in the SW480 cell line.

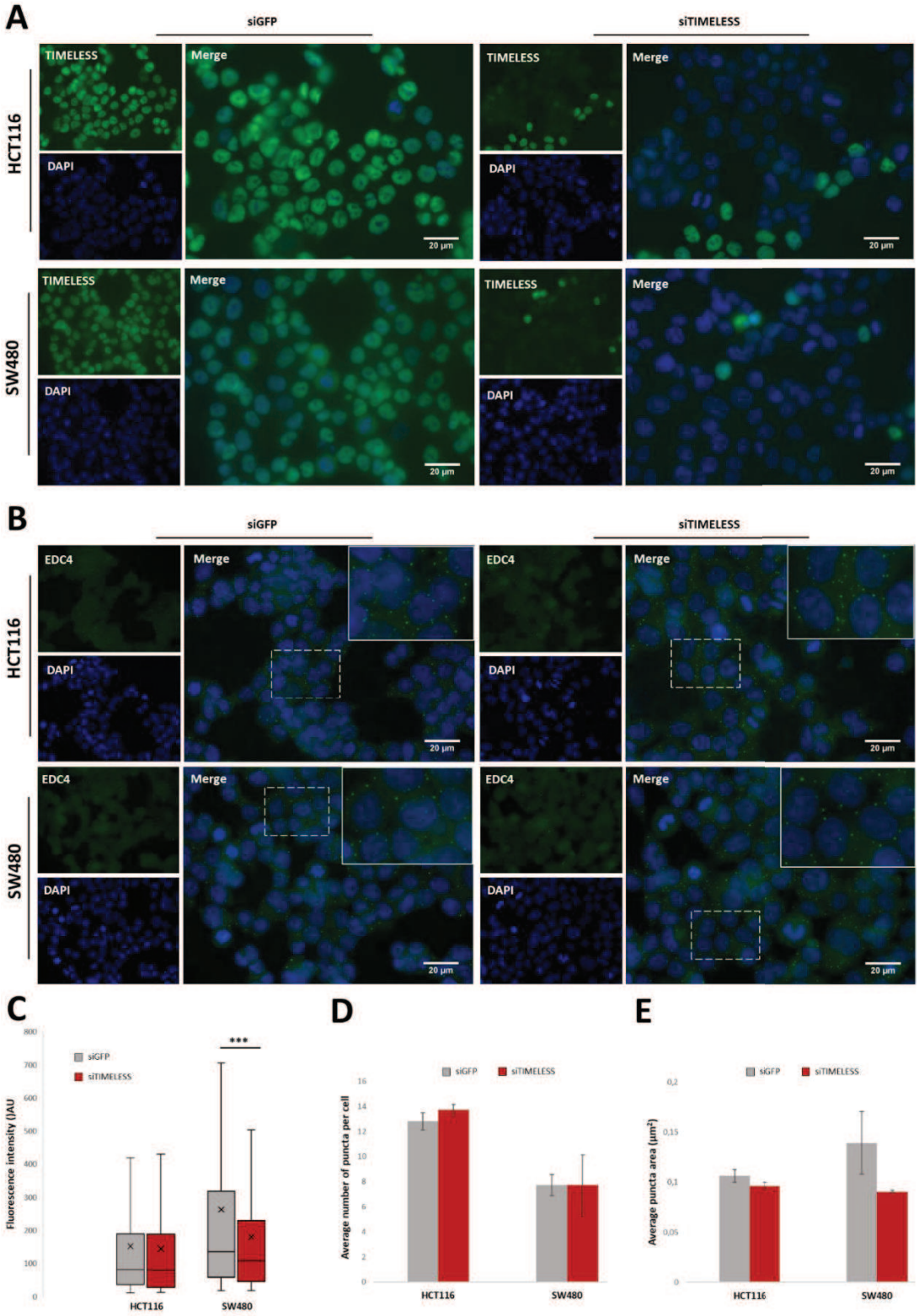

Figure 4.12. P-body dynamic upon TIMELESS. (A) Immunostaining for TIMELESS in siTIMELESS- and siGFP control-transfected cells. **(B)** Immunostaining for EDC4 in siTIMELESS- and siGFP control-transfected cells. **(C)** Fluorescence intensity distribution of EDC4 puncta (the x represents the mean). **(D)** Average number of puncta per cell. **(E)** Average puncta area. Values are expressed as mean ± SEM in D and E (A-E, n=2 independent experiment; Mann-Whitney U test, ***P<0,0001). Amplification of the original images is 400x and the amplified regions correspond to the boxed areas.

Chapter 5 - Discussion

Colorectal cancer is the third most common cancer and the second leading cause of cancer-related deaths worldwide. Despite the extensive characterization of the molecular mechanisms underlying its initiation and progression, little advances have been made in the last years in order to improve patient outcome. It is becoming increasingly clear that the disruption of the RNA life-cycle and its regulatory RBPs plays a role in stem cell biology (87) carcinogenesis (81,88), namely in the context of colorectal cancer (85,86). In this work, we aimed to uncover new stemness-related RBPs functionally relevant for CRC biology.

Our *in silico* approach led us to study three differentially expressed putative RBPs in CRC cases: ASMP, TIMELESS and ZBTB16. ASPM was shown to be upregulated at the transcriptional level in CRC samples when compared to normal tissue according to the TCGA data. It was also recently published that ASPM is upregulated at the transcriptional level in CRC compared to the normal tissue (120). In accordance, we found that the majority of CRC cases analysed in our series presented high ASPM protein expression levels as opposed to the normal tissue, reinforcing the notion that ASPM might be an important player associated with CRC tumour growth. In fact in another study it was shown that ASPM is associated with cancer cell proliferation by promoting G1/S transition, and apoptosis avoidance (121). The fact that ASPM had predominantly a cytoplasmatic staining partner, both by immunohistochemistry and immunofluorescence, indicates that CRC cells preferentially overexpress the cytoplasmatic ASPM isoform as it has been reported for other cancer types, rather than the nuclear isoform, which seems to be involved in the regulation of normal tissue turnover (122,123). The cytoplasmatic isoform specifically induces stem-like properties and enhances tumorigenic potential by its interaction with DVL-family members, the upstream regulator of β-catenin (122–125). This interaction with the Wnt signalling could explain the association found between ASPM-expressing tumours and the Wnt target gene *SOX9* (126).

ZBTB16 was shown to be downregulated at the transcriptional level in CRC samples compared to normal tissue according to the TCGA data. However, in our characterization of a series of human CRC cases, almost half of the tumours expressed high levels of ZBTB16 (57,2% vs 42,8%). It was also clear in the normal colon tissue that stromal cells showed higher ZBTB16-expression levels when compared to epithelial cells, and this stromal staining pattern was lost in high ZBTB16-expressing tumours. Therefore, we demonstrated that ZBTB16 is overexpressed in CRC cases when analysing

epithelial tumoral cells, supporting the hypothesis that ZBTB16 is in fact upregulated and might have a protumorigenic function in CRC (127). Intestinal cells and CRC cell lines specifically express a truncated isoform of ZBTB16 with 65kDa that lacks the BTB/POZ domain essential for ZBTB16 transcriptional activity, thereby localizing at the cytoplasm as we showed (128). The functional role of this isoform is yet to be clarified and further studies on its biological significance in intestinal epithelium homeostasis are required to fully understand its impact in CRC.

TIMELESS was observed to be upregulated at the mRNA level in tissue samples from CRC patients when compared to normal tissue according to the TCGA data, and as previously demonstrated (120). In our series of 192 CRC cases, the percentage of tumours expressing low and high levels of TIMELESS was similar (49,3% vs 50,7%). We could not establish a correlation between TIMELESS expression levels and patient's disease-free survival or overall survival. Another study also failed to found a correlation between TIMELESS expression levels and patient outcome. However, this study only included 19 patients (120). A larger study enrolling 114 patients correlated increased TIMELESS expression with shorter overall survival (129). Moreover, TIMELESS expression has been reported to be associated with tumour progression in other cancer contexts, specifically with stage III and IV patients in gliomas and hepatocellular carcinomas (130,131). This raises questions about TIMELESS role on cancer onset, since it seems globally more elevated in advanced tumour stages (129). Hence, the lack of correlation between patient's outcome and TIMELESS expression in our data might be due to the stage (II) of the patients whose tumours we analysed, and the low number of relapses between them. CRC cells selectively overexpress TIMELESS and other components of the replication fork complex to limit the checkpoint response on stalled forks. This gives cells an increased tolerance to tumorigenic replication stress avoiding excessive genomic instability and senescence, and supporting further tumour growth. (132). Contradicting previous findings (120), our larger cohort of CRC cases showed that tumours with high levels of TIMELESS expression are mainly associated with the MSS status. MSS tumours are commonly aneuploid due to chromosomal alterations, are well differentiated and exhibit less lymphocytic infiltration than MSI tumours in which novel immunogenic peptides are generated as a result of frameshift and missense mutations, leading to cytotoxic T lymphocytes recruitment to the tumour site (49). For this reason, MSS tumours are associated with worse patient outcome and are less responsive to

immunotherapy (133). The same type of association was found between ASPM and the MSS status. These associations, although weak, might indicate that TIMELESS and ASPM have a prognostic value in CRC.

High TIMELESS-expressing tumours were also significantly associated with SOX2 expression, despite the very low number of cases positive for this marker. SOX2 is a transcriptional factor essential for the maintenance of cell pluripotency and self-renewal capacity playing a major role in intestinal development by ensuring proper antero-posterior patterning between the glandular stomach and the intestine (134). SOX2 is not expressed in the adult intestinal epithelium, but it has been reported that its *de novo* expression can occur in CRC, which leads to more aggressive tumours, with a stem cell phenotype, chemotherapy resistant and prone to relapse (135,136). Interestingly, TIMELESS stimulated SOX2 expression through miR-5188-mediated activation of β-catenin transcription, promoting breast cancer stemness and progression (137). Based on the overall evaluation of the expression profile of the different markers in human CRC cases and in a panel of CRC cell lines, and also on the confidence level on the molecular tools we had available (namely the apparent quality of the antibodies), we decide to focus solely on the role of TIMELESS for further functional assessment.

We successfully downregulated TIMELESS expression in two CRC cell lines, which produced a similar response in terms of cell cycle distribution: a slight increase in cells at the G1 phase, especially for SW480 cells, and at the G2/M phase, especially in HCT116 cells, and a more prominent reduction in the S phase, for both cell lines. The increase in the percentage of cells in G2/M is in line with recent work that found a sharp increase in G2/M upon TIMELESS depletion, which was attributed to cell cycle arrest through the phosphorylation of CHK1 (p-CHK1) (138). However, that same study reported a decrease in cells in G1 as opposed to what was observed in this work. TIMELESS has been reported to form a complex with Tipin (TIMELESS-interacting protein) which stabilizes and controls the progression of replication forks during DNA replication (115,139,140). Upon DNA damage, this complex is essential to activate the CHK1-mediated checkpoint, which can lead to cell cycle arrest at G1/S such as in our cell lines. This indicates that TIMELESS expression prevents cell cycle arrest contributing to CRC cell proliferation (112,113).

It has been suggested in several studies that cell cycle progression may be under circadian clock regulation. In fact, TIMELESS is mainly expressed during the S and

G2/M phases in normal fibroblasts. Also, circadian regulators such as PER and CRY control WEE1 expression, which modulates the activity of the Cyclin B1-CDK1 kinase complex essential for mitosis initiation in mouse liver cells (141,142). Furthermore, TIMELESS couples replication termination with mitosis progression forming a complex with the mitotic entry kinases CDK1, Aurora A/B and PLK1 during metaphase. Therefore, depletion of TIMELESS impairs mitotic spindle structure and chromosome cohesion, preventing exit from mitosis and causing G2/M arrest (143).

Concomitantly, TIMELESS depletion also impacted cell death processes in a cell line-specific manner, including under 5-FU-induced genotoxic stress. 5-FU is a chemotherapeutic drug of the antimetabolite family and an uracil analogue. Once metabolized, it represses the thymidylate synthase leading to a dNTP imbalance and consequently DNA damage (144). 5-FU mechanism of action is S phase-specific and thus impairs DNA replication and repair, which might cause the decrease in TIMELESS expression that was observed in 5-FU-treated cells. TIMELESS-inhibited cells seem more prone to die by apoptosis or necrosis in the HCT116 and SW480 cell lines, respectively. In HCT116 cells, TIMELESS removal in the presence of 5-FU enhanced even more uncontrolled cell death by necrosis, but the levels in late apoptosis were equivalent to the ones observed in individual experimental conditions, despite the lower level of cells in early apoptosis. In SW480 cells, however, TIMELESS depletion combined with 5-FU had a more expressive increase in late apoptotic cells than each experimental condition individually. Overall, this indicates that, upon 5-FU-induced stress, TIMELESS depletion might render cells more susceptible for cell death, either through (late) apoptosis and/or necrosis, depending on the cell line background, therefore pointing to a TIMELESS role in cell viability maintenance and cell death avoidance under genotoxic stress.

The observed cell line-specific responses to TIMELESS depletion are likely related with the mutational profile of each cell line. HCT116 cells are reported to express wildtype P53 and thus might be more sensitive to TIMELESS depletion triggering controlled cell death via apoptosis. This result also correlates with the increase of HCT116 cells in G2/M phase, in the sense that retained P53 function could drive G2/M cell cycle arrest after TIMELESS ablation. Previous reports have shown that loss of TIMELESS sensitizes this cell line to G2/M checkpoint arrest (114). On the other hand, SW480 cells have a mutant P53 isoform, therefore might be unable to trigger P53-

dependent cell death upon TIMELESS depletion, which can lead to an increase in the percentage of uncontrolled cell death by necrosis. However, when TIMELESS depletion was combined with the 5-FU treatment a considerable increase in late apoptosis was observed, despite the weak decrease in cell viability induced by 5-FU. The low cellular response to 5-FU treatment is probably due to the fact that cells were only exposed to 5-FU 24h prior to analysis, which might be insufficient to detect changes in programmed cell death. Thereby, it would be interesting to prolong the time of exposure to 5-FU to further exploit TIMELESS role in cell death in response to stress.

Based on TIMELESS role in invasion and EMT promotion documented for other cancer models, we also explored a role for TIMELESS concerning the migratory capacity of CRC cells. TIMELESS has been previously implicated in CRC progression in mouse xenografts by mediating EMT and metastasis. However, no differences were found in siTIMELESS-transfected cells compared to the control condition. It should also be taken into consideration the possible limitation associated with the transient transfection methodology that was employed for the different functional assays, which might not be ideal to assess certain cellular phenotypes.

As we intended to explore the role of putative RBPs involved in stemness features, we looked into TIMELESS association with the intestinal stem cell phenotype. Our cohort of human CRC cases revealed that TIMELESS expression was restricted to a low number of epithelial cells in normal colonic tissue, particularly in lower crypts regions where $LGR5^+$ ISCs are located. With this in mind, we sought to determine if TIMELESS was under the regulation of Wnt signalling. Since the mutational profile of CRC cell lines did not allow proper modulation of the endogenous signalling pathway, we assessed the Wnt signalling modulation effect in TIMELESS expression in intestinal organoids. Intestinal organoids were chosen over colon organoids due to their independence of an exogenous Wnt source to grow, which allowed a more controlled condition for this assay. Although we observed higher TIMELESS expression in Wnt-enriched (WENR medium) organoids, this increase does not appear to be regulated at the transcriptional level, which led us to hypothesize that the increased TIMELESS levels are the result of Wnt-mediated expansion of the $LGR5^+$ cell population. However, definitive proof would only be possible through the analysis of TIMELESS transcriptional activity in response to Wnt signalling-related transcription factors, either by luciferase reporter assay or chromatin immunoprecipitation (ChIP). Interestingly, TIMELESS has been shown to stimulate Wnt

signalling including in CRC, where it stabilizes myosin-9 which promotes β-catenin transcriptional activity (129).

Surprisingly, TIMELESS depletion in CRC cell lines induced a general increase in known ISC markers, especially in SW480 cells, where an increase in *OLFM4* mRNA and MEX3A protein expression levels were observed. This contradicts not only the results mentioned above but also those in other cancer models. In breast cancer cells, TIMELESS was found to induce a stem-like phenotype through Wnt signalling overactivation which promoted EMT and metastasis (137). One might raise two hypotheses to explain these findings: first, knocking down TIMELESS induces the selection of subpopulations of CRC cells in which cell death occurs in non-stem-like cells, but not in stem-like cells; second, TIMELESS is regulating the stem-like phenotype and its silencing directly or indirectly affects the expression of ISC markers. A closer look would reject the first hypothesis based on the minor decrease in cell viability observed in TIMELESS-depleted cells. This means that CRC cells adopt a stem-like phenotype probably to compensate for the TIMELESS depletion-induced stress. Future work will also focus on understanding TIMELESS role in intestinal epithelium homeostasis starting with validation as a marker of the $LGR5^{+}$ cell population.

Finally, we demonstrated that TIMELESS expression directly or indirectly impacts P-bodies dynamics at least in the SW480 cell line. It is, however, not possible to state that TIMELESS has a definitive role as a RBP. The changes in mRNA metabolism could also be a consequence of the altered cellular phenotype observed in SW480 cells upon TIMELESS depletion considering that the MEX3A RBP expression is also altered. Nevertheless, it is known that TIMELESS accumulates at sites of double-strand breaks (DSB), where it physically interacts with poly(ADP-ribose) polymerase 1 (PARP1) independently of Tipin and is required for efficient PARP-1-mediated homologous recombination repair. And in fact, it was recently shown that PARP-1 directly binds RNA and supports mRNA splicing, nuclear export and stability (145,146). Furthermore, PARP-1-directed therapeutics increase the frequency of fork breakage and readily retain TIMELESS at DNA damage sites together with PARP-1 (147,148), and PARP-1 plays a key role during apoptosis, including in response to chemotherapeutics (149). Collectively, this underscores the importance of further studies to determine the role of the TIMELESS-PARP-1 interaction, considering that PARP-1 has also been implicated in ISC survival and is associated with worse patient outcome in stage II and III colon cancer receiving

adjuvant chemotherapy (150,151). To validate TIMELESS role as a RBP future studies would need to investigate its RNA interactome through RNA immunoprecipitation (RIP) or crosslinking and immunoprecipitation (CLIP) techniques, in which RBPs are crosslinked to their RNA targets by UV induction and then purified by electrophoretic methods.

Concluding remarks and future directions

Considering our results, we conclude that two of the putative RBPs identified, ASPM and ZBTB16, are preferentially overexpressed in human CRC cases, and so future work will focus on elucidating if they are functionally relevant in the context of CRC. We also provided further evidence that TIMELESS expression in implicated in key functional aspects of CRC cells, such as cell proliferation and resistance to cell death. Therefore, the molecular mechanisms underlying TIMELESS role in CRC should also be addressed in order to have a broader view on CRC pathogenicity.

This work also provided for the first time evidence that TIMELESS might be implicated with stemness potential in the context of CRC, and further studies will be conducted to determine TIMELESS role in ISCs and intestinal homeostasis. Finally, we also demonstrated that TIMELESS manipulation interferes with mRNA metabolism in SW480 cells, thereby highlighting that future work is needed to assess TIMELESS role in post-transcriptional regulation on CRC onset and progression, which might fuel novel cancer therapies.

References

1. Barker N, Clevers H. The intestinal stem cell. Genes Dev. 2008;96(C):157–73.

2. Barker N. Adult intestinal stem cells: Critical drivers of epithelial homeostasis and regeneration. Nat Rev Mol Cell Biol [Internet]. 2014;15(1):19–33.

3. Barrett K, Brooks H, Boitano S, Barman S. Ganong's: Review of Medical Physiology. Vol. 23rd editi, Lange. McGraw-Hill; 2010. 430 p.

4. Santos AJM, Lo YH, Mah AT, Kuo CJ. The Intestinal Stem Cell Niche: Homeostasis and Adaptations. Trends Cell Biol. 2018;28(12):1062–78.

5. Van Der Flier LG, Clevers H. Stem cells, self-renewal, and differentiation in the intestinal epithelium. Annu Rev Physiol. 2009;71:241–60.

6. Barker N, Van Es JH, Kuipers J, Kujala P, Van Den Born M, Cozijnsen M, et al. Identification of stem cells in small intestine and colon by marker gene Lgr5. Nature. 2007;449(7165):1003–7.

7. Snippert HJ, van der Flier LG, Sato T, van Es JH, van den Born M, Kroon-Veenboer C, et al. Intestinal crypt homeostasis results from neutral competition between symmetrically dividing Lgr5 stem cells. Cell [Internet]. 2010;143(1):134–44.

8. Lopez-Garcia C, Klein AM, Simons BD, Winton DJ. Intestinal stem cell replacement follows a pattern of neutral drift. Science (80-). 2010;330(6005):822–5.

9. Ritsma L, Ellenbroek SIJ, Zomer A, Snippert HJ, De Sauvage FJ, Simons BD, et al. Intestinal crypt homeostasis revealed at single-stem-cell level by in vivo live imaging. Nature [Internet]. 2014;507(7492):362–5.

10. Kozar S, Morrissey E, Nicholson AM, van der Heijden M, Zecchini HI, Kemp R, et al. Continuous clonal labeling reveals small numbers of functional stem cells in intestinal crypts and adenomas. Cell Stem Cell. 2013;13(5):626–33.

11. Muñoz J, Stange DE, Schepers AG, Van De Wetering M, Koo BK, Itzkovitz S, et al. The Lgr5 intestinal stem cell signature: Robust expression of proposed quiescent ′+4′ cell markers. EMBO J. 2012;31(14):3079–91.

12. Itzkovitz S, Lyubimova A, Blat IC, Maynard M, Van Es J, Lees J, et al. Single-molecule transcript counting of stem-cell markers in the mouse intestine. Nat Cell Biol. 2012;14(1):106–14.

13. Li N, Clevers H. Coexistence of quiescent and active adult stem cells in mammals. Science (80-). 2010;327(5965):542–5.

14. Murata K, Jadhav U, Madha S, van Es J, Dean J, Cavazza A, et al. Ascl2-Dependent Cell Dedifferentiation Drives Regeneration of Ablated Intestinal Stem Cells. Cell Stem Cell. 2020;26(3):377-390.e6.

15. van der Flier LG, van Gijn ME, Hatzis P, Kujala P, Haegebarth A, Stange DE, et al. Transcription Factor Achaete Scute-Like 2 Controls Intestinal Stem Cell Fate. Cell [Internet]. 2009;136(5):903–12.

16. Tetteh PW, Basak O, Farin HF, Wiebrands K, Kretzschmar K, Begthel H, et al. Replacement of Lost Lgr5-Positive Stem Cells through Plasticity of Their Enterocyte-Lineage Daughters. Cell Stem Cell [Internet]. 2016;18(2):203–13.

17. Yu S, Tong K, Zhao Y, Balasubramanian I, Yap GS, Ferraris RP, et al. Paneth Cell Multipotency Induced by Notch Activation following Injury. Cell Stem Cell [Internet]. 2018;23(1):46-59.e5.

18. Kikuchi A, Yamamoto H, Sato A, Matsumoto S. New Insights into the Mechanism of

Wnt Signaling Pathway Activation [Internet]. 1st ed. Vol. 291, International Review of Cell and Molecular Biology. Elsevier Inc.; 2011. 21–71 p.

19. Nusse R, Clevers H. Wnt/β-Catenin Signaling, Disease, and Emerging Therapeutic Modalities. Cell [Internet]. 2017;169(6):985–99.

20. Zhan T, Rindtorff N, Boutros M. Wnt signaling in cancer. Oncogene. 2017;36(11):1461–73.

21. Yu J, Virshup DM. Updating the Wnt pathways. Biosci Rep. 2014;34(5):593–607.

22. Cruciat CM, Niehrs C. Secreted and transmembrane Wnt inhibitors and activators. Cold Spring Harb Perspect Biol. 2013;5(3).

23. Martin-Orozco E, Sanchez-Fernandez A, Ortiz-Parra I, Ayala-San Nicolas M. WNT Signaling in Tumors: The Way to Evade Drugs and Immunity. Front Immunol. 2019;10(December):1–21.

24. Wen X, Wu Y, Awadasseid A, Tanaka Y, Zhang W. New advances in canonical wnt/β-catenin signaling in cancer. Cancer Manag Res. 2020;12:6987–98.

25. Farin HF, Van Es JH, Clevers H. Redundant sources of Wnt regulate intestinal stem cells and promote formation of paneth cells. Gastroenterology [Internet]. 2012;143(6):1518-1529.e7.

26. Degirmenci B, Valenta T, Dimitrieva S, Hausmann G, Basler K. GLI1-expressing mesenchymal cells form the essential Wnt-secreting niche for colon stem cells. Nature [Internet]. 2018;558(7710):449–53.

27. Greicius G, Kabiri Z, Sigmundsson K, Liang C, Bunte R, Singh MK, et al. PDGFRα+ pericryptal stromal cells are the critical source of Wnts and RSPO3 for murine intestinal stem cells in vivo. Proc Natl Acad Sci U S A. 2018;115(14):E3173–81.

28. Aoki R, Shoshkes-Carmel M, Gao N, Shin S, May CL, Golson ML, et al. Foxl1-Expressing Mesenchymal Cells Constitute the Intestinal Stem Cell Niche. Cmgh [Internet]. 2016;2(2):175–88.

29. Gregorieff A, Pinto D, Begthel H, Destrée O, Kielman M, Clevers H. Expression Pattern of Wnt Signaling Components in the Adult Intestine. Gastroenterology. 2005;129(2):626–38.

30. Scoville DH, Sato T, He XC, Li L. Current View: Intestinal Stem Cells and Signaling. Gastroenterology. 2008;134(3):849–64.

31. Qi Z, Chen YG. Regulation of intestinal stem cell fate specification. Sci China Life Sci. 2015;58(6):570–8.

32. Batlle E, Henderson JT, Beghtel H, Van den Born MMW, Sancho E, Huls G, et al. β-catenin and TCF mediate cell positioning in the intestinal epithelium by controlling the expression of EphB/EphrinB. Cell. 2002;111(2):251–63.

33. de Lau W, Peng WC, Gros P, Clevers H. The R-spondin/Lgr5/Rnf43 module: Regulator of Wnt signal strength. Genes Dev. 2014;28(4):305–16.

34. Yoon JK, Lee JS. Cellular signaling and biological functions of R-spondins. Cell Signal [Internet]. 2012;24(2):369–77.

35. De Lau W, Barker N, Low TY, Koo BK, Li VSW, Teunissen H, et al. Lgr5 homologues associate with Wnt receptors and mediate R-spondin signalling. Nature. 2011;476(7360):293–7.

36. Meran L, Baulies A, Li VSW. Intestinal Stem Cell Niche: The Extracellular Matrix and Cellular Components. Stem Cells Int. 2017;2017.

37. Philpott A, Winton DJ. Lineage selection and plasticity in the intestinal crypt. Curr Opin Cell Biol [Internet]. 2014;31:39–45.

38. Reid IR. Recent advances in understanding and managing paget's disease [version 1; peer review: 3 approved]. F1000Research. 2019;8:1–12.

39. Horvath S, Zhang B, Carlson M, Lu K V., Zhu S, Felciano RM, et al. Analysis of oncogenic signaling networks in glioblastoma identifies ASPM as a molecular target. Proc Natl Acad Sci U S A. 2006;103(46):17402–7.

40. Spit M, Koo BK, Maurice MM. Tales from the crypt: Intestinal niche signals in tissue renewal, plasticity and cancer. Open Biol. 2018;8(9).

41. Sato T, Vries RG, Snippert HJ, Van De Wetering M, Barker N, Stange DE, et al. Single Lgr5 stem cells build crypt-villus structures in vitro without a mesenchymal niche. Nature [Internet]. 2009;459(7244):262–5.

42. Brenner H, Kloor M, Pox CP. Colorectal cancer. Lancet. 2014;383(9927):1490–502.

43. Arnold M, Sierra MS, Laversanne M, Soerjomataram I, Jemal A, Bray F. Global patterns and trends in colorectal cancer incidence and mortality. Gut. 2017;66(4):683–91.

44. Cunningham D, Atkin W, Lenz HJ, Lynch HT, Minsky B, Nordlinger B, et al. Colorectal cancer. Lancet [Internet]. 2010;375(9719):1030–47.

45. Kuipers EJ, Grady WM, Lieberman D, Seufferlein T, Sung JJ, Boelens PG, et al. Colorectal cancer. Nat Rev Dis Prim [Internet]. 2015;1:1–25.

46. Dekker E, Tanis PJ, Vleugels JLA, Kasi PM, Wallace MB. Colorectal cancer. Lancet [Internet]. 2019;394(10207):1467–80.

47. Fearon E, Vogelstein B. A genetic model for colorectal tumorigenesis. Cell Press. 1989;19(2):170–2.

48. Fearon ER. Molecular genetics of colorectal cancer. Annu Rev Pathol Mech Dis. 2011;6:479–507.

49. Drescher KM, Sharma P, Lynch HT. Current hypotheses on how microsatellite instability leads to enhanced survival of lynch syndrome patients. Clin Dev Immunol. 2010;2010.

50. Li XL, Zhou J, Chen ZR, Chng WJ. P53 mutations in colorectal cancer- Molecular pathogenesis and pharmacological reactivation. World J Gastroenterol. 2015;21(1):84–93.

51. Pastushenko I, Blanpain C. EMT Transition States during Tumor Progression and Metastasis. Trends Cell Biol [Internet]. 2019;29(3):212–26.

52. Tomasetti C, Vogelstein B. Variation in cancer risk among tissues can be explained by the number of stem cell divisions. Science (80-). 2015;347(6217):78–81.

53. de Sousa e Melo F, de Sauvage FJ. Cellular Plasticity in Intestinal Homeostasis and Disease. Cell Stem Cell. 2019;24(1):54–64.

54. Vermeulen L, de Sousa e Melo F, Richel DJ, Medema JP. The developing cancer stem-cell model: Clinical challenges and opportunities. Lancet Oncol [Internet]. 2012;13(2):e83–9.

55. Anderson EC, Hessman C, Levin TG, Monroe MM, Wong MH. The role of colorectal

cancer stem cells in metastatic disease and therapeutic response. Cancers (Basel). 2011;3(1):319–39.

56. Ricci-Vitiani L, Lombardi DG, Pilozzi E, Biffoni M, Todaro M, Peschle C, et al. Identification and expansion of human colon-cancer-initiating cells. Nature. 2007;445(7123):111–5.

57. O'Brien CA, Pollett A, Gallinger S, Dick JE. A human colon cancer cell capable of initiating tumour growth in immunodeficient mice. Nature. 2007;445(7123):106–10.

58. Dalerba P, Dylla SJ, Park IK, Liu R, Wang X, Cho RW, et al. Phenotypic characterization of human colorectal cancer stem cells. Proc Natl Acad Sci U S A. 2007;104(24):10158–63.

59. Schepers AG, Clevers H. Lineage tracing reveals Lgr5+ stem cell activity in mouse intestinal adenomas. 2012;337(August):730–6.

60. Kemper K, Prasetyanti PR, De Lau W, Rodermond H, Clevers H, Medema JP. Monoclonal antibodies against Lgr5 identify human colorectal cancer stem cells. Stem Cells. 2012;30(11):2378–86.

61. Barker N, Ridgway RA, Van Es JH, Van De Wetering M, Begthel H, Van Den Born M, et al. Crypt stem cells as the cells-of-origin of intestinal cancer. Nature [Internet]. 2009;457(7229):608–11.

62. Ziskin JL, Dunlap D, Yaylaoglu M, Fodor IK, Forrest WF, Patel R, et al. In situ validation of an intestinal stem cell signature in colorectal cancer. Gut. 2013;62(7):1012–23.

63. Snippert HJ, Schepers AG, Van Es JH, Simons BD, Clevers H. Biased competition between Lgr5 intestinal stem cells driven by oncogenic mutation induces clonal expansion. EMBO Rep. 2014;15(1):62–9.

64. Merlos-Suárez A, Barriga FM, Jung P, Iglesias M, Céspedes MV, Rossell D, et al. The intestinal stem cell signature identifies colorectal cancer stem cells and predicts disease relapse. Cell Stem Cell. 2011;8(5):511–24.

65. Seshagiri S, Stawiski EW, Durinck S, Modrusan Z, Storm EE, Conboy CB, et al. Recurrent R-spondin fusions in colon cancer. Nature. 2012;488(7413):660–4.

66. Vermeulen L, De Sousa E Melo F, Van Der Heijden M, Cameron K, De Jong JH, Borovski T, et al. Wnt activity defines colon cancer stem cells and is regulated by the microenvironment. Nat Cell Biol [Internet]. 2010;12(5):468–76.

67. Schwitalla S, Fingerle AA, Cammareri P, Nebelsiek T, Göktuna SI, Ziegler PK, et al. Intestinal tumorigenesis initiated by dedifferentiation and acquisition of stem-cell-like properties. Cell. 2013;152(1–2):25–38.

68. Lenos KJ, Miedema DM, Lodestijn SC, Nijman LE, van den Bosch T, Romero Ros X, et al. Stem cell functionality is microenvironmentally defined during tumour expansion and therapy response in colon cancer. Nat Cell Biol [Internet]. 2018;20(10):1193–202.

69. De Sousa E Melo F, Kurtova A V., Harnoss JM, Kljavin N, Hoeck JD, Hung J, et al. A distinct role for Lgr5 + stem cells in primary and metastatic colon cancer. Nature [Internet]. 2017;543(7647):676–80.

70. Shimokawa M, Ohta Y, Nishikori S, Matano M, Takano A, Fujii M, et al. Visualization and targeting of LGR5 + human colon cancer stem cells. Nature [Internet]. 2017;545(7653):187–92.

71. Fumagalli A, Oost KC, Kester L, Morgner J, Bornes L, Bruens L, et al. Plasticity of

Lgr5-Negative Cancer Cells Drives Metastasis in Colorectal Cancer. Cell Stem Cell. 2020;26(4):569-578.e7.

72. Hsu HC, Liu YS, Tseng KC, Hsu CL, Liang Y, Yang TS, et al. Overexpression of Lgr5 correlates with resistance to 5-FU-based chemotherapy in colorectal cancer. Int J Colorectal Dis. 2013;28(11):1535–46.

73. Moore MJ. From birth to death: The complex lives of eukaryotic mRNAs. Science (80-). 2005;309(5740):1514–8.

74. Re A, Joshi T, Kulberkyte E, Morris Q, Workman CT. Chapter 23 RNA – Protein Interactions : An Overview. Vol. 1097, RNA sequence, Structure and Function: Computational and Bioinfromatic Methods. 2014. 491–521 p.

75. Parker R, Sheth U. P Bodies and the Control of mRNA Translation and Degradation. Mol Cell. 2007;25(5):635–46.

76. Balagopal V, Parker R. Polysomes, P bodies and stress granules: states and fates of eukaryotic mRNAs. Curr Opin Cell Biol. 2009;21(3):403–8.

77. Liao JY, Yang B, Zhang YC, Wang XJ, Ye Y, Peng JW, et al. EuRBPDB: A comprehensive resource for annotation, functional and oncological investigation of eukaryotic RNA binding proteins (RBPs). Nucleic Acids Res. 2020;48(D1):D307–13.

78. Gerstberger S, Hafner M, Tuschl T. A census of human RNA-binding proteins. Nat Rev Genet [Internet]. 2014;15(12):829–45.

79. Schwanhüusser B, Busse D, Li N, Dittmar G, Schuchhardt J, Wolf J, et al. Global quantification of mammalian gene expression control. Nature. 2011;473(7347):337–42.

80. Vogel C, De Sousa Abreu R, Ko D, Le SY, Shapiro BA, Burns SC, et al. Sequence signatures and mRNA concentration can explain two-thirds of protein abundance variation in a human cell line. Mol Syst Biol [Internet]. 2010;6(400):1–9.

81. Pereira B, Billaud M, Almeida R. RNA-Binding Proteins in Cancer: Old Players and New Actors. Trends in Cancer [Internet]. 2017;3(7):506–28. Available from: http://dx.doi.org/10.1016/j.trecan.2017.05.003

82. Hogan DJ, Riordan DP, Gerber AP, Herschlag D, Brown PO. Diverse RNA-binding proteins interact with functionally related sets of RNAs, suggesting an extensive regulatory system. PLoS Biol. 2008;6(10):2297–313.

83. Anderson P, Kedersha N, Ivanov P. Stress granules, P-bodies and cancer. Biochim Biophys Acta - Gene Regul Mech [Internet]. 2015;1849(7):861–70.

84. Wurth L, Gebauer F. RNA-binding proteins, multifaceted translational regulators in cancer. Biochim Biophys Acta - Gene Regul Mech [Internet]. 2015;1849(7):881–6.

85. García-Cárdenas JM, Guerrero S, López-Cortés A, Armendáriz-Castillo I, Guevara-Ramírez P, Pérez-Villa A, et al. Post-transcriptional Regulation of Colorectal Cancer: A Focus on RNA-Binding Proteins. Front Mol Biosci. 2019;6(August):1–18.

86. Chatterji P, Rustgi AK. RNA Binding Proteins in Intestinal Epithelial Biology and Colorectal Cancer. Trends Mol Med [Internet]. 2018;24(5):490–506.

87. Ye J, Blelloch R. Regulation of pluripotency by RNA binding proteins. Cell Stem Cell. 2014;15(3):271–80.

88. Coppin L, Leclerc J, Vincent A, Porchet N, Pigny P. Messenger RNA life-cycle in cancer cells: Emerging role of conventional and non-conventional RNA-binding proteins? Int J Mol Sci. 2018;19(3).

89. Hong S. RNA Binding Protein as an Emerging Therapeutic Target for Cancer Prevention and Treatment. J Cancer Prev. 2017;22(4):203–10.

90. Deloria AJ, Höflmayer D, Kienzl P, Lopatecka J, Sampl S, Klimpfinger M, et al. Epithelial splicing regulatory protein 1 and 2 paralogues correlate with splice signatures and favorable outcome in human colorectal cancer. Oncotarget. 2016;7(45):73800–16.

91. Fagoonee S, Picco G, Orso F, Arrigoni A, Longo DL, Forni M, et al. The RNA-binding protein ESRP1 promotes human colorectal cancer progression. Oncotarget. 2017;8(6):10007–24.

92. Leontieva O V., Ionov Y. RNA-binding motif protein 35A is a novel tumor suppressor for colorectal cancer. Cell Cycle. 2009;8(3):490–7.

93. Liao B, Hu Y, Brewer G. Competitive binding of AUF1 and TIAR to MYC mRNA controls its translation. Nat Struct Mol Biol. 2007;14(6):511–8.

94. Dong R, Lu JG, Wang Q, He XL, Chu YK, Ma QJ. Stabilization of Snail by HuR in the process of hydrogen peroxide induced cell migration. Biochem Biophys Res Commun. 2007;356(1):318–21.

95. Hamilton KE, Noubissi FK, Katti PS, Hahn CM, Davey SR, Lundsmith ET, et al. IMP1 promotes tumor growth, dissemination and a tumor-initiating cell phenotype in colorectal cancer cell xenografts. Carcinogenesis. 2013;34(11):2647–54.

96. Rivera Vargas T, Boudoukha S, Simon A, Souidi M, Cuvellier S, Pinna G, et al. Post-transcriptional regulation of cyclins D1, D3 and G1 and proliferation of human cancer cells depend on IMP-3 nuclear localization. Oncogene. 2014;33(22):2866–75.

97. Mura M, Hopkins TG, Michael T, Abd-Latip N, Weir J, Aboagye E, et al. LARP1 post-transcriptionally regulates mTOR and contributes to cancer progression. Oncogene. 2015;34(39):5025–36.

98. Ma F, Zhou Z, Li N, Zheng L, Wu C, Niu B, et al. Lin28a promotes self-renewal and proliferation of dairy goat spermatogonial stem cells (SSCs) through regulation of mTOR and PI3K / AKT. 2016;(December):1–12.

99. Tu HC, Schwitalla S, Qian Z, LaPier GS, Yermalovich A, Ku YC, et al. LIN28 cooperates with WNT signaling to drive invasive intestinal and colorectal adenocarcinoma in mice and humans. Genes Dev. 2015;29(10):1074–86.

100. Rezza A, Skah S, Roche C, Nadjar J, Samarut J, Plateroti M. The overexpression of the putative gut stem cell marker Musashi-1 induces tumorigenesis through Wnt and Notch activation. J Cell Sci. 2010;123(19):3256–65.

101. Ji S, Ye G, Zhang J, Wang L, Wang T, Wang Z, et al. MiR-574-5p negatively regulates Qki6/7 to impact β-catenin/Wnt signalling and the development of colorectal cancer. Gut. 2013;62(5):716–26.

102. Das S, Anczuków O, Akerman M, Krainer AR. Oncogenic Splicing Factor SRSF1 Is a Critical Transcriptional Target of MYC. Cell Rep. 2012;1(2):110–7.

103. Buchet-Poyau K, Courchet J, Le Hir H, Séraphin B, Scoazec JY, Duret L, et al. Identification and characterization of human Mex-3 proteins, a novel family of evolutionarily conserved RNA-binding proteins differentially localized to processing bodies. Nucleic Acids Res. 2007;35(4):1289–300.

104. Barriga FM, Montagni E, Mana M, Mendez-Lago M, Hernando-Momblona X, Sevillano M, et al. Mex3a Marks a Slowly Dividing Subpopulation of Lgr5+ Intestinal Stem Cells. Cell Stem Cell [Internet]. 2017;20(6):801-816.e7.

105. Pereira B, Amaral AL, Dias A, Mendes N, Muncan V, Silva AR, et al. MEX3A regulates Lgr5 + stem cell maintenance in the developing intestinal epithelium . EMBO Rep. 2020;21(4):1–17.

106. Pereira B, Sousa S, Barros R, Carreto L, Oliveira P, Oliveira C, et al. CDX2 regulation by the RNA-binding protein MEX3A: Impact on intestinal differentiation and stemness. Nucleic Acids Res. 2013;41(7):3986–99.

107. Huttner WB, Fish JL, Kosodo Y, Enard W, Pa S. Aspm specifically maintains symmetric proliferative divisions of neuroepithelial cells ¨ a. 2006;

108. Capecchi MR, Pozner A. ASPM regulates symmetric stem cell division by tuning Cyclin E ubiquitination. 2015;(May):1–17.

109. Buchman JJ, Durak O, Tsai LH. ASPM regulates Wnt signaling pathway activity in the developing brain. Genes Dev. 2011;25(18):1909–14.

110. Koike N, Hida A, Numano R, Hirose M, Sakaki Y, Tei H. Identification of the mammalian homologues of the Drosophila timeless gene, Timeless1. FEBS Lett. 1998;441(3):427–31.

111. Cho W, Kang Y, An Y, Tappin I, Hurwitz J, Lee J. Human Tim-Tipin complex affects the biochemical properties of the replicative DNA helicase and DNA polymerases. 2013;110(7):2523–7.

112. Yoshizawa-Sugata N, Masai H. Human Tim/Timeless-interacting protein, Tipin, is required for efficient progression of S phase and DNA replication checkpoint. J Biol Chem [Internet]. 2007;282(4):2729–40.

113. Smith-Roe SL, Patel SS, Zhou Y, Simpson DA, Rao S, Ibrahim JG, et al. Separation of intra-S checkpoint protein contributions to DNA replication fork protection and genomic stability in normal human fibroblasts. Cell Cycle. 2013;12(2):332–45.

114. Yang X, Wood PA, Hrushesky WJM. Mammalian TIMELESS Is Required for ATM-dependent CHK2 Activation and G 2 / M Checkpoint Control *. 2010;285(5):3030–4.

115. Leman AR, Noguchi C, Lee CY, Noguchi E. Human Timeless and Tipin stabilize replication forks and facilitate sister-chromatid cohesion. J Cell Sci. 2010;123(5):660–70.

116. Smith-Roe SL, Patel SS, Simpson DA, Zhou YC, Rao S, Ibrahim JG, et al. Timeless functions independently of the Tim-Tipin complex to promote sister chromatid cohesion in normal human fibroblasts. Cell Cycle. 2011;10(10):1618–24.

117. Leman AR, Dheekollu J, Deng Z, Lee SW, Das MM, Lieberman PM. Timeless preserves telomere length by promoting efficient DNA replication through human telomeres Do not distribute . © 2012 Landes Bioscience . 2012;2337–47.

118. Clotaire DZJ, Wei Y, Yu X, Ousman T, Hua J. Functions of promyelocytic leukaemia zinc finger (Plzf) in male germline stem cell development and differentiation. Reprod Fertil Dev. 2019;31(8):1315–20.

119. Sambuy Y, De Angelis I, Ranaldi G, Scarino ML, Stammati A, Zucco F. The Caco-2 cell line as a model of the intestinal barrier: Influence of cell and culture-related factors on Caco-2 cell functional characteristics. Cell Biol Toxicol. 2005;21(1):1–26.

120. Mazzoccoli G, Panza A, Valvano MR, Palumbo O, Carella M, Pazienza V, et al. Clock Gene Expression Levels and Relationship With Clinical and Pathological Features in Colorectal Cancer Patients. 2011;28(10):841–51.

121. Yang Q, Qi M, Dong W. ASPM is a novel candidate gene associated with colorectal

cancer cell growth. DNA Cell Biol. 2021;10(FEB):1–7.

122. Pai VC, Hsu C, Chan T, Chen WLCCW, Lin CLC, Chen SHL, et al. ASPM promotes prostate cancer stemness and progression by augmenting Wnt − Dvl-3 − β -catenin signaling. Oncogene [Internet]. 2018;

123. Hsu CC, Liao WY, Chang KY, Chan TS, Huang PJ, Chiang CT, et al. A multi-mode Wnt- and stemness-regulatory module dictated by FOXM1 and ASPM isoform I in gastric cancer. Gastric Cancer [Internet]. 2021;24(3):624–39.

124. Liao WY, Hsu CC, Chan TS, Yen CJ, Chen WY, Pan HW, et al. Dishevelled 1-Regulated Superpotent Cancer Stem Cells Mediate Wnt Heterogeneity and Tumor Progression in Hepatocellular Carcinoma. Stem Cell Reports. 2020;14(3):462–77.

125. Hsu CC, Liao WY, Chan TS, Chen WY, Lee CT, Shan YS, et al. The differential distributions of ASPM isoforms and their roles in Wnt signaling, cell cycle progression, and pancreatic cancer prognosis. J Pathol. 2019;249(4):498–508.

126. Prévostel C, Blache P. The dose-dependent effect of SOX9 and its incidence in colorectal cancer. Eur J Cancer. 2017;86:150–7.

127. Mariani F, Sena P, Magnani G, Mancini S, Palumbo C, Leon MP De, et al. PLZF Expression during Colorectal Cancer Development and in Normal Colorectal Mucosa according to Body Size , as Marker of Colorectal Cancer Risk. 2013;2013.

128. Fr I. Identification of a novel promyelocytic leukemia zinc-finger isoform required for colorectal cancer cell growth and survival. 2013;67:58–66.

129. Cao M, Wang Y, Xiao Y, Zheng D, Zhi C, Xia X, et al. Activation of the clock gene TIMELESS by H3k27 acetylation promotes colorectal cancer tumorigenesis by binding to Myosin-9. J Exp Clin Cancer Res. 2021;40(1):1–17.

130. Wang F, Chen QX. The analysis of deregulated expression of the timeless genes in gliomas. J Cancer Res Ther. 2018;14(10):S708–12.

131. Elgohary N, Pellegrino R, Neumann O, Elzawahry HM, Schemmer P, Schirmacher P, et al. Protumorigenic role of Timeless in hepatocellular carcinoma. 2015;597–606.

132. Bianco JN, Bergoglio V, Lin YL, Pillaire MJ, Schmitz AL, Gilhodes J, et al. Overexpression of Claspin and Timeless protects cancer cells from replication stress in a checkpoint-independent manner. Nat Commun [Internet]. 2019;10(1).

133. Popat S, Hubner R, Houlston RS. Systematic review of microsatellite instability and colorectal cancer prognosis. J Clin Oncol. 2005;23(3):609–18.

134. Sarkar A, Hochedlinger K. The Sox family of transcription factors: Versatile regulators of stem and progenitor cell fate. Cell Stem Cell [Internet]. 2013;12(1):15–30.

135. Takeda K, Mizushima T, Yokoyama Y, Hirose H, Wu X, Qian Y, et al. Sox2 is associated with cancer stem-like properties in colorectal cancer. Sci Rep. 2018;8(1):1–9.

136. Schaefer T, Lengerke C. SOX2 protein biochemistry in stemness, reprogramming, and cancer: the PI3K/AKT/SOX2 axis and beyond. Oncogene [Internet]. 2020;39(2):278–92.

137. Zou Y, Lin X, Bu J, Lin Z, Chen Y, Qiu Y, et al. Timeless-Stimulated miR-5188-FOXO1/β-Catenin-c-Jun Feedback Loop Promotes Stemness via Ubiquitination of β-Catenin in Breast Cancer. Mol Ther [Internet]. 2019;28(13):1–15.

138. Neilsen BK, Id DEF, Mccall JL, Fisher KW, Lewis E. ERK-mediated TIMELESS expression suppresses G2 / M arrest in colon cancer cells. 2019;1–19.

139. Gotter AL. Tipin, a novel timeless-interacting protein, is developmentally co-expressed with Timeless and disrupts its self-association. J Mol Biol. 2003;331(1):167–76.

140. Ünsal-Kaçmaz K, Chastain PD, Qu P-P, Minoo P, Cordeiro-Stone M, Sancar A, et al. The Human Tim/Tipin Complex Coordinates an Intra-S Checkpoint Response to UV That Slows Replication Fork Displacement. Mol Cell Biol. 2007;27(8):3131–42.

141. Ünsal-Kaçmaz K, Mullen TE, Kaufmann WK, Sancar A. Coupling of Human Circadian and Cell Cycles by the Timeless Protein. Mol Cell Biol. 2005;25(8):3109–16.

142. Matsuo T, Yamaguchi S, Mitsui S, Emi A, Shimoda F, Okamura H. Control mechanism of the circadian clock for timing of cell division in vivo. Science (80-). 2003;302(5643):255–9.

143. Dheekollu J, Wiedmer A, Hayden J, Speicher D, Gotter AL, Lieberman PM. Timeless Links Replication Termination to Mitotic Kinase Activation. 2011;6(5).

144. Longley DB, Harkin DP, Johnston PG. 5-Fluorouracil: Mechanisms of action and clinical strategies. Nat Rev Cancer. 2003;3(5):330–8.

145. Ke Y, Zhang J, Lv X, Zeng X, Ba X. Novel insights into PARPs in gene expression: regulation of RNA metabolism. Cell Mol Life Sci [Internet]. 2019;76(17):3283–99.

146. Melikishvili M, Chariker JH, Rouchka EC, Fondufe-Mittendorf YN. Transcriptome-wide identification of the RNA-binding landscape of the chromatin-associated protein PARP1 reveals functions in RNA biogenesis. Cell Discov [Internet]. 2017;3:1–21.

147. Xie S, Mortusewicz O, Ma HT, Herr P, Poon RRY, Helleday T, et al. Timeless Interacts with PARP-1 to Promote Homologous Recombination Repair. Mol Cell [Internet]. 2015;60(1):163–76.

148. Young LM, Marzio A, Perez-Duran P, Reid DA, Meredith DN, Roberti D, et al. TIMELESS Forms a Complex with PARP1 Distinct from Its Complex with TIPIN and Plays a Role in the DNA Damage Response. Cell Rep [Internet]. 2015;13(3):451–9.

149. Li M, Yu X. The role of poly(ADP-ribosyl)ation in DNA damage response and cancer chemotherapy. Oncogene. 2015;34(26):3349–56.

150. Ishizuka S, Martin K, Booth C, Potten CS, de Murcia G, Bürkle A, et al. Poly(ADP-ribose) polymerase-1 is a survival factor for radiation-exposed intestinal epithelial stem cells in vivo. Nucleic Acids Res. 2003;31(21):6198–205.

151. Abdelrahman AE, Ibrahim DA, El-Azony A, Alnagar AA, Ibrahim A. ERCC1, PARP-1, and AQP1 as predictive biomarkers in colon cancer patients receiving adjuvant chemotherapy. Cancer Biomarkers. 2020;27(2):251–64.